ADDIS ABABA UNIVERSITY

ADDIS ABABA UNIVERSITY INSTITUTE OF TECHNOLOGY SCHOOL OF ELECTRICAL AND COMPUTER ENGINEERING

DESIGN AND SIMULATION OF MOBILE PICK AND PLACE ROBOT MANIPULATOR (MPPRM)

Thesis Submitted to Addis Ababa Institute of Technology in Partial Fulfillment of the Requirements for the Degree of Master of Science in Electrical and Computer Engineering (Control Engineering)

By: Kalkidan Yirmed

Advisor: Dr. Dereje Shiferaw

February 24, 2020

Addis Ababa, Ethiopia

Addis Ababa University

Addis Ababa Institute of Technology

School of Electrical and Computer Engineering

DESIGN AND SIMULATION OF MOBILE PICK AND PLACE ROBOT MANIPULATOR (MPPRM)

Thesis Submitted to Addis Ababa Institute of Technology in Partial Fulfillment of the Requirement for the Degree of Master of Science in Electrical and Computer Engineering (Control Engineering)

By: Kalkidan Yirmed

Approval by Board of Examiners

Chairman Department of Graduate Committee	Signature
Dr. Dereje Shiferaw Advisor's Name	Signature
Internal Examiner	Signature
External Examiner	Signature

DECLARATION

I hereby declare that this thesis entitled **"DESIGN AND SIMULATION OF MOBILE PICK AND PLACE ROBOT MANIPULATOR (MPPRM)"** was composed by myself, with the guidance of my advisor, that the work contained herein is my own except where explicitly stated otherwise in the text, and that this work has not been submitted, in whole or in part, for any other degree or professional qualification in any other institute.

Kalkidan Yirmed _____

Name Signature

Addis Ababa _____

Place Date of submission

This thesis work has been submitted for examination with my approval as a University Advisor.

Dr. Dereje Shiferaw _____

Advisor's Name Signature

ACKNOWLEDGEMENT

First of all, I would like to thank Almighty GOD, for being a tower of strength and guiding force, giving me faith and courage to carry on even during difficult times.

I am extremely grateful to my thesis advisor Dr. Dereje Shiferaw, who guided me at every stage of preparation of this thesis. His support, encouragement, valuable ideas and many excellent comments have been crucial for accomplishing this thesis work. I am truly thankful for his guidance and many interesting discussions.

There are no words that describe how grateful I am to my grandfather Aba Mulu Gebeyehu taught me how to take scarifies in wrong time. My deepest thanks go to my wife Brikabu Abebe for their patience and understanding during my busy schedule.

Last but not least, I want to acknowledge my gratitude towards my parents and uncles, for their great support, encouragement and kind understanding.

ABSTRACT

Self-balanced two-wheeled mobile robot manipulators (TWMRMs), which is based on an inverted pendulum system, is dynamically (for handling a payload) and statically unstable. While different configurations of self-balanced two-wheeled mobile robot manipulators (TWMRMs) exist, the workspace of these systems is restricted by their current configurations and designs. This study presents the performance of using a fuzzy-PID control algorithm as part of a PID control scheme for the control of 5 DOFs self-balanced TWMPPRM that could be useful for industrial applications such as pick and place and materials handling hazardous products in the chemical manufacturing industry. The system under investigation offers solutions for industrial robotic applications requiring a limited working space. The non-linear mathematical model system derived from Lagrangian modeling approach is simulated in the MATLAB / SIMULINK framework. Fuzzy-PID control of a decoupled nature is designed and implemented. Various operating scenarios with several initial conditions are used to test the robustness and performance of the system. Using integral absolute error (IAE) strategy for payload free movement, it is observable that the system takes around 2.2870 seconds to settle by implementing the PID control strategy, which is greater than the settling time (0.7800 seconds) of the Fuzzy-PID control, and for peak time and rise time it takes 0.5710s and 0.2790s respectively for PID. Furthermore, for peak time and rise time it takes 0.4400s and 0.2300s respectively using Fuzzy-PID control strategy. The simulation results showed the effectiveness of the Fuzzy-PID control approach in improving system performance compared to the PID control system.

Keywords: PID controller, Fuzzy logic, Fuzzy-PID controller, TWMPPRM.

CONTENTS

LIST OF FIGURES

LIST OF TABLES

LIST OF ABBREVIATIONS

MPPRM	Mobile pick and place robotic manipulator
FPID	Fuzzy-PID
DOFs	Degrees of freedoms
TWMRMs	Two-wheeled mobile robot manipulators
TWMR	Two-wheeled mobile robot
MRMs	Mobile robot manipulators
IB	Intermediate body
IP	Inverted pendulum
WIP	Wheeled inverted pendulum
COM	Center of mass
ZN	Ziegler-Nichols
FLC	Fuzzy Logic Controller
FIS	Fuzzy inference System
ITAE	Integral Time Absolute Error
ITSE	Integral Time Square Error
IAE	Integral Absolute Error
ISE	Integral Square Error

LIST OF SYMBOLS

θ	Tilt angle of the intermediate body around the vertical Z axis
δ_R, δ_L	Angular displacement of right and left wheels respectively
h_1, h_2	Vertical and Horizontal linear link displacement respectively
F_1, F_2	Force generated by the vertical and horizontal linear actuator respectively
F_d	Disturbance force
τ_R, τ_L	Right and left wheels torque per meter respectively
m_1	Mass of the chassis
m_2	Mass of the linear actuators
m_w	Mass of wheel
R	Wheel radius
J_1	Chassis moment of inertia
J_2	Moving mass moment of inertia
J_w	Wheel moment of inertia
l	Distance of chassis′ center of mass for wheel axle
μ_1	Coefficient of friction of vertical linear actuator
μ_2	Coefficient of friction of horizontal linear
μ_w	Coefficient of friction between wheel and ground
μ_c	Coefficient of friction between chassis and wheel
g	Gravitational acceleration
V_R, V_L	Input voltage of right and left wheel actuator/motor respectively
V_1, V_2	Input voltage of vertical and horizontal link linear actuator/motor respectively

CHAPTER ONE

1. INTRODUCTION

1.1 Background

Two wheeled robots, which operate on the inverted pendulum principle, are unstable, nonlinear, and under actuated in nature. Basically, the robot consists of two driving wheels attached on each side of the robot chassis and there is an arm added to give additional freedom which driven by DC motors. Just as the inverted pendulum, two wheeled robots are balanced at upright position by controlling the rotation of the DC motors. There are wheeled human transporters, wheeled space robots, industrial robots etc. which can work complete autonomous and fulfill hazardous and dangerous tasks. However, under actuated mobile robots are still under-development and researchers trying to make them perfect. There are under actuated robots with wheel and walking gait. Walking robots are good for human service and rough terrain with manual control or semi-automatic. They have superior maneuver but they are very slow. These robots are used in civil and military applications.

Two wheeled systems are designed for human transportation at the beginning. But in the past, two wheeled systems are built for mobile robotics applications as mapping, industrial carriers, servant robots and etc. To give more flexibility and freedom, these two wheeled systems are combined with manipulators thus mobile manipulators come around. Mobile manipulator can achieve many tasks as obstacle avoidance, pushing, picking and placing etc. Walking robots can also achieve these kinds of tasks but their complex structure restricts usage most of the cases. These wheeled part and manipulator are constructing a hybrid platform. Hybrid platforms can mimic the biological creatures like insects and animals. These platforms make us understand the posture stability and complex control techniques.

In this thesis, two wheeled under actuated robot is designed. There is an arm added to give additional freedom. Hence, self-balanced two wheeled mobile pick and place robot manipulator (TWMPPRM) designed. This arm can be used as a manipulator and disturbance source, arm source also can be effective for posture stability. The system has different functions in the mathematical model and the real system. In the mathematical model arms have two different functions. First function is to create disturbances while the controller strives for balancing and

linear movement. Second function is to help balancing when there is an external disturbance effects or when the initial conditions are non-zero.

The TWMPPRMs consists three main subsystems namely, mechanical system, electrical system, and control system [1]. Mechanical system comprises of all movable parts and is used to move the end effector to the desired position with respect to the mobile base/platform. This movement depends on the electrical system (separately excited DC motors). The third system in mobile manipulators is the control system and consists of some devices and tools (i.e. sensors, controllers, and knowledge base) that provide convenient duty to mobile manipulators. Control system provides some function for the plant (TWMPPRM) such as: a) providing the capability to move in the surrounding environments. b) Collecting information about the robot in the working place. c) Using this information to give a methodology to control robot. d) Storing the data providing it to the robot updating it at an instant.

One of the most vital and powerful issues in this work is to investigate and resolve the issue of stability, balance by controlling the motion state of mobile manipulator for pick and place application. Controlling TWMPPRM is a major research area to limit the time history of base and joint inputs that required stabilizing, balance, and move the end-effector to execute the required mission. Therefore, the control technique must apply to achieve the desired behavior. FLC is better than the PID controllers with nonlinear systems. On the other hands, more than 90% of the controllers in application today are PID controllers because they are easy to understand and implement. It is costly to replace the PID controller with FLC in all applications. Therefore, one of the attractive solutions is to combine the PID controllers and FLC to structure the Fuzzy-PID controller in industrial applications to overcome drawbacks of PID controllers with nonlinear system [2]. Many papers [3-5] discussed the Fuzzy-PID method. Fuzzy-PID is a multilayer controller with the FLC at the highest level which has the capabilities to tune the PID parameters under varying process conditions best than classical method (e.g. Ziegler-Nichols) and PID controllers at lowest level.

1.1.1. Fuzzy Logic system

Fuzzy logic was introduced by Zadeh [18], is a mathematical tool for dealing with uncertainties and imprecision in modeling and data available. The fuzzy logic provides an inference structure that enables appropriate human reasoning capabilities. The traditional binary set theory describes

crisp events, events that either do or do not occur. Fuzzy logic uses probability theory to explain if an event will occur, measuring the chance with which a given event is expected to occur. The theory of fuzzy logic is based upon the notion of relative graded membership.

A fuzzy logic system accepts imprecise data and vague statements and provides decisions. It provides means to model the uncertainty associated with vagueness, imprecision, and lack of information regarding a problem or a plant. The basic elements of a fuzzy logic system, as shown in figure 1.1, are Fuzzifier, Fuzzy inference system, and Defuzzifier [19].

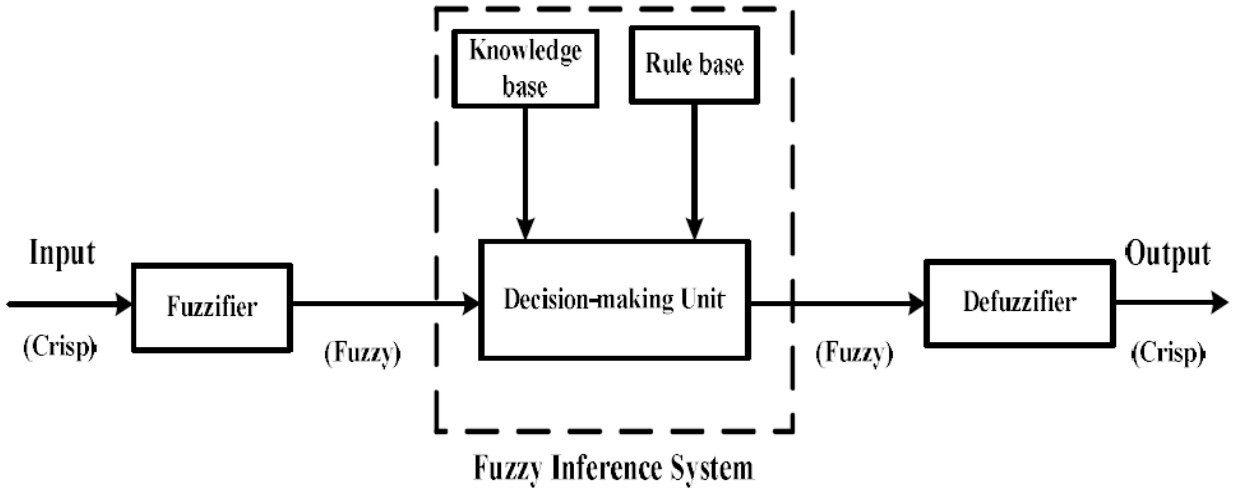

Figure 1.1 Fuzzy logic system [19]

Input data are most often crisp values. The task of the fuzzifier is to map crisp inputs into fuzzy. Inference system consists of a decision-making unit based on knowledge base and rule base. Models based on fuzzy logic consist of "If-Then" rules. The fact following "If" is called a premise or hypothesis or antecedent. Based on this fact, one can infer another fact that is called a conclusion or consequent (the fact following "Then"). A set of a large number of rules of the type: *IF* (antecedent) *THEN* (consequent) is called a fuzzy rule base. Knowledge base contains the information about the model based on the experience of the experts. Defuzzifier converts inferred fuzzy actions into crisp output action.

Fuzzification

Fuzzification is the process where the crisp quantities are converted to fuzzy values. By identifying the uncertainties in the crisp values, the fuzzy values are formed. The conversion of fuzzy values is represented by membership functions. In any practical application, there may be error in the measured variable. This causes imprecision in the data. This imprecision may be

represented by membership functions. Thus, fuzzification process involves assigning membership functions to the fuzzy values. For example, speed of dc motor can be considered in several speed bands, identified as membership functions. The shape of universe of speed is shown in figure 1.2.

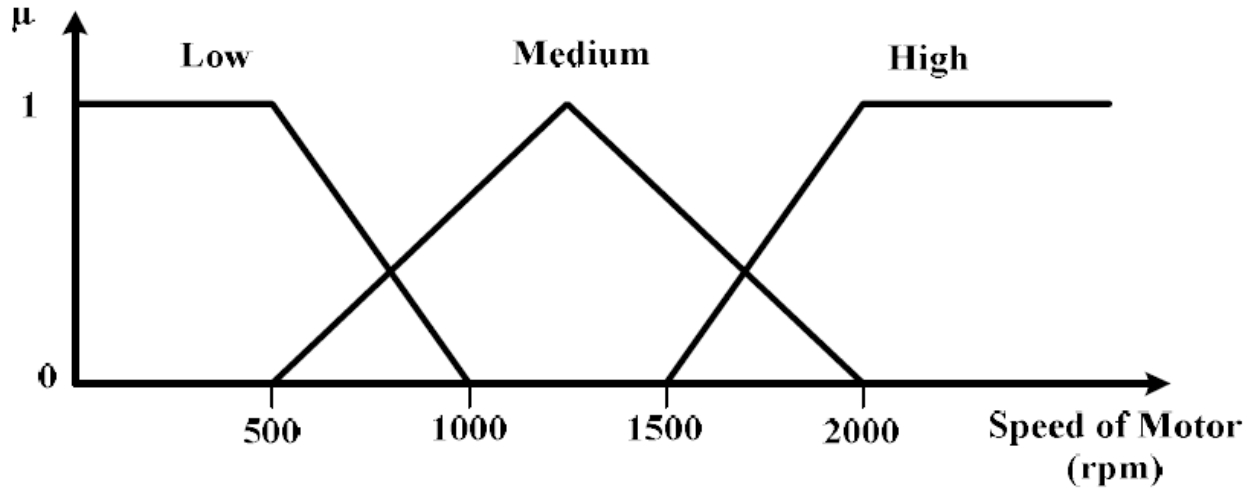

Figure 1.2 Membership function for Speed of motor [20]

The range of speed is classified into low, medium and high. The curves represent membership functions corresponding to various fuzzy variables. These curves differentiate the range of speed, decided by a certain person. Different persons can decide the range differently. The placements of curves are approximated over the universe of discourse. The number of curves and the overlapping of curves are important criteria to be considered while defining membership functions.

Defuzzification

The fuzzy results generated cannot be used as such to applications; hence it is necessary to convert fuzzy quantities to crisp quantities for further processing. Defuzzification is the process of making inferred fuzzy outputs to crisp value. It is the conversion of a fuzzy quantity to a precise quantity, just as fuzzification is the conversion of a precise quantity to a fuzzy quantity. The output of a fuzzy process can be the logical union of two or more fuzzy membership functions defined on the universe of discourse of the output variable. Defuzzification reduces the collection of membership functions to single sealed scalar quantity. Following are some of the methods for defuzzification:

- Max membership principle
- Centroid method

- Weighted average method
- Mean max membership

Among the above methods, Centroid method is the most widely used. It is also called center of gravity or center of mass method. It can be explained by the algebraic expression:

$$z^* = \frac{\int \mu_{C(z)}.zdz}{\int \mu_{C(z)}dz} \tag{1.1}$$

Where, $\mu_{C(z)}$ membership functions for fuzzy set C.

Figure 1.3 shows the graphical representation of the centroid method of defuzzification.

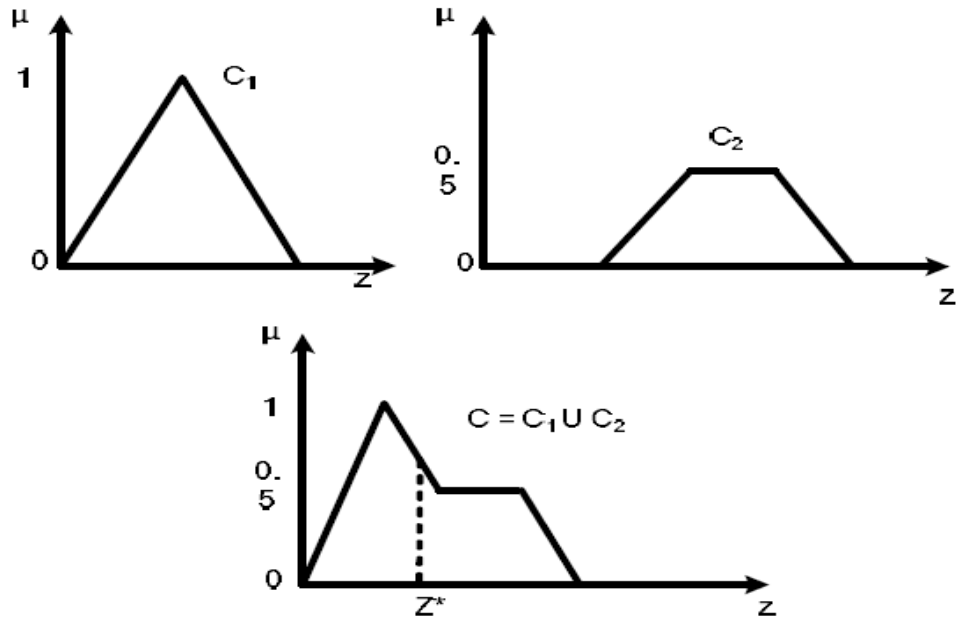

Figure 1.3 Centroid method of defuzzification

Fuzzy Inference System

Fuzzy inference systems (FISs) are also known as fuzzy rule-based systems. Fuzzy inference system consists of a rule base, a database and a decision-making unit. Rule base consists of a number of If-Then rules. Database defines the membership functions of the fuzzy sets used in the fuzzy rules and the decision-making unit performs the inference operations on the rules. FIS formulates suitable rules and based upon the rules, the decision is made. This is based mainly on the concepts of fuzzy set theory, fuzzy IF-THEN rules and fuzzy reasoning.

The most important two types of fuzzy inference methods are:

- Mamdani fuzzy inference method

- Sugeno or Takagi-Sugeno-Kang method of fuzzy inference

The main difference between the two methods lies in the consequent of fuzzy rules. Mamdani method uses fuzzy sets as rule consequent whereas Sugeno method employs linear function of input variables as rule consequent. Mamdani inference expects the output membership functions to be fuzzy set whereas the Sugeno output membership functions are either constant or linear. In Sugeno method, a large number of fuzzy rules must be employed to approximate periodic or highly oscillatory functions. Sugeno controllers usually have far more adjustable parameters in the rule consequent and the number of parameters grows exponentially with increase in number of input variables.

Mamdani Inference Mechanism:

This method was introduced by Mamdani [21]. The concept of Mamdani inference mechanism can be explained with the help of an example explained in figure 1.4. There are two inputs, *x*0 and *y*0.

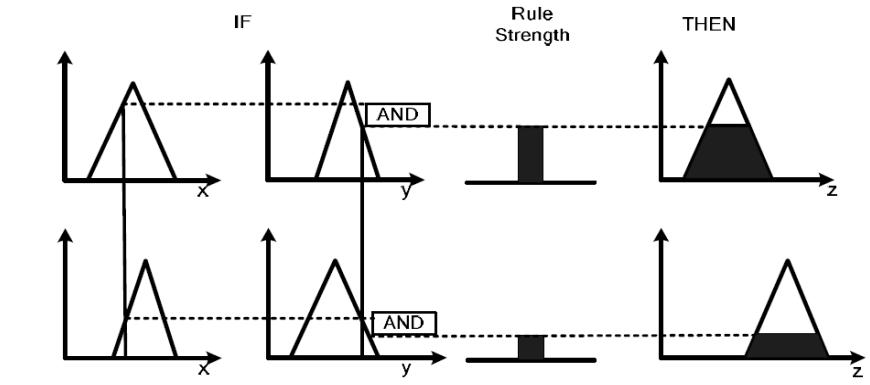

(a)

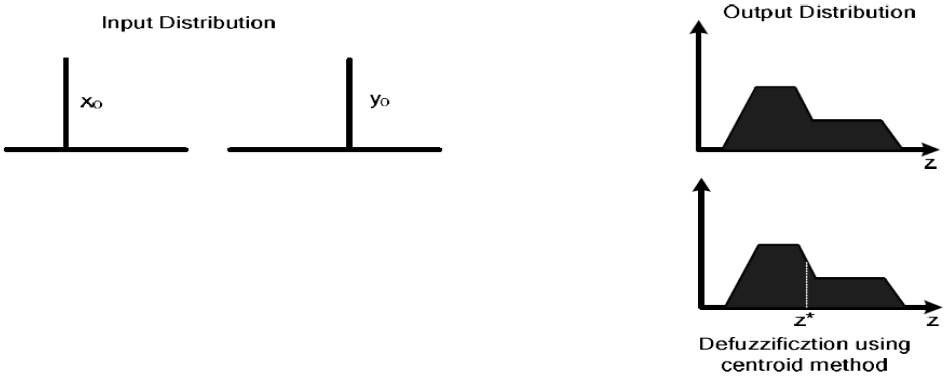

(b)

Figure 1.4 (a) & (b) Mamdani Inference Scheme [19]

These inputs are mapped into fuzzy numbers by assigning membership functions to them. The fuzzy "AND" is used to combine the membership functions to compute the rule strength. The outputs of all of the fuzzy rules are combined to obtain one fuzzy output distribution. This is usually, but not always, done by using the fuzzy "OR.". If it is desired to come up with a single crisp output from an FIS, it is obtained from the process of defuzzification.

Sugeno Inference Mechanism:

The Sugeno fuzzy model was proposed by Takagi, Sugeno, and Kang. A typical fuzzy rule in a Sugeno fuzzy model has the format "IF x is A and y is B THEN $z = f(x, y)$". Where A, B are fuzzy sets in the antecedent; $z = f(x, y)$ is a crisp function in the consequent. Usually $f(x, y)$ is a polynomial in the input variables *x* and *y*, but it can be any other function that can approximate the output within the fuzzy region specified by the antecedent of the rules. When f is constant, it is a zero order Sugeno fuzzy model. When f (x, y) is a first order polynomial, then it is first order Sugeno fuzzy model and so on. Figure 1.5 explains Sugeno inference mechanism with an example.

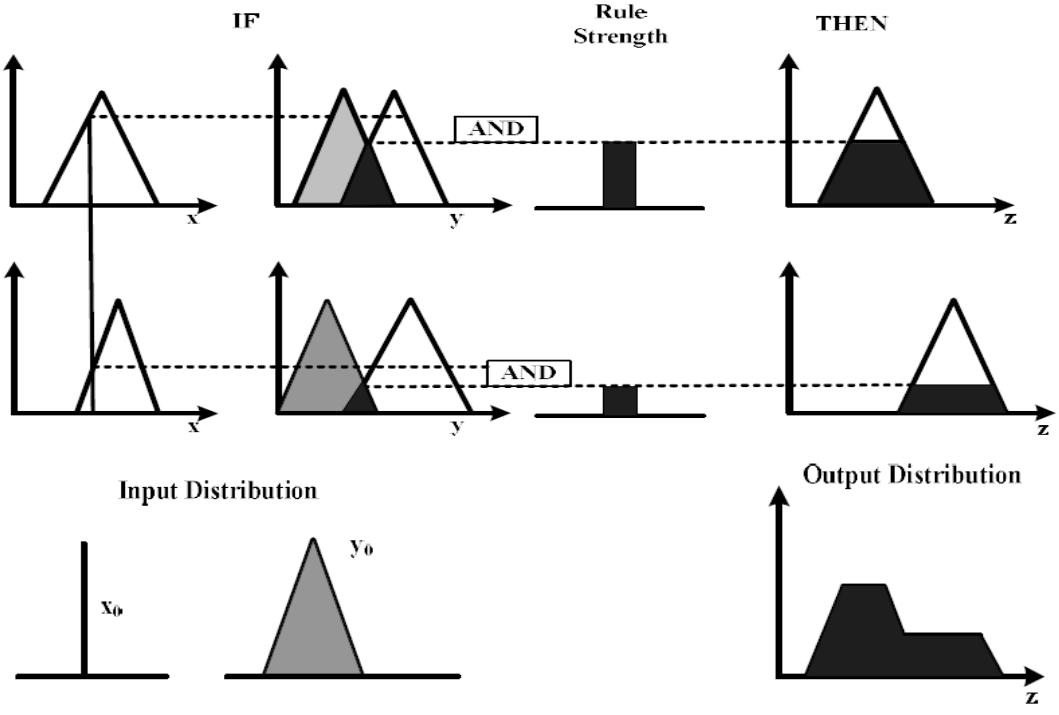

Figure 1.5 Sugeno Inference mechanism [19]

Advantages of Mamdani Method

- It is intuitive.
- It has widespread acceptance.

- It is well suited to human input.
- It is easy to form compared to Sugeno method.

Advantages of Sugeno Method

- It is computationally efficient and well suited to mathematical analysis
- It works well with linear techniques.
- It works well with optimization and adaptive techniques.
- It has guaranteed continuity of the output surface.

1.1.2. Fuzzy Logic Controller

Fuzzy logic controllers are used to reduce the development time or to improve the performance of an existing controller. Figure 1.6 shows the basic construction of a fuzzy logic controller. It consists of a fuzzification unit, a knowledge base and rule-based inference system and defuzzication unit.

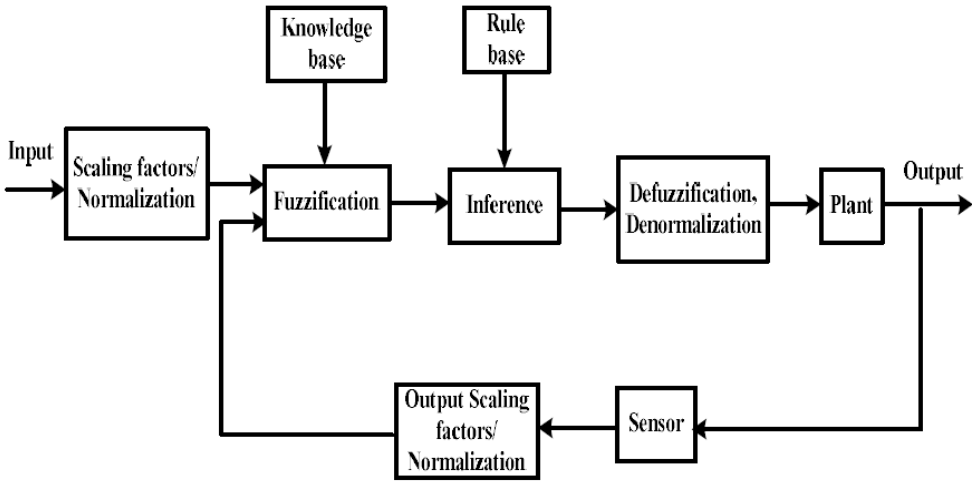

Figure 1.6 Fuzzy logic controller

Scaling factors map input/output values to the domain of fuzzy variables. The values of input scaling factors connect input values to suitable rules, and the values of output scaling factors adjust the amplitude of a control action.

Assumptions in a Fuzzy Control System Design

A number of assumptions are implicit in a fuzzy control system design. Following basic assumptions are commonly made whenever a fuzzy rule-based control policy is selected [22].

- The plant is observable and controllable: state, input, and output variables are usually available for observation and measurement or computation.

- There exists a body of knowledge comprised of a set of linguistic rules, engineering common sense, intuition, or a set of input – output measurements data from which rules can be extracted.
- A solution exists.
- The control engineer is looking for a ‘‘good enough’’ solution, not necessarily the optimum one.
- The controller will be designed within an acceptable range of precision.

1.2. Statement of the Problem

Mobile robots are increasingly designed today and are used in a variety of different applications, including pick and place, material handling and packaging. Wheeled robots are more energy efficient, tend to have a simpler mechanical structure, as well as simpler dynamics compared to that required by legged robots to make contact with the ground and provide a driving force. Robots with at least three wheels can achieve static stability, further simplifying dynamics. The inverted pendulum system is naturally unstable. Therefore, a suitable control system technique and method needs to be investigated to control the system. The two-wheel balancing robot is an application of the inverted pendulum that requires a controller to maintain its upright position. To achieve this, a controller needs to be designed and implement on the robot to balance and stabilize the inverted pendulum. The robot is inherently unstable and without external control it would roll around the wheels rotation axis and eventually fall, and various types of controllers were implemented on two wheeled balancing robots. The controller is used to balance and stabilizing the system (TWMPPRM).

1.3. Objective of the Thesis

1.3.1. General Objective

The general objective of this thesis is to design and simulate Fuzzy-PID based control of self-balanced two wheeled mobile pick and place robot manipulator (TWMPPRM) using MATLAB /SIMULINK software.

1.3.2. Specific Objective

Specifically, the core objectives of the research are:

- To develop the mathematical models of the self-balanced TWMPPRM.
- To design and simulate Fuzzy-PID controller for self-balanced TWMPPRM using MATLAB Simulink.

- To analyze and compare the performance of Fuzzy-PID for self-balanced TWMPPRM with conventional PID controller.

1.4. Significance of the research

Presently, in Ethiopia (chemical manufacturing factories), the focus given to the use of mobile robots in many applications is minimal. This is mainly due to the fact that such vehicles are just thought as luxury and of no use in the country. However, applications such as pick and place certain object from place to place in hazardous product in chemical manufacturing industries. This is, consequently, where mobile robotics comes to fill the gap to satisfy the safety, huge manpower requirement, efficiency, and accuracy needs. Furthermore, this work will lay the foundation where future researchers and students gain experience and motivation, and the University will start building its name as one of the newly established technological research institutes.

1.5. Scope of the Thesis

In order to realize the objectives of the project, there are several scopes had been outlined. The scopes of the project are:

- Understanding the mobile manipulator control background, analyzing the problem and investigate Fuzzy-PID controller theory which has been applied to the mobile manipulator system.
- Apply the combination of Fuzzy-PID controller to the self-balanced TWMPPRM system.

The performance of the PID controller is to be compared with Fuzzy-PID in terms of controller performance index. MATLAB/Simulink is used to simulate the output performance of the robot.

1.6. Methodology

The proposed thesis first concentrated at study of the literatures about controller design and theoretical and structural backgrounds about mobile robot manipulator and controller. Then after we get a good understanding about mobile robot manipulator and controller from the reviewed literature, we have compared the performance various controller and then we have selected our technique which can remove the shortcoming of the proportional integral derivative controller. The dynamic analysis of self-balanced TWMPPRMs is introduced that enables handling a payload attached to the intermediate body (IB) in two mutually perpendicular directions. The second is the model of actuator dynamics of robot with some assumption. These actuators are

separately-excited DC motor. And finally, the overall nonlinear system model or mobile manipulator dynamic and actuator dynamics is developed. After the dynamic models have been developed, based on the Fuzzy-PID controller theory five degree of freedom self -balanced TWMPPRMs controllers are designed. The performance of the proposed method is tested by simulation using MATLAB/SIMULINK.

1.7. The Outlines of the thesis

This thesis is organized in to five chapters. The first chapter presents the overview of self-balanced TWMPPRM control mechanism, statement of the problem, objectives of the study, Significance of the study, Scope of the study, and applied methodology. Chapter two gives a historical background of Fuzzy-PID controller used to TWMPPRM and describes the principal working of them, then a literature review of previous studies in this field are presented. Chapter three focuses on Mathematical modeling of TWMPPRM, Proposed Control Design of TWMPPRM and Simulink model of overall system. Simulation and experimental results are presented and discussed in chapter four. Finally, chapter five presents conclusions and recommendations.

CHAPTER TWO

2. LITERATURE REVIEW

2.1. Introduction

Generally speaking, the most conventional widely known problems in the discipline of control, inverted pendulum (IP) systems are highly nonlinear and unstable systems that have been extensively investigated in the previous researchers. Different linear and nonlinear identification approaches are used to develop an accurate IP model. Recently, there has been much more interest in two-wheeled mobile pick and place robot manipulators (TWMPPRMs). A huge number of researchers are proposing various modeling and control methods that have been applied to both investigate and control these highly nonlinear systems, some of literatures are listed next.

2.2. Inverted pendulum-based systems

In a number of robotic laboratories around the world, the research on wheeled inverted pendulum (WIP) robots has significantly expanded.

Chinnadurai and Ranganathan [3] applied the idea of an inverted pendulum by developing a two-wheel self-supporting robot. This low power robot is equipped with an infrared (IR) sensor, an attitude sensor and a tilting camera. The robot can be controlled worldwide using the IOC (Internet-On-Chip) Controller.

Mayr et al. [6] took the idea of the inverted pendulum and developed a three-dimensional (3D) pendulum, also known as the inertia wheel cube (IWC), which has the form of a cube and is capable of balancing its edges and tip. Similar to the two-dimensional (2D) inverted pendulum systems, the IWC uses the reaction wheels for balancing purposes.

Lee et al. [7] focused on developing a new one-wheel inverted pendulum system that balances itself around its equilibrium position using air power. The roll angle was regulated by the air pressure from the ducted fans controlled by linear control approaches, while the pitch angle was controlled by the direct current (DC) motor.

Goher and Tokhi [8] also developed a novel configuration of wheeled robotic machines with an extended intermediate body (IB). The proposed system is equipped with a linear actuator to provide different lifting levels for the payload to be carried out. Given the fact that the designed wheeled robotic machine (WRM) provided an additional degree of freedom (DOF) through the

linear actuator connected to its IB, the workspace was still limited by the extension of the IB in a single vertical direction.

2.3. Control Strategies

Two wheeled robots are nonlinear systems; however, the most common controllers used in the literature are linear due to simple implementation process. New approaches in nonlinear control systems which have been encouraged by developments in neural network and fuzzy logic are used in this area. Many researchers have suggested that intelligent control approaches will improve the robustness and control stability for two wheeled robots and some have suggested hybrid control approaches. Some of literatures are listed next.

A large number of studies have been conducted to determine the optimal control method for the stabilization of different forms of underactuated IP.

Bettayeb et al. [9] proposed a novel controller concept based on pole placement fractional PI-state feedback to control an integer order system. The developed control method was applied to the proportional integral (PI)-cart system and illustrated satisfactory results in terms of robustness, stability and accuracy when applying external disturbances to the pendulum as well as varying cart masses.

Boussaada et al. [10] focused on the consideration of stabilization issues related to systems having multiple zero values at origin. A multi-delayed-proportional controller was proposed to overcome the problem. The controller was tested numerically on an IP on a horizontally moving cart. The simulation results of the study showed a major improvement in the efficiency of the closed loop system, taking into consideration noise measurements and/or system uncertainties.

Brisilla and Sankaranarayanan [11] presented a non-linear control strategy for maneuvering a four-degree freedom mobile inverted robotic pendulum system while stabilizing the pendulum. Using a nonlinear co-ordinate transformation that led to a three-step navigation design procedure, the controller was developed. Compared to the available control techniques, the developed controller does not require any switching between controllers and had shown good stability results.

Cui et al. [12] also proposed an adaptive backstepping control for a wheeled inverted pendulum model. The Lagrangian approach was utilized for deriving the nonlinear model and through a coordinate transformation, the system was divided into three sub-systems. The proposed control

method was applied to each subsystem. The simulation results showed that the proposed control was effective and that the output trajectory could be tracked as close as the reference trajectory.

Vinodh Kumar and Jerome [13] focused on developing a control strategy based on robust linear quadratic regulator (LQR) and proportional velocity (PV) controllers for the stabilization and trajectory of a single inverted pendulum. To swing the pendulum to an upright position, an energy-based PV controller was used. A robust LQR-stabilizer turns on immediately after the system reaches the vertical position to catch the pendulum and force it to track the predefined reference signal.

Prasad et al. [14] also used LQR and developed a simple approach comprising of a proportional-integral-derivative (PID) controller and LQR to control the inverted pendulum-cart dynamic system. The study of the response of the control schemes showed that the performance of the proposed PID+LQR control system was better than the PID control approach only.

Olivares and Albertos [15] studied several control methods for the control of a flywheel inverted pendulum, which is an under-actuated mechanical system. At first, a simple PID controller was tested, lead to an internally unstable controlled plant. In order to overcome the stability problem, two control options have been implemented and developed. These developed methods were an internal stabilizing controller and an observer-based state feedback control that replaced the PID controller.

Raffo et al. [16] also developed a non-linear H∞ controller for the stability of two wheeled self-balancing vehicles. The proposed controller takes into consideration the whole dynamics of the system in its structure, ensuring the stability of the closed loop system as a whole.

Yue et al. [17] proposed a new composite controller for a two-wheeled inverted pendulum vehicle with an unstable suspension, subject to a non-holonomic constraint. The developed control system consists of an adaptive sliding mode technique to generate an additional disturbance-like signal and a direct fuzzy controller that approximates the optimal velocity control effort of the adaptive mechanism.

Ali et al. [37] presented an Implementation and Design of Fuzzy Supervisory Controller for Mobile Robot Manipulator. In that paper, the range of the PID parameters is chosen by two ways: First, determine the optimal PID parameters, which is obtained previous using Artificial Bee Colony (ABC) optimization algorithm. Second, choose the range of the each parameter around the optimal value.

Liu et al. [38] presented Fuzzy PID Control of Space Manipulator for Both Ground Alignment and Space Applications. In that paper, the range of the PID parameters is chosen by a classical tuning technique such as Z-N method, The results proved that the self-tuning fuzzy PID control achieved better performance as compared with PID controller without fuzzy tuning.

Zhao et al. [39] presented Fuzzy gain scheduling of PID controllers. In that paper, proposed the uses of fuzzy rules and reasoning to determine the PID controller parameter and how to control it online.

2.4. Design of Fuzzy-PID controller

Conventional control techniques require linear and accurate modeling of the plant. In many cases, the plant becomes non-linear, so making a linear model becomes very complicated. Additionally, the system parameters may have some uncertainties that lead to imprecision. The conventional control techniques do not provide satisfactory performance for such cases. While, emerging intelligent techniques were developed, and extensively used to improve or replace conventional control techniques. Such intelligent techniques don't need an accurate model. Some of the techniques are:

- Fuzzy logic
- Neural Network
- Particle Swarm Optimization (PSO)
- Genetic Algorithm (GA)
- Ant Colony Optimization

Fuzzy logic is very popular among the above techniques and is extensively used. Fuzzy logic is easy to understand conceptually. It is tolerant of imprecise data and is based on expert experience. Fuzzy logic can model arbitrary complexity of nonlinear functions and can be coupled with conventional control techniques. Fuzzy control provides a convenient method for constructing non-linear controllers. While conventional controllers depend on the system model and parameter precision, Fuzzy Logic Controllers (FLCs) use a different approach to control system operation. Instead of using a system model, FLC works on the basis of heuristic knowledge and linguistic description to perform some task. This reduces the effect of inaccurate parameters and models because FLC does not require a system model.

We know that mobile manipulator has nonlinear dynamics, and even more the system parameters can vary. In general, it is difficult to find an accurate model of an actual mobile manipulator;

so, parameter values obtained from system identifications may only be approximate values. Although conventional cascade PID technique is widely used in trajectory control of mobile manipulators, it is not appropriate for non-linear systems or when complicated or unknown to the system model. With the help of Fuzzy logic, PID controllers can be made adaptive to improve performance.

2.4.1. Fuzzy-PID controller

The PID controller is mainly to adjust an appropriate proportional gain (KP), integral gain (KI), and differential gain (KD) to achieve the optimal control performance. Figure 2.1 shows a basic structure of PID controller.

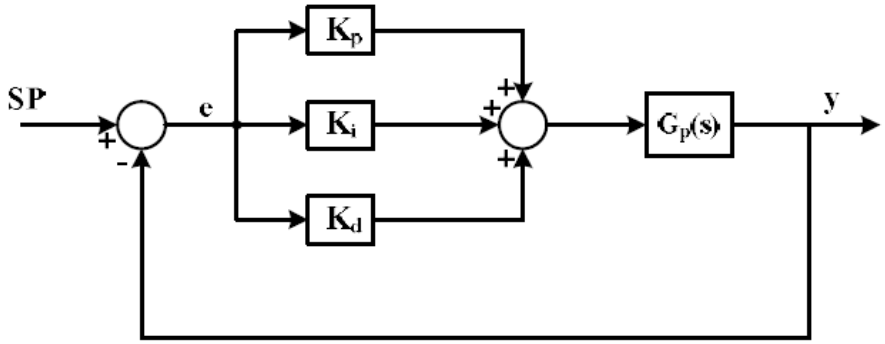

Figure 2.1 PID controller

PID controllers work efficiently with the linear system but for a non-linear system, the parameters of PID controller may not give satisfactory performance and therefore need to be tuned frequently. Fuzzy logic may be used to tune the parameters of a PID controller corresponding to the changes that may occur during the system operation or due to data imprecision or uncertainty or due to nonlinearity in behavior. Figure 2.2 shows the basic construction of a fuzzy-PID controller.

Steps involved in designing a Fuzzy-PID controller

Following steps are involved during the development of a fuzzy-PID controller:

- **Tuning of a crisp PID controller**

This is the first step involved in the development of a fuzzy-PID controller. The parameters of the PID controllers are tuned as it is done in the conventional controller. This can be done by Ziegler-Nichols method or any other tuning method.

- **Designing a linear fuzzy controller**

The first step in designing linear fuzzy controller involves identification of the input and output variables. Input variables are selected as: error between desired and actual values of output (e)

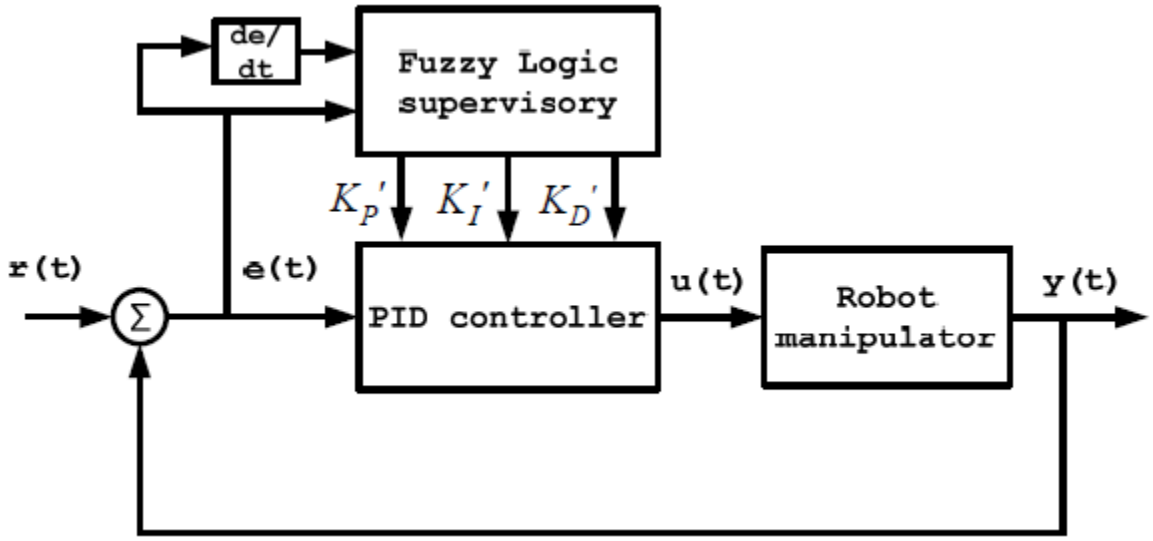

Figure 2.2 Fuzzy-PID controller [2]

and rate of change of error (ė) and output variables as incremental changes in gain parameters (ΔKP, ΔKI and ΔKD). The input and output variables are normalized by using appropriate scaling factors to map them in the domain of fuzzy variables. Universe of discourse of each variable is defined and linguistic label is assigned to each one. The linguistic variables defined in this study are shown in Table 2.1.

Table 2.1 Linguistic variables for fuzzy-PID controller

NL	NM	NS	ZE	PS	PM	PL
Negative Large	Negative Medium	Negative Small	Zero	Positive Small	Positive Medium	Positive Large

Once linguistic variables are defined, membership functions are assigned to them. Then a rule base is formed by assigning relationship between input and output. Then the inference method is chosen. In this study, Mamdani inference mechanism is considered for the development of the fuzzy-PID controller. The fuzzy output generated from the inference system is defuzzified to obtain a crisp value. Here, Centroid method is chosen for defuzzification. The output value is de-normalized by choosing appropriate scaling factor to adjust the amplitude of control action. The output from the fuzzy controller i.e. ΔKP, ΔKI and ΔKD are combined with the initial PID parameters to update them corresponding to the changes that occur during system operation.

CHAPTER THREE

3. MATHEMATICAL MODELING AND CONTROL SYSTEM DESIGN

3.1 System Description

The two-wheeled mobile pick and place robotic manipulator (TWMPPRM) contains all the main components, sensors and motors that the system consists of, and the design focuses on multiple features, including: a symmetrical mass distribution of entire parts and components of the robot at the initial position, the light weight without affecting the robot's stiffness in order to be able to carry the payload mass, and the compactness of the room for the system electronics and accessories.

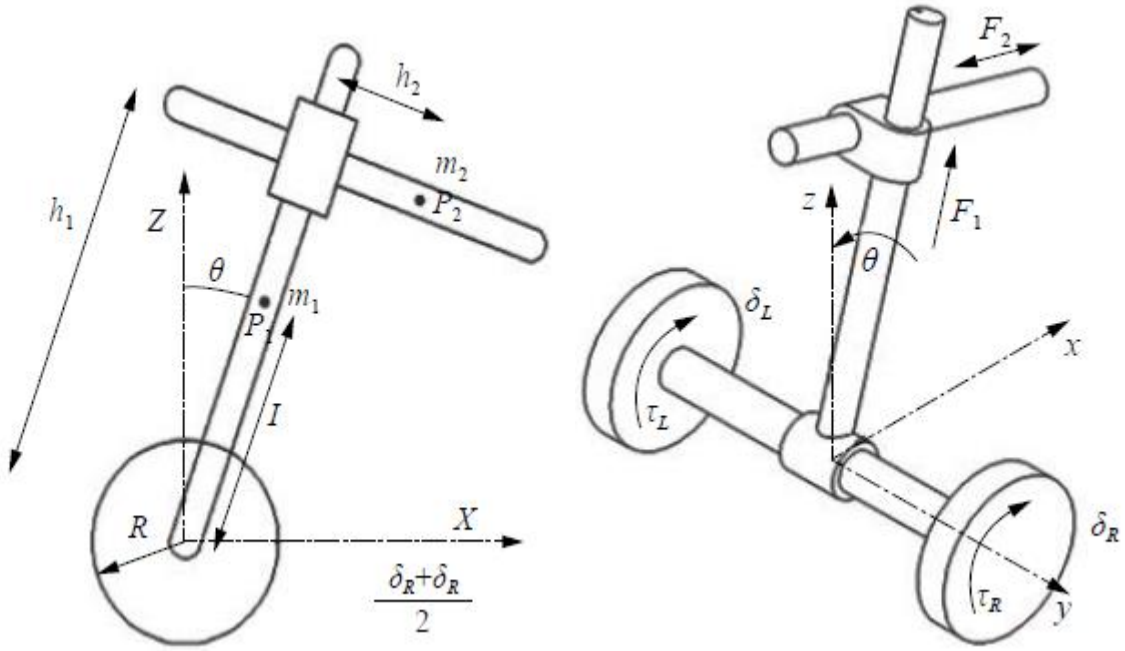

Figure 3.1 Schematic diagram of the system showing motion variables [16]

Referring to the figure 3.1, the system consists mainly of a chassis with a center of gravity at the point P_1 and a linear actuator mass with a center of gravity at the point P_2. P_1 and P_2 coordinates will change as long as the robot moves away from its initial location in the XY plane. The dynamics of the five DOF's TWMPPRM are fully described in these variables. The two motors attached to each wheel are responsible for providing the proper torque, τ_R and τ_L, and the other two motors are attached to the robot link, so the two-wheeled robot manipulator can be controlled.

The TWMPPRM uses two encoders and two potentiometers embedded in the wheel motors and linear actuator/motor to measure the system's position and velocity, and an accelerometer and a gyroscope to sense the body's angular tilt rate. The signals measured from these sensors allow the TWMPPRM control system to maintain the robot in a continuous upright position.

Advantages of using the proposed design with standard wheels over omnidirectional wheels

Different types of wheels are used for wheeled mobile robots, including: standard, castor and omni-directional wheels. The proposed design of this thesis uses two standard wheels driven by two DC motors. The advantages of the standard wheels used include simplicity in design and manufacturing, and relatively good reliability. The small size of the used wheels leads to better stability and a stronger grip on the floor. This adds to the stability and rigidity of the entire system when performing material handling tasks. The simple manufacturing process of standard wheels assures minimal positioning errors while moving.

Omnidirectional wheels are used in mobile robots conducting material handling tasks and other industrial applications, while mobile robots with omnidirectional wheels can be controlled with a reduced number of actuators and are highly maneuverable in narrow or crowded areas. Accuracy of motion is influenced by systematic errors caused by unavoidable errors in control and mechanical and non-systematic subsystems caused by unpredicted phenomenon such as wheel slippage and surface irregularities. Calibration would be required to compensate for these errors due to the use of omni-directional wheels. Certain odometry errors, while robot movements, can also occur due to unequal wheel diameters, misalignment of joints, backlash and slipping in encoder pulses [23]. Omnidirectional vehicles are widely used in mobile robots for logistics material handling applications. However, in general, they are designed for flat, smooth terrain motion and are not feasible for outdoor use [24]. Slippage is there when omnidirectional wheels are in motion and the manufacturing of these wheels is expensive and requires high accuracy. Additionally, there is poor efficiency since not all wheels rotate in the direction of motion, which causes friction loss, and are more computationally complex due to angle of motion calculations.

Description of the system DOFs

Just as shown in Figure 3.1, the proposed DOF system is characterized by four types of translations: the angular rotation of the right and left wheels δ_R and δ_L respectively, and the linear movement of the attached payload in vertical and horizontal directions h_1 and h_2,

respectively. The fifth DOF is represented by the IB tilt angle of the vertical Z axis, θ. Object pick and place, assembly lines, etc. are all applications that can be used with the new TWMPPRM configuration, particularly with applications that require limited space activity. In order for the robot to perform the pick-up and placement scenario, the description of the course of motion can be explained as follows:

1) The robot starts maneuvering on its two-wheels until it reaches the desired position to pick the target while maintaining its balance. At this point, the two control torque signals from the motors connected to the robot's wheels are the dominant control efforts.
2) The TWMPPRM linear actuators start the IB's extension process in the vertical direction up to the position of the object by displacing the vertical link (h_1). At this stage the vehicle's center of mass (COM) moves up and the operated wheels′ motors are responsible for maintaining a state of balance.
3) The linear actuator extends the end-effector in a lateral direction from the control system to the location of the target. As a result, the entire vehicle's COM changes its location and the wheels′ motors are responsible for producing the motor torque required to compensate for the COM's change of position. The TWMPPRM is most likely to experience a sudden disturbance caused by the object impact when picking the object. This disturbance can be resolved by wheel motors′ control signals.
4) The end-effector at this point undergoes a reverse motion back to its original position. In this course of motion, the vehicle's linear actuator should apply the required force signal with the appropriate speed in order to provide the TWMPPRM with safety against tipping over. The TWMPPRM needs to maintain balance based on the torque signals generated from the wheels′ motors.
5) Once the linear actuator rod returns to its original location, the IB robot starts moving down to the desired elevation to place the picked object in the assigned location. The control effort on the motor wheels increases as the COM gets closer to the chassis of the vehicle.
6) The end-effector of the vehicle extends until it reaches the desired place for positioning of the object. For the sake of adjusting the end-effector, maneuvering the entire TWMPPRM might be required to perform this task properly.

Table 3.1 shows the activation of each of the actuators of the TWMPPRM against each subtask for an object picking and placing motion scenario, as well as the degrees of freedom involved in each process. As can be seen, the motors connected to the wheels of the robot remain activated throughout the entire process as a result of the continuous change in the position of the COM, along with the external disturbances that occur during the picking and/or placing of the object. Both motors of the wheels require a sufficient torque signal to maintain the balance position (upright vertical position) of the TWMPPRM. The activating the linear actuators of robot will depend on the selected subtask. Switching mechanisms are developed as the main element of the control algorithms to evaluate the engagement time of each of the actuators in operation at the TWMPPRM.

Table 3.1 Engagement of individual actuators against subtasks

Ser.	Subtask	DOFs Associated	Right wheel Motor τ_R	Left wheel Motor τ_L	Linear actuator I F_1	Linear actuator II F_2
1	Moving to the picking place	$\delta_R, \delta_L, \theta$	✓	✓	X	X
2	Extension of the IB	$\delta_R, \delta_L, \theta, h_1$	✓	✓	✓	X
3	Extension of the end-effector	$\delta_R, \delta_L, \theta, h_2$	✓	✓	X	✓
4	Reverse motion of the end-effector	$\delta_R, \delta_L, \theta, h_2$	✓	✓	X	✓
5	Contraction of the IB	$\delta_R, \delta_L, \theta, h_1$	✓	✓	✓	X
6	Placing of the object	$\delta_R, \delta_L, \theta, h_2$	✓	✓	X	X

3.2 Mathematical modeling

The mathematical model of the mechanical system is used to analyze the different behavior of the model. There are a variety of methods used to derive the equations of motion. Based on the fact that it provides a powerful technique to derive any complicated motion equations from the system, the Lagrangian modeling approach is used to model the TWMPPRM. Use the TWMPPRM parameters listed in Table 3.2 and referring to the TWMPPRM schematic diagram in Figure 3.1, the mathematical model of the vehicle is derived in order to relate the kinematics of the mechanical system to the forces / torques applied to its links and to analyze the various behaviors of the model.

Regarding chassis–wheel, wheel–ground interaction and for the coulomb frictional model in the linear actuator, the friction on the mating surfaces was simplified. The coefficient values were selected according to the surface type. Under all vehicle and actuator working conditions, the selected constant values are assumed to be valid. This did not take into account variations in speed, configuration of the path, profile of the terrain etc. To validate the model of the system, the constant values were used. However, the modeling interactions between surfaces need to be examined for different surfaces, different terrain profiles and different vehicle operating conditions. The system equations of motion, details are provided in previous research that describes the system dynamics [25].

3.2.1. Deriving equations of motion

Based on the diagram indicated in Figure 3.1, linear Chassis Displacement COM, point P1, can be derived as shown in Eqns. 3.1, 3.2 and 3.3 along the X, Y and Z axes, respectively, as follows:

$$x_1 = \frac{R}{2}(\delta_R + \delta_L) + l\sin\theta \tag{3.1}$$

$$y_1 = \frac{R}{2}\left(\delta_R + \delta_L\right) + l\cos\theta \tag{3.2}$$

$$z_1 = l\cos\theta \tag{3.3}$$

Where for the lateral linear displacement point P_2 can be calculated as follows:

$$x_2 = h_1\sin\theta + h_2\cos\theta + \frac{R}{2}(\delta_R + \delta_L) \tag{3.4}$$

$$y_2 = \frac{R}{2}\left(\delta_R + \delta_L\right) + h_1 \cos\theta + h_2 \sin\theta \tag{3.5}$$

$$z_2 = h_1 \cos\theta - h_2 \sin\theta \tag{3.6}$$

3.2.2. Modeling using Lagrange formulation

Throughout this section, the lagrange formulation is used to derive model of the system, as it provides a powerful technique for obtaining motion equations. The general form of the Lagrange equation is defined as shown in the Eqn.3.7.

$$\frac{d}{dt}\left(\frac{\partial L}{\partial \dot{q}_i}\right) - \frac{\partial L}{\partial q_i} + \frac{\partial D}{\partial \dot{q}_i} = f_i \tag{3.7}$$

Where *L* represents the Lagrange equation and it is determined as:

$$L = T - U \tag{3.8}$$

Where, *T* and *U* are the total kinetic energies and potential energies of the system, respectively.

- q_i (i = 1, 2, . . ., n) are generalized coordinates such as: $q_i = [h_1 \quad h_2 \quad \theta \quad \delta_L \quad \delta_R]$
- f_i is generalized forces that contain all the given forces in the system acting along the coordinates such as: $f_i = [F_1 \quad F_2 \quad 0 \quad \tau_L \quad \tau_R]$
- D is the dissipation function and illustrated as: $D = \frac{1}{2} b q_i^2$

The chassis ' total kinetic energy can be calculated in the following way:

$$T_c = \frac{1}{2} m_1 (v_{x1}^2 + v_{y1}^2 + v_{z1}^2) + \frac{1}{2} m_2 (v_{x2}^2 + v_{y2}^2 + v_{z2}^2) + \frac{1}{2} J_1 \dot{\theta}^2 + \frac{1}{2} J_2 \dot{\theta}^2 \tag{3.9}$$

Where,

$$v_{x1} = \frac{1}{2} v_R + \frac{1}{2} v_L + l\dot{\theta} \cos\theta \tag{3.10}$$

$$v_{y1} = \frac{1}{2} v_R + \frac{1}{2} v_L + l\dot{\theta} \sin\theta \tag{3.11}$$

$$v_{z1} = -l\dot{\theta} \sin\theta \tag{3.12}$$

$$v_{x2} = \dot{h}_1 \sin\theta + h_1 \dot{\theta} \cos\theta + \dot{h}_2 \cos\theta - h_2 \dot{\theta} \sin\theta + \frac{1}{2} v_R + \frac{1}{2} v_L \tag{3.13}$$

$$v_{y2} = \frac{1}{2} v_R + \frac{1}{2} v_L + \dot{h}_1 \cos\theta - h_1 \dot{\theta} \sin\theta + \dot{h}_2 \sin\theta + h_2 \dot{\theta} \cos\theta \tag{3.14}$$

$$v_{z2} = \dot{h}_1 \cos\theta - h_1 \dot{\theta} \sin\theta - \dot{h}_2 \sin\theta - h_2 \dot{\theta} \cos\theta \tag{3.15}$$

$$v_L = R\dot{\delta}_L \tag{3.16}$$

$$v_R = R\dot{\delta}_R \tag{3.17}$$

Calculate the total kinetic energy per wheel as follows:

$$T_w = \frac{1}{2} m_w v_R^2 + \frac{1}{2} m_w v_L^2 + \frac{1}{2} J_w (\frac{v_R^2}{R^2}) + \frac{1}{2} J_w (\frac{v_L^2}{R^2}) \tag{3.18}$$

The total kinetic energy of the chassis and wheels can be calculated as follows:

$$T = T_c + T_w \tag{3.19}$$

The total potential energy of the chassis and wheels can be calculated as follows:

$$U = m_1 gl\cos\theta + m_2 g(h_1\cos\theta - h_2\sin\theta) \tag{3.20}$$

The total dissipation power of the chassis and wheels can be calculated as follows:

$$D = \frac{1}{2}\mu_1\dot{h}_1^2 + \frac{1}{2}\mu_2\dot{h}_2^2 + \frac{1}{2}\mu_w(v_R^2 + v_L^2) + \frac{1}{2}\mu_c(v_R^2 + v_L^2) \tag{3.21}$$

Substituting Eqns. 3.19 and 3.20 in Eqn. 3.8, the Lagrange equation can be expressed as follows:

$$\begin{aligned} L = {} & \frac{1}{2} m_1 (v_{x1}^2 + v_{y1}^2 + v_{z1}^2) + \frac{1}{2} m_2 (v_{x2}^2 + v_{y2}^2 + v_{z2}^2) \\ & + \frac{1}{2} J_1 \dot{\theta}^2 + \frac{1}{2} J_2 \dot{\theta}^2 + \frac{1}{2} m_w (v_R^2 + v_L^2) \\ & \frac{1}{2} J_w (\frac{v_R^2 + v_L^2}{R^2}) - m_1 gl\cos\theta - m_2 g(h_1\cos\theta - h_2\sin\theta) \end{aligned} \tag{3.22}$$

Deriving the equation for h_1 :

$$\begin{aligned} & \frac{1}{2} m_2 (2g\cos\theta - 2h_1\dot{\theta}^2 - 4\dot{h}_2\dot{\theta} - 2h_2\ddot{\theta} + 2\ddot{h}_1 \\ & + R(\ddot{\delta}_R + \ddot{\delta}_L)\sin\theta) = F_1 - \mu_1\dot{h}_1 \end{aligned} \tag{3.23}$$

Deriving the equation for h_2 :

$$\begin{aligned} & \frac{1}{2} m_2 (2g\sin\theta + 2h_2\dot{\theta}^2 - 4\dot{h}_1\dot{\theta} - 2h_1\ddot{\theta} - 2\ddot{h}_2 \\ & - R(\ddot{\delta}_R + \ddot{\delta}_L)\cos\theta) = F_2 - \mu_2\dot{h}_2 \end{aligned} \tag{3.24}$$

Deriving the equation for δ_L :

$$\begin{aligned}
&\frac{1}{2}m_1(\frac{R}{2}\ddot{\delta}_R+\frac{R}{2}\ddot{\delta}_L-l\dot{\theta}^2\sin\theta+l\ddot{\theta}\cos\theta)\\
&+\frac{1}{2}m_2(\ddot{h}_1\sin\theta+2\dot{h}_1\dot{\theta}\cos\theta-h_1\dot{\theta}^2\sin\theta+h_1\ddot{\theta}\cos\theta\\
&+\ddot{h}_2\cos\theta-2\dot{h}_2\dot{\theta}\sin\theta-h_2\dot{\theta}^2\cos\theta\\
&-h_2\ddot{\theta}\sin\theta+\frac{R}{2}\ddot{\delta}_R+\frac{R}{2}\ddot{\delta}_L)+2m_wR\ddot{\delta}_L+2J_w\frac{\ddot{\delta}_L}{R}\\
&=\tau_L-R(\mu_w+\mu_c)\dot{\delta}_L
\end{aligned}\tag{3.25}$$

Deriving the equation for δ_R:

$$\begin{aligned}
&\frac{1}{2}m_1(\frac{R}{2}\ddot{\delta}_R+\frac{R}{2}\ddot{\delta}_L-l\dot{\theta}^2\sin\theta+l\ddot{\theta}\cos\theta)\\
&+\frac{1}{2}m_2(\ddot{h}_1\sin\theta+2\dot{h}_1\dot{\theta}\cos\theta-h_1\dot{\theta}^2\sin\theta+h_1\ddot{\theta}\cos\theta\\
&+\ddot{h}_2\cos\theta-2\dot{h}_2\dot{\theta}\sin\theta-h_2\dot{\theta}^2\cos\theta\\
&-h_2\ddot{\theta}\sin\theta+\frac{R}{2}\ddot{\delta}_R+\frac{R}{2}\ddot{\delta}_L)+2m_wR\ddot{\delta}_R+2J_w\frac{\ddot{\delta}_R}{R}=\tau_R-R(\mu_w+\mu_c)\dot{\delta}_R
\end{aligned}\tag{3.26}$$

Deriving the equation for θ:

$$\begin{aligned}
&2m_2\dot{\theta}\left(\dot{h}_2h_2+\dot{h}_1h_1\right)+\frac{1}{2}m_2R\left(h_1\cos\theta-h_2\sin\theta\right)\left(\ddot{\delta}_R+\ddot{\delta}_L\right)+\frac{1}{2}m_1lR\cos\theta\left(\ddot{\delta}_R+\ddot{\delta}_L\right)\\
&-m_2g\left(h_1\sin\theta+h_2\cos\theta\right)+\ddot{\theta}\left(J_1+J_2+m_1l^2+m_2h_2^2+m_2h_1^2\right)\\
&+m_2\left(\ddot{h}_2h_1+\ddot{h}_1h_2\right)-m_1gl\sin\theta=0
\end{aligned}\tag{3.27}$$

Equations (3.23–3.27) represent the differential equations of the nonlinear second order which describe the dynamics of the system under consideration.

State space modeling

To linearize the system, a point of equilibrium at the vertical upright position is considered. This is applied when the angle of inclination (tilt angle) approaches a zero value. We can rewrite the system equations of motion as follows:

$$\frac{1}{2}m_2\left(2g-4\dot{h}_2\dot{\theta}-2h_2\ddot{\theta}+2\ddot{h}_1+R\left(\ddot{\delta}_R+\ddot{\delta}_L\right)\theta\right)=F_1-\mu_1\dot{h}_1\tag{3.28}$$

$$\frac{1}{2}m_2\left(2g\theta-4\dot{h}_1\dot{\theta}-2h_1\ddot{\theta}-2\ddot{h}_2-R(\ddot{\delta}_R+\ddot{\delta}_L)\right)=F_2-\mu_2\dot{h}_2\tag{3.29}$$

$$\frac{1}{2}m_1\left(\frac{R}{2}\ddot{\delta}_R+\frac{R}{2}\ddot{\delta}_L+l\ddot{\theta}\right)+$$
$$\frac{1}{2}m_2\left(\ddot{h}_1\theta+2\dot{h}_1\dot{\theta}+h_1\ddot{\theta}+\ddot{h}_2-2\dot{h}_2\dot{\theta}\theta-h_2\ddot{\theta}\theta+\frac{R}{2}\ddot{\delta}_R+\frac{R}{2}\ddot{\delta}_L\right) \tag{3.30}$$
$$+2m_w\ddot{\delta}_L+2J_w\frac{\ddot{\delta}_L}{R}=\tau_L-R(\mu_w+\mu_c)\dot{\delta}_L$$

$$\frac{1}{2}m_1\left(\frac{R}{2}\ddot{\delta}_R+\frac{R}{2}\ddot{\delta}_L+l\ddot{\theta}\right)+$$
$$\frac{1}{2}m_2\left(\ddot{h}_1\theta+2\dot{h}_1\dot{\theta}+h_1\ddot{\theta}+\ddot{h}_2-2\dot{h}_2\dot{\theta}\theta-h_2\ddot{\theta}\theta+\frac{R}{2}\ddot{\delta}_R+\frac{R}{2}\ddot{\delta}_L\right) \tag{3.31}$$
$$+2m_wR\ddot{\delta}_R+2J_w\frac{\ddot{\delta}_R}{R}=\tau_R-R(\mu_w+\mu_c)\dot{\delta}_R$$

$$2m_2\dot{\theta}\left(\dot{h}_2h_2+\dot{h}_1h_1\right)+\frac{1}{2}m_2R\left(h_1-h_2\theta\right)\left(\ddot{\delta}_R+\ddot{\delta}_L\right)+\frac{1}{2}m_1lR\left(\ddot{\delta}_R+\ddot{\delta}_L\right)$$
$$-m_2g\left(h_1\theta+h_2\right)+\ddot{\theta}\left(J_1+J_2+m_1l^2+m_2h_2^2+m_2h_1^2\right) \tag{3.32}$$
$$+m_2\left(\ddot{h}_2h_1+\ddot{h}_1h_2\right)-m_1gl\theta=0$$

Then, as shown in the following equation, the dynamics of the five DOFs robot can be represented by ten state vectors X of the dynamic system:

$$X=\begin{bmatrix}\delta_R & \delta_L & \theta & h_1 & h_2 & \dot{\delta}_R & \dot{\delta}_L & \dot{\theta} & \dot{h}_1 & \dot{h}_2\end{bmatrix} \tag{3.33}$$

Where the variables on the state vector can be identified as follows:

- Right wheel angular displacement, δ_R
- Left wheel angular displacement, δ_L
- Chassis pitch angle, θ
- Vertical linear link displacement, h_1
- Horizontal linear link displacement, h_2
- Right wheel velocity, $\dot{\delta}_R$
- Left wheel velocity, $\dot{\delta}_L$
- Chassis angular velocity, $\dot{\theta}$
- Vertical linear link velocity, $\dot{h}_1$

Table 3.2 TWMPPRM parameters associated with their description

Terminology	Description	Unit
θ	Tilt angle of the intermediate body around the vertical Z axis	◦
δ_R, δ_L	Angular displacement of right and left wheels	Rad
h_1	Vertical linear link displacement	M
h_2	Horizontal linear link displacement	M
F_1	Force generated by the vertical linear actuator	N
F_2	Force generated by the horizontal linear actuator	N
τ_R, τ_L	Right and left wheels torque per meter	N
m_1	Mass of the chassis	Kg
m_2	Mass of the linear actuators	Kg
m_w	Mass of wheel	Kg
R	Wheel radius	M
J_1	Chassis moment of inertia	$kg.m^2$
J_2	Moving mass moment of inertia	$kg.m^2$
J_w	Wheel moment of inertia	$kg.m^2$
l	Distance of chassis′ center of mass for wheel axle	M
μ_1	Coefficient of friction of vertical linear actuator	Ns/m
μ_2	Coefficient of friction of horizontal linear Actuator	Ns/m
μ_w	Coefficient of friction between wheel and ground	Ns/m
μ_c	Coefficient of friction between chassis and wheel	Ns/m
g	Gravitational acceleration	m/s^2

- Horizontal linear link velocity, $\dot{h}_2$

State variables of wheel velocity, angular velocity and linear link velocity derive from link displacements, links linear displacements and pitch angle, respectively, which can be formulated as follows:

$$X_1 = \delta_R \tag{3.34}$$

$$X_2 = \delta_L \tag{3.35}$$

$$X_3 = \theta \tag{3.36}$$

$$X_4 = h_1 \tag{3.37}$$

$$X_5 = h_2 \tag{3.38}$$

$$X_6 = \dot{X}_1 = \dot{\delta}_R \tag{3.39}$$

$$X_7 = \dot{X}_2 = \dot{\delta}_L \tag{3.40}$$

$$X_8 = \dot{X}_3 = \dot{\theta} \tag{3.41}$$

$$X_9 = \dot{X}_4 = \dot{h}_1 \tag{3.42}$$

$$X_{10} = \dot{X}_5 = \dot{h}_2 \tag{3.43}$$

The System input variables are as follows:

$$u_1 = \tau_R \tag{3.44}$$

$$u_2 = \tau_L \tag{3.45}$$

$$u_3 = F_1 \tag{3.46}$$

$$u_4 = F_2 \tag{3.47}$$

Where,

- τ_R and τ_L Are the torques needed for both right and left wheels,
- F1 and F2 are linear force generated by the linear actuator to move the payload vertically and horizontally, respectively.

$$\begin{bmatrix} \dot{X}_1 \\ \dot{X}_2 \\ \dot{X}_3 \\ \dot{X}_4 \\ \dot{X}_5 \\ \dot{X}_6 \\ \dot{X}_7 \\ \dot{X}_8 \\ \dot{X}_9 \\ \dot{X}_{10} \end{bmatrix} = \begin{bmatrix} A_{11} & A_{12} & A_{13} & A_{14} & A_{15} & A_{16} & A_{17} & A_{18} & A_{19} & A_{110} \\ A_{21} & A_{22} & A_{23} & A_{24} & A_{25} & A_{26} & A_{27} & A_{28} & A_{29} & A_{210} \\ A_{31} & A_{32} & A_{33} & A_{34} & A_{35} & A_{36} & A_{37} & A_{38} & A_{39} & A_{310} \\ A_{41} & A_{42} & A_{43} & A_{44} & A_{45} & A_{46} & A_{47} & A_{48} & A_{49} & A_{410} \\ A_{51} & A_{52} & A_{53} & A_{54} & A_{55} & A_{56} & A_{57} & A_{58} & A_{59} & A_{510} \\ A_{61} & A_{62} & A_{63} & A_{64} & A_{65} & A_{66} & A_{67} & A_{68} & A_{69} & A_{610} \\ A_{71} & A_{72} & A_{73} & A_{74} & A_{75} & A_{76} & A_{77} & A_{78} & A_{79} & A_{710} \\ A_{81} & A_{82} & A_{83} & A_{84} & A_{85} & A_{86} & A_{87} & A_{88} & A_{89} & A_{810} \\ A_{91} & A_{92} & A_{93} & A_{94} & A_{95} & A_{96} & A_{97} & A_{98} & A_{99} & A_{910} \\ A_{101} & A_{102} & A_{103} & A_{104} & A_{105} & A_{106} & A_{107} & A_{108} & A_{109} & A_{1010} \end{bmatrix} \begin{bmatrix} X_1 \\ X_2 \\ X_3 \\ X_4 \\ X_5 \\ X_6 \\ X_7 \\ X_8 \\ X_9 \\ X_{10} \end{bmatrix} + \begin{bmatrix} B_{11} & B_{12} & B_{13} & B_{14} \\ B_{21} & B_{22} & B_{23} & B_{24} \\ B_{31} & B_{32} & B_{33} & B_{34} \\ B_{41} & B_{42} & B_{43} & B_{44} \\ B_{51} & B_{52} & B_{53} & B_{54} \\ B_{61} & B_{62} & B_{63} & B_{64} \\ B_{71} & B_{72} & B_{73} & B_{74} \\ B_{81} & B_{82} & B_{83} & B_{84} \\ B_{91} & B_{92} & B_{93} & B_{94} \\ B_{101} & B_{102} & B_{103} & B_{104} \end{bmatrix} \begin{bmatrix} u_1 \\ u_2 \\ u_3 \\ u_4 \end{bmatrix} \tag{3.48}$$

where, A, B, C and D matrices are shown as follows:

$$A = \begin{bmatrix} 0 & 0 & 0 & 0 & 0 & 1 & 0 & 0 & 0 & 0 \\ 0 & 0 & 0 & 0 & 0 & 0 & 1 & 0 & 0 & 0 \\ 0 & 0 & 0 & 0 & 0 & 0 & 0 & 1 & 0 & 0 \\ 0 & 0 & 0 & 0 & 0 & 0 & 0 & 0 & 1 & 0 \\ 0 & 0 & 0 & 0 & 0 & 0 & 0 & 0 & 0 & 1 \\ 0 & 0 & A_{63} & 0 & A_{65} & A_{66} & A_{67} & 0 & 0 & A_{610} \\ 0 & 0 & A_{73} & 0 & A_{75} & A_{76} & A_{77} & 0 & 0 & A_{710} \\ 0 & 0 & A_{83} & 0 & A_{85} & A_{86} & A_{87} & 0 & 0 & A_{810} \\ 0 & 0 & 0 & A_{94} & 0 & 0 & 0 & 0 & 0 & 0 \\ 0 & 0 & A_{103} & 0 & A_{105} & A_{106} & A_{107} & 0 & 0 & A_{1010} \end{bmatrix} B = \begin{bmatrix} 0 & 0 & 0 & 0 \\ 0 & 0 & 0 & 0 \\ 0 & 0 & 0 & 0 \\ 0 & 0 & 0 & 0 \\ 0 & 0 & 0 & 0 \\ B_{61} & B_{62} & 0 & B_{64} \\ B_{71} & B_{72} & 0 & B_{74} \\ B_{81} & B_{82} & 0 & B_{84} \\ 0 & 0 & B_{93} & 0 \\ B_{101} & B_{102} & B_{103} & B_{104} \end{bmatrix}$$

$$C = \begin{bmatrix} 1 & 0 & 0 & 0 & 0 & 0 & 0 & 0 & 0 & 0 \\ 0 & 1 & 0 & 0 & 0 & 0 & 0 & 0 & 0 & 0 \\ 0 & 0 & 1 & 0 & 0 & 0 & 0 & 0 & 0 & 0 \\ 0 & 0 & 0 & 1 & 0 & 0 & 0 & 0 & 0 & 0 \\ 0 & 0 & 0 & 0 & 1 & 0 & 0 & 0 & 0 & 0 \end{bmatrix} D = \begin{bmatrix} 0 & 0 & 0 & 0 \\ 0 & 0 & 0 & 0 \\ 0 & 0 & 0 & 0 \\ 0 & 0 & 0 & 0 \\ 0 & 0 & 0 & 0 \end{bmatrix}$$

And finally, the state space model of the system can be formulated as follows:

$$X = \begin{bmatrix} 0 & 0 & 0 & 0 & 0 & 1 & 0 & 0 & 0 & 0 \\ 0 & 0 & 0 & 0 & 0 & 0 & 1 & 0 & 0 & 0 \\ 0 & 0 & 0 & 0 & 0 & 0 & 0 & 1 & 0 & 0 \\ 0 & 0 & 0 & 0 & 0 & 0 & 0 & 0 & 1 & 0 \\ 0 & 0 & 0 & 0 & 0 & 0 & 0 & 0 & 0 & 1 \\ 0 & 0 & A_{63} & 0 & A_{65} & A_{66} & A_{67} & 0 & 0 & A_{610} \\ 0 & 0 & A_{73} & 0 & A_{75} & A_{76} & A_{77} & 0 & 0 & A_{710} \\ 0 & 0 & A_{83} & 0 & A_{85} & A_{86} & A_{87} & 0 & 0 & A_{810} \\ 0 & 0 & 0 & A_{94} & 0 & 0 & 0 & 0 & 0 & 0 \\ 0 & 0 & A_{103} & 0 & A_{105} & A_{106} & A_{107} & 0 & 0 & A_{1010} \end{bmatrix} \begin{bmatrix} \delta_R \\ \delta_L \\ \theta \\ h_1 \\ h_2 \\ \dot{\delta}_R \\ \dot{\delta}_L \\ \dot{\theta} \\ \dot{h}_1 \\ \dot{h}_2 \end{bmatrix} + \begin{bmatrix} 0 & 0 & 0 & 0 \\ 0 & 0 & 0 & 0 \\ 0 & 0 & 0 & 0 \\ 0 & 0 & 0 & 0 \\ 0 & 0 & 0 & 0 \\ B_{61} & B_{62} & 0 & B_{64} \\ B_{71} & B_{72} & 0 & B_{74} \\ B_{81} & B_{82} & 0 & B_{84} \\ 0 & 0 & B_{93} & 0 \\ B_{101} & B_{102} & B_{103} & B_{104} \end{bmatrix} \begin{bmatrix} \tau_R \\ \tau_L \\ F_1 \\ F_2 \end{bmatrix} \tag{3.49}$$

Constants A and B in Eqs. 3.48 and 3.49 are described in the "Appendix A" at the end of the thesis.

3.3. Actuators Dynamics of Robot

DC motors are commonly used in robotic applications and are the main types of actuators used in mobile robots. Consequently, it is important to analyze and integrate their dynamics into the robot model. There are two classes of DC motors: Filed-Current Controlled and Armature-Current Controlled. In a Field-Current Controlled motor, the armature current $\dot{i}_a$ is kept constant while the field-current is controlled using field voltage V_f commands.

On the other hand, in a Armature-Current Controlled motor, the armature voltage V_a is the command to control the armature current while keeping the field-current i_f constant. Armature-current controlled DC motors are more common choice in mobile robots.

It is modeled as circuit with resistance and inductance connected in series. The input voltage $v_a(t)$ is the voltage supplied by amplifier to move the motor. The back EMF voltage $v_b(t)$ is induced by the rotation of the armature windings in the fixed magnetic field. To derive the transfer function of the DC motor, the system is divided into three major components of equation: electrical equation, mechanical equation, and electro-mechanical equation [26].

The differential equation (electrical equation) for the equivalent circuit can be derived by applying the Kirchhoff voltage laws around the electrical loop. Kirchhoff's voltage law states that, the sum of all voltages around the loop must be equal to zero, or

$$v_a - v_{Ra} - v_{La} - v_b(t) = 0 \tag{3.50}$$

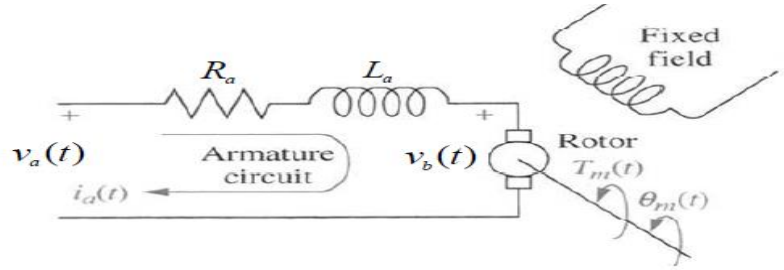

Figure 3.2 Electrical Representation of Separately excited DC motor [27].

According to Ohm's law, the voltage across the resistor can be represented as:

$$v_{Ra} = i_a R_a \tag{3.51}$$

Where, i_a is the armature current.

The voltage across the inductor is proportional to the current change through the coil with respect to time and can be written as:

$$v_{La} = L_a \frac{d}{dt} i_a \tag{3.52}$$

Where, La is the inductance of the armature coil. Finally, the back emf can be written as:

$$v_b(t) = k_b \omega_m \tag{3.53}$$

Where k_b is the velocity constant, determined by the flux density of the permanent magnets, the reluctance of the iron core of the armature, and the number of turns of the armature winding. ω is the rotational velocity of the armature.

Substituting eqns. (3.51), (3.52), and (3.53) into eqn. (3.50) gives the following differential equation:

$$v_a - i_a R_a - L_a \frac{d}{dt} i_a - k_b \omega_m = 0 \tag{3.54}$$

Mechanical Characteristics

On the other side, the mechanical equation (Newton low of motion) is obtained as follows:

$$\tau_m(t) = J_m \frac{d^2\theta(t)}{dt^2} + B_m \frac{d\theta(t)}{dt} = J_m \ddot{\theta}(t) + B_m \dot{\theta}(t) \tag{3.55}$$

Where, τ_m is the motor torque produced by the motor shaft, J_m and B_m are denoted as the moment of inertia and motor friction coefficient.

Based on the previous two equations (3.54) and (3.55), when the input voltage $v_a(t)$,is applied, the armature current $i_a(t)$ goes through resistance R_a and inductance L_a producing magnetic flux and causing the motion of the rotor according to the motor torque as illustrated in equation (3.56).

$$\tau_m(t) = K_t i_a(t) \tag{3.56}$$

Where K_t is the torque constant and like the velocity constant, it depends on the flux density of the fixed magnets, the reluctance of the iron core, and the number of turns in the armature winding.

The equations (3.53), (3.54), (3.55) and (3.56) are combined as follow:

$$L_a \frac{di_a(t)}{dt} + R_a i_a(t) = v_a(t) - K_b \frac{d\theta(t)}{dt} \tag{3.57}$$

$$J_m \frac{d^2\theta(t)}{dt^2} + B_m \frac{d\theta(t)}{dt} = K_t i_a(t) \tag{3.58}$$

Then, transforming the above two equations using Laplace transformation, we obtain the two equations as follows:

$$L_a sI(s) + R_a I(s) = V_a(s) - K_b s\theta(s) \tag{3.59}$$

$$J_m s^2\theta(s) + B_m s\theta(s) = K_t I(s) \tag{3.60}$$

The transfer function of the motor speed is:

$$G_{speed}(s) = \frac{s\theta(s)}{V_a(s)} = \frac{K_t}{J_m L_a s^2 + (L_a B_m + R_a J_m)s + B_m R_a + K_t R_a} \tag{3.61}$$

In addition, the transfer function of the motor position is determined by multiplying the transfer function of the motor speed by the term $\frac{1}{s}$:

$$G_{position}(s) = \frac{\theta(s)}{V_a(s)} = \frac{K_t}{J_m L_a s^2 + (L_a B_m + R_a J_m)s + B_m R_a + K_t R_a} \tag{3.62}$$

State Space Representation

The differential equation in eqns. (3.57) and (3.58) for the armature current and angular velocity can be written as follows:

$$\frac{d}{dt} i_a = -\frac{R_a}{L_a} i_a - \frac{k_b}{L_a} \omega + \frac{V_a}{L_a} \tag{3.63}$$

$$\frac{d}{dt} \omega = \frac{k_t}{J_m} i_a - \frac{B_m}{J_m} \omega \tag{3.64}$$

Which describe the dc motor system, putting differential equations in the state space form gives the following:

$$\frac{d}{dt}\begin{bmatrix} i_a \\ \omega \end{bmatrix} = \begin{bmatrix} -\frac{R_a}{L_a} & -\frac{k_b}{L_a} \\ \frac{k_t}{J_m} & -\frac{B_m}{J_m} \end{bmatrix} \begin{bmatrix} i_a \\ \omega \end{bmatrix} + \begin{bmatrix} \frac{1}{L_a} & 0 \\ 0 & 0 \end{bmatrix} \begin{bmatrix} V_a \\ 0 \end{bmatrix} \tag{3.65}$$

$$\begin{bmatrix} y_1 \\ y_2 \end{bmatrix} = \begin{bmatrix} 1 & 0 \\ 0 & 1 \end{bmatrix} \begin{bmatrix} i_a \\ \omega \end{bmatrix} + \begin{bmatrix} 0 & 0 \\ 0 & 0 \end{bmatrix} \begin{bmatrix} V_a \\ 0 \end{bmatrix} \tag{3.66}$$

Symbolically expressed as:

$$\frac{d}{dt} x = Ax + Bu \tag{3.67}$$

$$y = Cx + Du \tag{3.68}$$

Where, x is the state vector, u is the input vector, and y is the output vector.

Table 3.3 DC motor parameter and values

Parameter	**Value**
Moment of inertia	$J_m = 0.0000155 Kg.m^2$
Friction coefficient	$B_m = 0.000104667 N.ms$
Back EMF constant	$K_b = 0.0726 V / ms^{-1}$
Torque constant	$K_t = 0.0726 Nm / A$
Rated current	2A
Rated terminal voltage	$60V$
Rated power	40 *watts*
Rated torque	0.10Nm
Electric resistance	$R_a = 4\Omega$
Electric inductance	$L_a = 0.23H$

3.4 Control System Design

There are different types of controllers used for control of self-balanced TWMPPRM among those in the following section we discussed on PID and FPID controllers.

3.4.1. Design and Analysis of PID Controller

PID controller is considered to be the most popular control technique widely used in control applications. A huge number of applications and control engineers used the PID controller in their daily lives. PID control provides an easy way to control a process by varying its parameters and works well in industrial applications such as mobile manipulators where large components of joint inertia are added by actuators. PID controllers were dominant and popular issues in control theory due to simplicity of implementation, simplicity of design, and the ability to be used in a wide range of applications [28, 29]. In addition, they are available at low cost and provide robust and reliable performance for most systems when the parameters are properly tuned. According to different sources, PID controllers or PID variations (P, PD, and PI) are commonly used in more than 90% to 95% of control applications. However, the PID controller has its own limitations; the performance of the PID can only be satisfactory if the requirement is reasonable and the variation of the process parameters is limited. Setting the PID parameters is called tuning. There are a number of methods for determining PID gains for the controller. Some of these methods use the knowledge on the characteristics of the open-loop, such as the Cohen-Coon method. Other methods use the Nyquist curve plotting of the plant such as Ziegler-Nichols tuning method [30]. All these tuning formulas need to have prior knowledge of the system. The PID control technique is used to control and enhance the characteristics of the system, such as reducing overshoot, speed uprising time, and eliminating steady-state error. Each of the PID parameters has specific criteria for enhancing the characteristics of the controlled system. In this paper we use PID online tuner on MATLAB and then we can obtain the maximum and minimum gain for each gain parameter. Figure 4.2 in section 4.2 demonstrates the strategy schematics to control the self-balanced TWMPPRM. The strategy is based on developing a feed- back control mechanism that consists of five major control loops. The IB's angular position is controlled by the IB's error measurement in the tilt angle. From the five feedback loops, two are developed for the sake of driving the robot to undergo a particular planar motion in the XY plane. The error in the angular position of each wheel, also defined as the difference between the corresponding wheels desired and actual angular positions, is considered as the input to both control loops. The

two remaining feedback control loops are designed for controlling the object′s position. Both control loops consider the object position′s error as an input and the actuation force as an output. The driving torques of the right and left wheels′ motors (τ_R, τ_L) and the linear actuator forces of the vertical and horizontal links′ motors (F_1, F_2) are inputs to the TWMPPRM system. Five main PID control loops are utilized to control the system's five outputs; the angular position of the IB (θ), the left and right wheels' angular positions (δ_R, δ_L), and the object's linear displacements (h_1, h_2).

$$e_{\delta_L} = \delta_{Ld} - \theta_{Lm} \tag{3.69}$$

$$e_{\delta_R} = \delta_{Rd} - \theta_{Rm} \tag{3.70}$$

$$e_{\theta} = \theta_{d} - \theta_{m} \tag{3.71}$$

$$e_{h_1} = h_{1d} - h_{1m} \tag{3.72}$$

$$e_{h_2} = h_{2d} - h_{2m} \tag{3.73}$$

Where, *m* and *d* subscripts indicate desired and actual measured variable, respectively.

3.4.4. Design and Analysis of Fuzzy-PID Controller

As discussed in section 1.1.1, fuzzy logic is an artificial intelligence branch that deals with algorithms of reasoning used to emulate human thinking and machine decision-making. Fuzzy logic combines a grade or level with an information spectrum giving a maximum value of 1 and a minimum value of 0. There are no systematic procedures for the fuzzy logic controller architecture, such as root locus, Nyquist plots, pole placement, and stability tests and so on. The basic difficulty in developing the procedures is that there is no mathematical description of the basic rule [31].

Fuzzy logic control depends primarily on the rules of the linguistic variables. Fuzzy logic control is free from complex numerical calculations, unlike other methods. This uses simple mathematical calculations to control the model. While relying on basic mathematical analysis, it provides good performance in the control system. Hence, this method is one of the best methods available and also easier one to control a plant.

The fuzzy logic controller does not need to update precise information for system variables. This is contrary to the classical controller, which does need to update precise information for the

system variable to perform to the sensitivity of the classical controller within variations in the system variables. However, the classical controller is better able cannot eliminate steady-state error. Combining of these two controller structures, to control and minimize the steady state error of the system, therefore, is one good way to take advantage of categories, i.e., fuzzy logic control and PID controller [32].

Initially the PID controller gain Kp, Ki, Kd are calculated from linearized system by tuning online, this is better to estimate the maximum and minimum stable gain value, but we can also use other tuning method. The typical PID control law in its standard form is:

$$U(t) = K_p(e(t) + \frac{1}{T_i}\int_0^t e(t)dt + T_d \frac{e(t)}{dt})$$
$$U(t) = K_p e(t) + K_i \int_0^t e(t)dt + K_d \frac{e(t)}{dt}) \quad (3.74)$$

Where, $K_d = K_p * T_d$, $K_i = K_p / T_i$ and $e(t)$ is the difference between desired value and actual value, U(t) control variable, K_p is proportional gain, T_d is derivative time constant, T_i is the integral time constant, K_d is derivative gain, and K_i the integral gain.

Fuzzy System for Tuning the PID Gains

The PID controller's efficiency is based on a suitable tuning of PID gains. It is not a trivial challenge to tune the PID gains to optimize efficiency. The PID gains are generally tuned by qualified human specialists on the basis of some "thumb rule." and in practice; the PID gains are usually tuned by experienced human experts. In the next step, we will first determine a set of tuning rules for the PID gains (fuzzy IF-THEN rules) and then combine these rules into a fuzzy system that adjusts the PID gains online [33].

We have seen from the block diagram in Chapter 2, the fuzzy system takes two inputs (e and Δe) and gives three outputs ($K_P^{'}, K_I^{'}, K_D^{'}$). The Fuzzy-PID controller has comparatively smaller errors than the PID controller and has a better capability to dismiss disturbances. A fuzzy system that adjusts the PID controller gains, have been designed as follows [33].

The Fuzzy PID system with Fuzzy rule parameters or If-Then logic can be applied to decrease the error value on output in the MPPRM system. Mamdani-type inference is used for the

inference engine with centroid defuzzification method, it is more recommended for nonlinear system [34]. The output of fuzzy PID controller is given by:

$$U_{fPID} = K_{pf} e(t) + K_{if} \int_0^t e(t)dt + K_{df} \frac{e(t)}{dt} \tag{3.75}$$

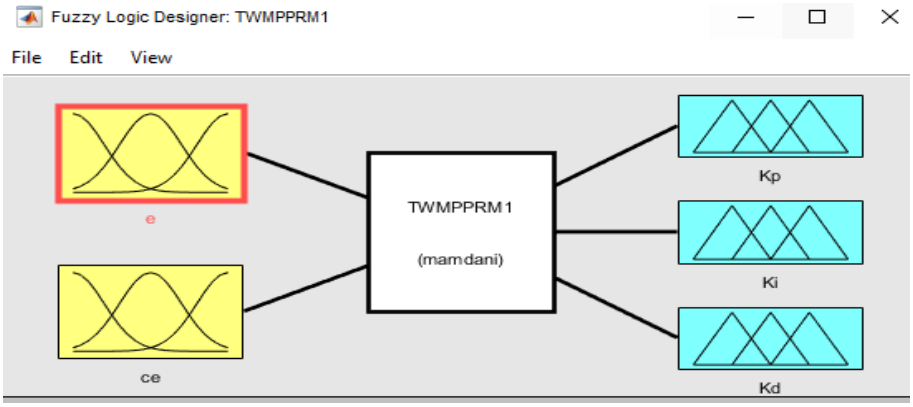

Figure 3.3 Fuzzy Inference System of the proposed system

K_{pf}, K_{if} and K_{df} are fuzzy PID controller gains for proportional, integral and derivative respectively. Initially we can calculate the PID gain using linearized system and then use PID online tuner on MATLAB and then we can obtain the maximum and minimum gain for each gain parameter. The self-tuning fuzzy PID controller, which takes error "e" and rate of change-in-error "Δe" as the input to make the controller use of the fuzzy controller rules to update PID gains Kp, Ki, Kd online. The Fuzzy PID controller refers to finding the fuzzy relationship between the three gains of PID controller and "e" and "Δe", and according to the principle of fuzzy control modifying the three gains in order to meet different requirements for control gains when "e" and "Δe" are different and making the controller produce a best control performance.

The first step in the design of a fuzzy logic controller is to define membership functions for the inputs. Five fuzzy levels or sets are chosen and defined by fuzzy set values for the error "e" and change in error "Δe". Fuzzy values (NB, NS, Z, PS, PB) which denotes Negative Big, Negative Small, Zero, Positive Small, and Positive Big respectively, and for the outputs we are chosen four fuzzy values (S, M, B, VB) which denotes, Small, Medium, Big and Very Big respectively.

The membership functions of the all inputs and outputs have been choice identical. Figure 3.4 shows these membership functions. We choice triangular membership functions, and the range of the fuzzy sets used for controllers are not same and they have been determined by tuning linearized system and taking range of stability of the linear system and we obtain by using trial

and error experience [34]. The fuzzy interface system has 25 rules. The range of the fuzzy sets for output range of Kp have been chosen between [-1 1], Ki have been chosen [-0.1 -0.1] and for Kd [-0.05 0.05] are for self-balanced TWMPPRM. For inputs, the range for the error and error rate have been chosen [-2 2] and [-3 3] respectively, and if these inputs are out of these ranges, we use a saturation for putting in to the range.

The relation between fuzzy system and PID controller which is called fuzzy PID controller output gain is calculated from its range of fuzzy controller gain [34, 35].

$$UfPID(t) = K_{Xf} e(t) + K_{Xf} \int_0^t e(t)dt + K_{Xf} \frac{de(t)}{dt} \tag{3.76}$$

$$K_{Xf} = K_X^{'} (K_{X\max} - K_{X\min}) + K_{X\min} \tag{3.77}$$

Where, subscribe X means P, I, or D.

The range of the PID parameters is chosen by two ways: First, determine the optimal PID parameters, which is obtained PID online tuner on MATLAB.

Second, choose the range of each parameter around the optimal value as:

$$K_{X_{\min}} < K_{Xf} < K_{X_{\max}}$$

In this work, the model has four PID controllers with fifteen parameters explained in vectors: $[K_{P1} \quad K_{I1} \quad K_{D1} \quad K_{P2} \quad K_{I2} \quad K_{D2} \quad K_{P3} \quad K_{I3} \quad K_{D3} \quad K_{P4} \quad K_{I4} \quad K_{D4} \quad K_{P5} \quad K_{I5} \quad K_{D5}]$

Where, $[K_{P1} \quad K_{I1} \quad K_{D1}]$ and $[K_{P2} \quad K_{I2} \quad K_{D2}]$ represented the parameters of displacement of right and left wheels respectively, $[K_{P3} \quad K_{I3} \quad K_{D3}]$ represented the parameters of tilt angle of the intermediate body around the vertical Z axis, $[K_{P4} \quad K_{I4} \quad K_{D4}]$ represented the parameters of vertical linear link displacement and $[K_{P5} \quad K_{I5} \quad K_{D5}]$ represented the parameters of horizontal linear link displacement.

Rule Base Construction

Deriving fuzzy rule base is an important part in FLC design and implementation [27, 36]. Two approaches for deriving rule base: heuristic and deterministic approaches. The first, heuristic approach it is based on the qualitative knowledge of the system behavior. The rule is formed by analyzing the behavior of the process such as the convergence from the proposed output may be correct. The second approach can systematically determine the parameters and the linguistic

structure of the rules, which satisfy the desired control. Consider a unit-step response for control system is shown in Figure 3.5(a). The error signal, which is the difference between the unit step input and the output response, is shown in Figure 3.5(b).

Table 3.4 Minimum & Maximum values of PID controller for FPID.

Parameter Name	$K_{X_{\min}}$	$K_{X_{\max}}$
K_{P1}	80.01	84.92
K_{I1}	0.052	0.063
K_{D1}	75.34	76.16
K_{P2}	80.01	84.92
K_{I2}	0.052	0.063
K_{D2}	75.34	76.16
K_{P3}	80.72	85.29
K_{I3}	0.020	0.026
K_{D3}	9.011	10.082
K_{P4}	8.190	9.031
K_{I4}	0.011	0.026
K_{D4}	10.31	11.28
K_{P5}	27.36	28.29
K_{I5}	0.051	0.059
K_{D5}	32.09	33.25

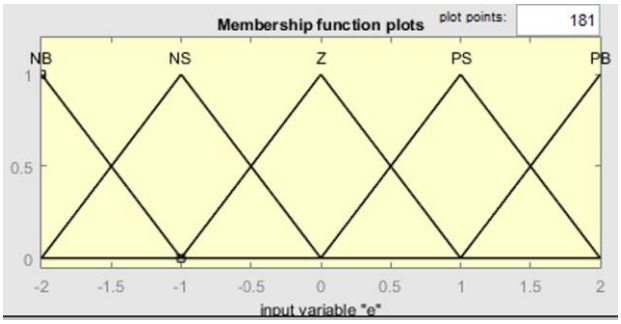

(a)

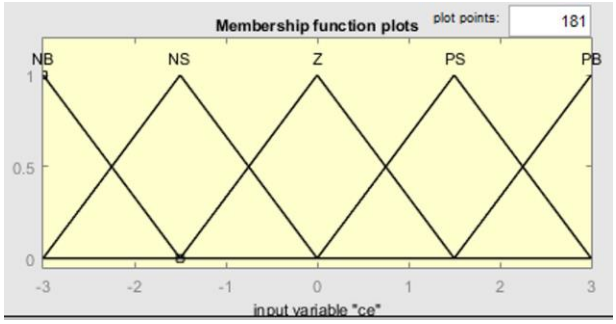

(b)

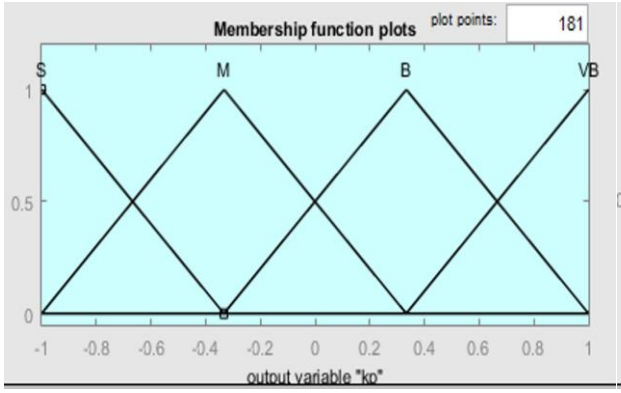

(c)

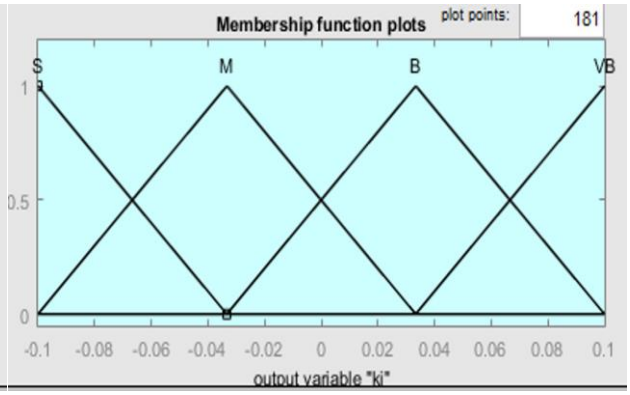

(d)

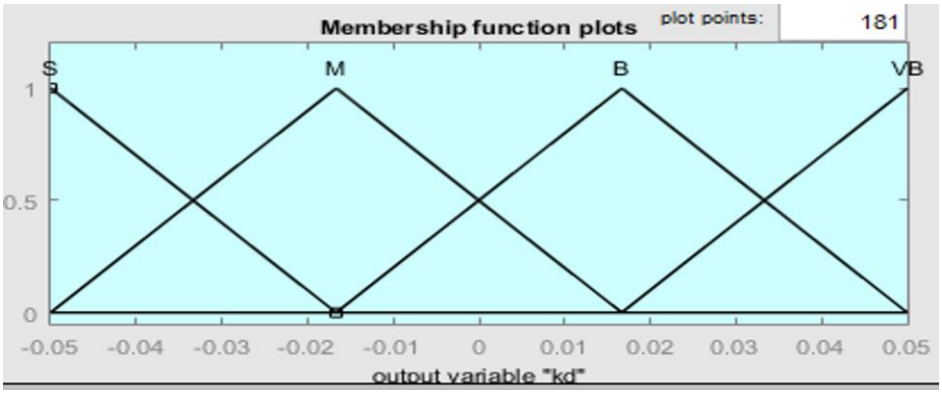

(e)

Figure 3.4 Membership functions of input and output. (a) e ,(b) ce ,(c) $K_P^{'}$,(d) $K_I^{'}$ and (e) $K_D^{'}$

Assume the system consists of a motor with torque $\tau(t)$ that proportional to $e(t)$. The performance of the system is analyzed as follows: During the time interval $0 < t < t_1$,the error signal is positive, and corresponding motor torque is positive and it is rising rapidly. In the time interval, $t_1 < t < t_3$, the error signal is negative and the motor torque is negative.

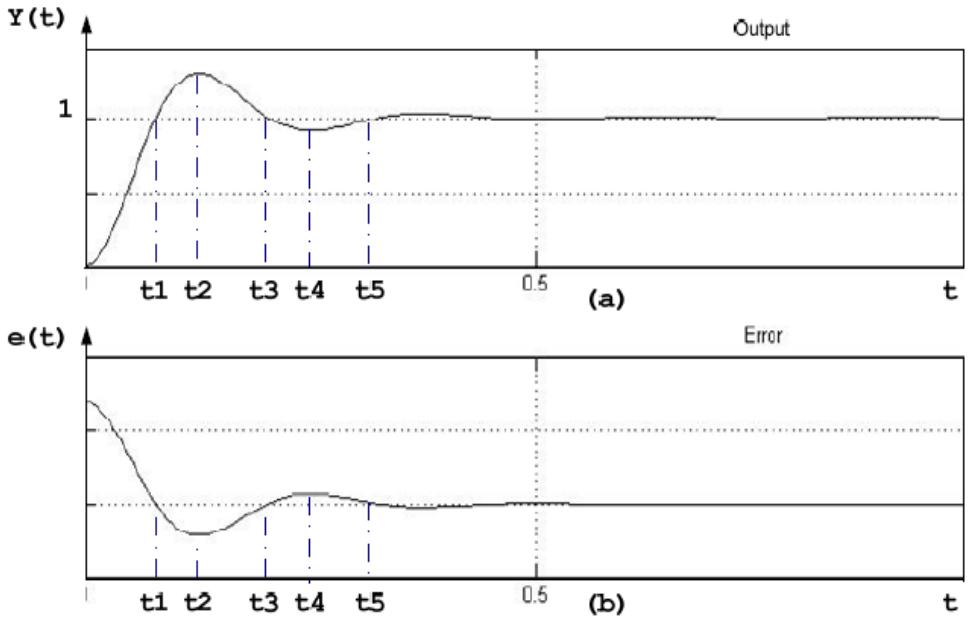

Figure 3.5 Waveform showing (a) output, (b) error [27]

The negative torque tends to slow down the output acceleration and cause the direction of the output $y(t)$ to opposite direction. During the time interval $t_3 < t < t_5$, the motor torque is a gain positive; thus, tends to reduce the response caused negative torque in previous time interval. Since the system will be considered stable along *t*. To illustrate the above mechanism for rule derivation, Figure 3.8 shows the response of a process to be controlled, where the input of the fuzzy controller is the error and change of error. In the first region ($e > 0$ and $\Delta e < 0$) i.e. between point and point a_1 and point b_1 the control signal *u* should increase to speed up the rising time, and then decreased gradually as *e* will approaches zero to reduce the overshoot. Similarly, (e and Δe smaller than zero) so the control signal should decrease to slow divergence of the response and eliminating the overshoot. The other two cases similarly as the above two cases. Let studying first case around point a_1. If the error is positive big and its derivative is positive big, then the PID parameters should have large proportional gain, the integral time constant must be smaller, and the derivative time constant must be smaller. In this case, the proportional gain Kp may represented by a fuzzy set (Very Big) and the derivative gain is Kd represented by a fuzzy set (Small), and the integral gain Ki is represented by a fuzzy set (Small). Therefore, the rule base a round a_1 reads as:

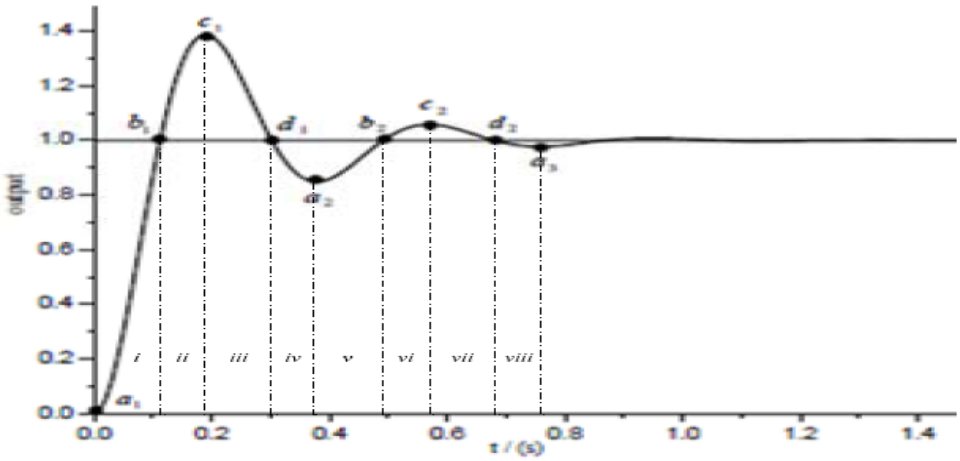

Figure 3.6 Step response [27]

IF e (t) is PB and Δe(t) is PB, THEN $K_P^{'}$ is VB, $K_I^{'}$ is S, $K_D^{'}$ is S.

Around point b_1 small control signal to avoid large overshoot. If the error is NS and its derivative is PS, then the PID controller have to be smaller value of the proportional gain, larger value for the integral time constant, larger value for derivative time constant. Thus, the following fuzzy rule is written as:

IF e (t) is NS and Δe(t) is PS, THEN $K_P^{'}$ is S, $K_I^{'}$ is B, $K_D^{'}$ is B.

If the error is PB and its difference is PS (i.e. the system output will approach the steady state, at point d_2), then parameters of PID controller must keep the values of the last state (i.e. the changes of these parameters must be very small). Therefore, this step will maintain the system output at set point, and let the system output approach the steady state. The desired rule is written as follows:

Table 3.5 Fuzzy control rule of K'P/K'I/K'D

$e / \Delta e$	NB	NS	Z	PS	PB
NB	VB/S/S	VB/M/S	S/M/VB	S/M/B	M/S/S
NS	VB/B/S	B/B/S	S/B/B	S/B/B	B/B/S
Z	B/B/S	M/B/M	S/VB/B	S/VB/M	VB/VB/S
PS	M/B/M	S/B/B	S/B/B	M/B/S	VB/B/S
PB	S/S/M	S/S/VB	S/M/VB	B/M/S	VB/S/S

IF e (t) is PB and Δe(t) is PS, THEN $K_P^{'}$ is B, $K_I^{'}$ is M, $K_D^{'}$ is S.

The fuzzy control rules of the proposed algorithm have been derived experimentally from studying the step response of the process to be controlled. All rule bases derived in the same way. The rule base table of $K_P^{'}$, $K_I^{'}$ and $K_D^{'}$ are shown in Table (3.5).

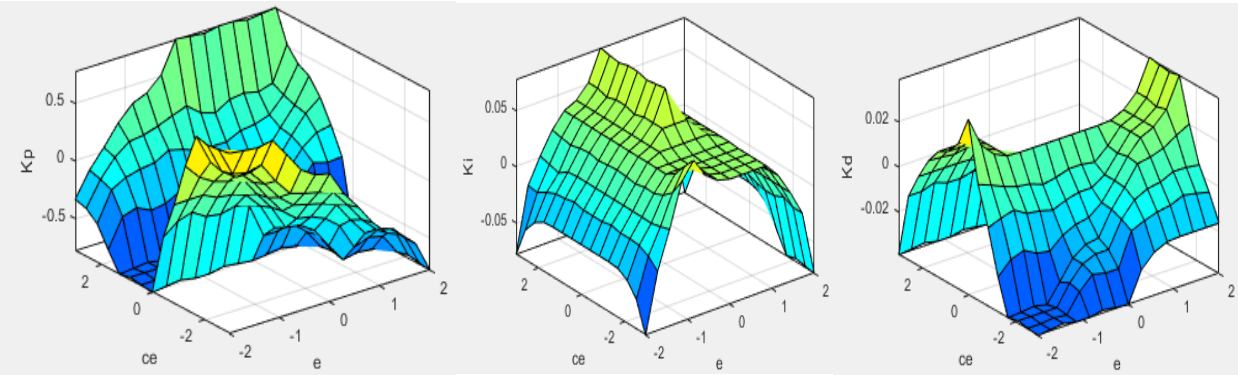

Figure 3.7 Surface viewer for Kp, Ki, Kd with respect to e and ce

CHAPTER FOUR

4. SIMULATION RESULTS AND DISCUSSIONS

This chapter deals with the results and discussions of MATLAB simulations. It is deals with simulation results of the open loop system response, and closed loop control of the system using PID and Fuzzy-PID in different conditions with MATLAB/SIMULINK. Then, the simulation studies the system in dynamic and transient performance using MATLAB/Simulink 2016b environment and the results are discussed. The Simulink model shown in Figure 4.2, 4.6, 4.10, 4.17& 4.19 is used to carry out simulation studies and analyze the performance of the controllers under different operating conditions.

4.1. Open loop system response

This section investigates the response and performance of the system using MATLAB/Simulink. In order to study the behavior of the developed model, an open loop system response needs to be investigated. The model is implemented in the MATLAB / Simulink environment using the simulation parameters described in Tables B1 and 3.3, where the following initial conditions are used: $\theta = 0, \delta_R = 0, \delta_L = 0, h_1 = 0, h_2 = 0, v_R = 0, v_L = 0, \dot{h}_1 = 0, \dot{h}_2 = 0$. Figure 4.1 illustrates the open-loop system response of pitch angle (θ), angular velocity ($\dot{\theta}$), right wheel angular displacement (δ_R), right wheel velocity (v_R), left wheel angular displacement (δ_L), left wheel velocity (v_L), vertical link displacement (h_1), vertical link velocity ($\dot{h}_1$), horizontal link displacement (h_2), and horizontal link velocity ($\dot{h}_2$). As for the simulation results shown in Figure 4.1, the output of the system is infinite. It is obvious that the system is an unstable non-linear system; therefore, a closed-loop system is required to stabilize the system and improve its performance.

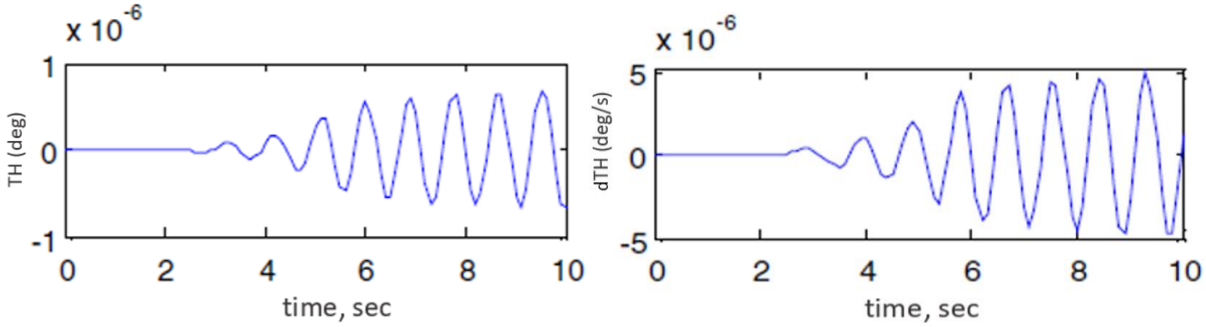

(a) (b)

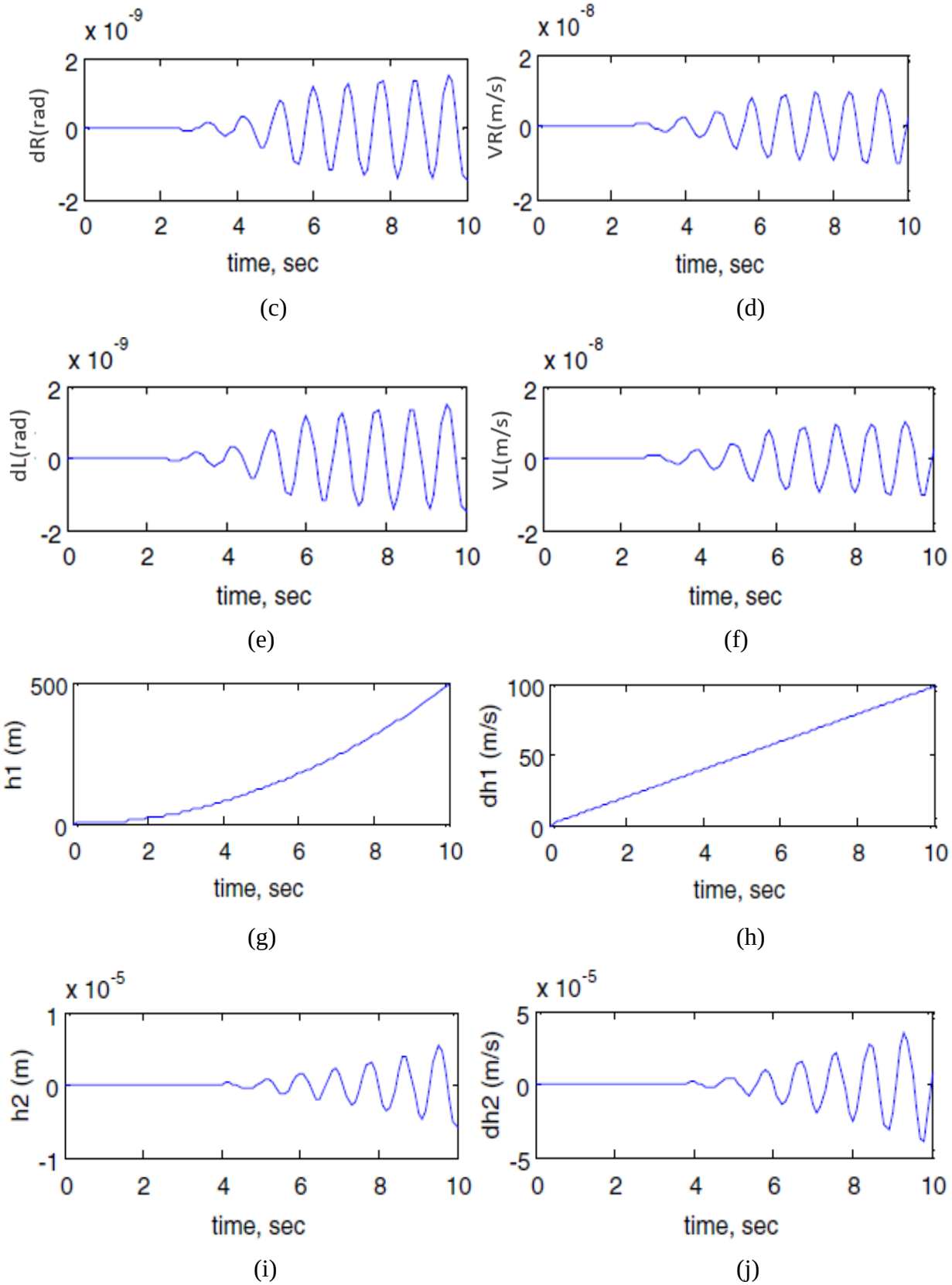

Figure 4.1 (a)-(j): TWMPPRM open loop response

4.2. PID control without and with switching mechanisms

4.2.1. PID control without switching mechanisms

In this section, and based on the mathematical model derived in Section 3.2 and the robot dynamic actuators in Section 3.3, the developed control strategy is implemented using the TWMPPRM model. Initially, testing the following simulation exercises will not include switching mechanisms. Two specific conditions are considered when evaluating both the control scheme and the behavior of the system: the free movement of the payload and the activation of the two linear actuators associated with both horizontal and vertical movement of the payload. After using switching mechanisms, which are intended to determine when the linear actuators of the self-balanced TWMPPRM will perform, the same exercise is repeated.

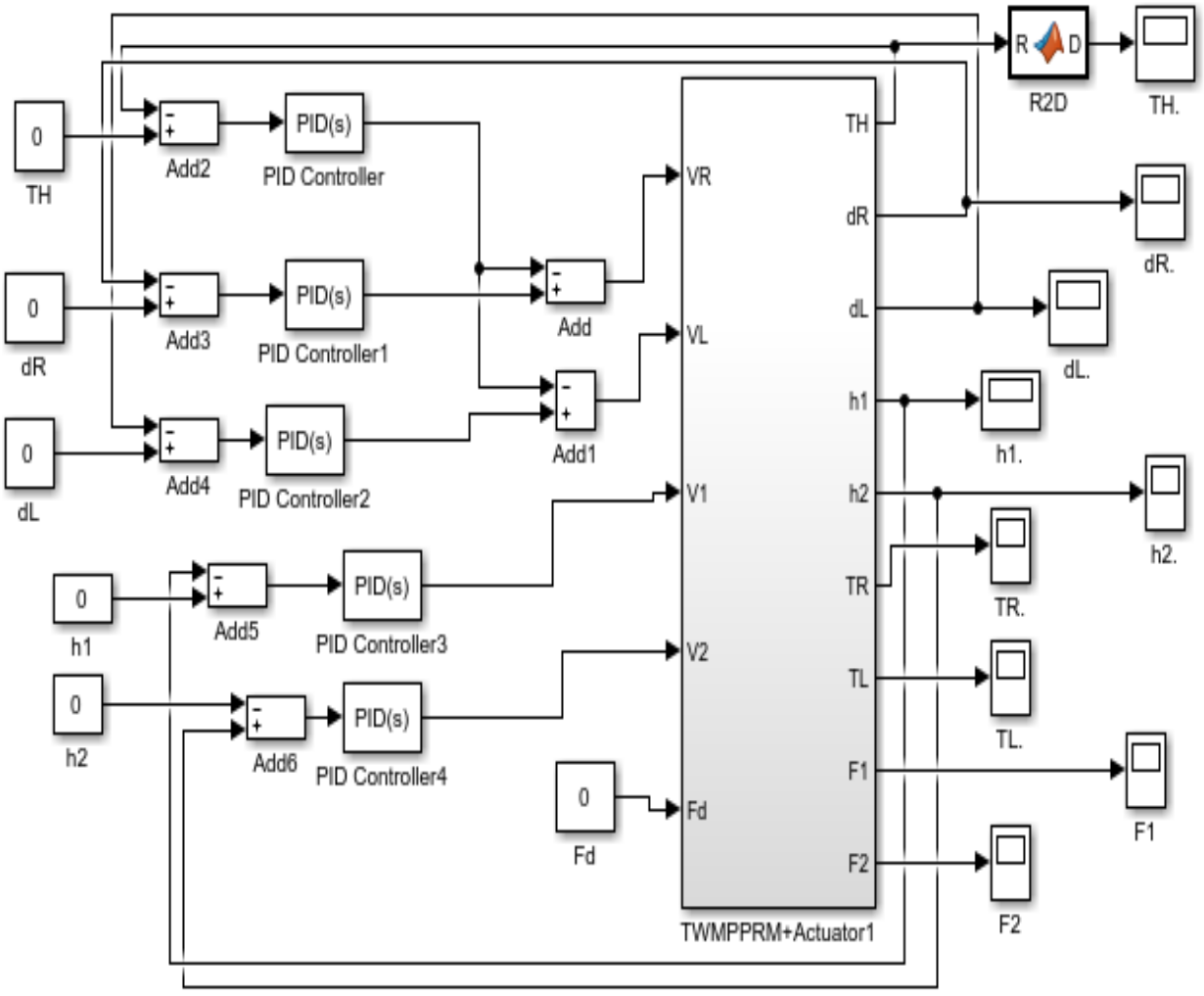

Figure 4.2 Simulink model of PID controller without switching mechanism

A. Payload free movement (Vertical and horizontal linear actuators not activated)

Figure 4.3 demonstrates the TWMPPRM simulation output considering the tilting angle $\theta = 5^{\circ}$ and setting the effect of the linear actuators h_1 and h_2 to zero during the stabilization mode. Based on Figure 4.3, the control mechanism takes less than 2s to stabilize the vehicle in order to reach the balancing position. It has been noted that the vehicle's motion is unbound and continues to move in order to preserve stability. For such types of vehicles used in applications with limited working space, this behavior is unsatisfactory and the vehicle, once it has achieved stability, is considered to be running at a fixed speed.

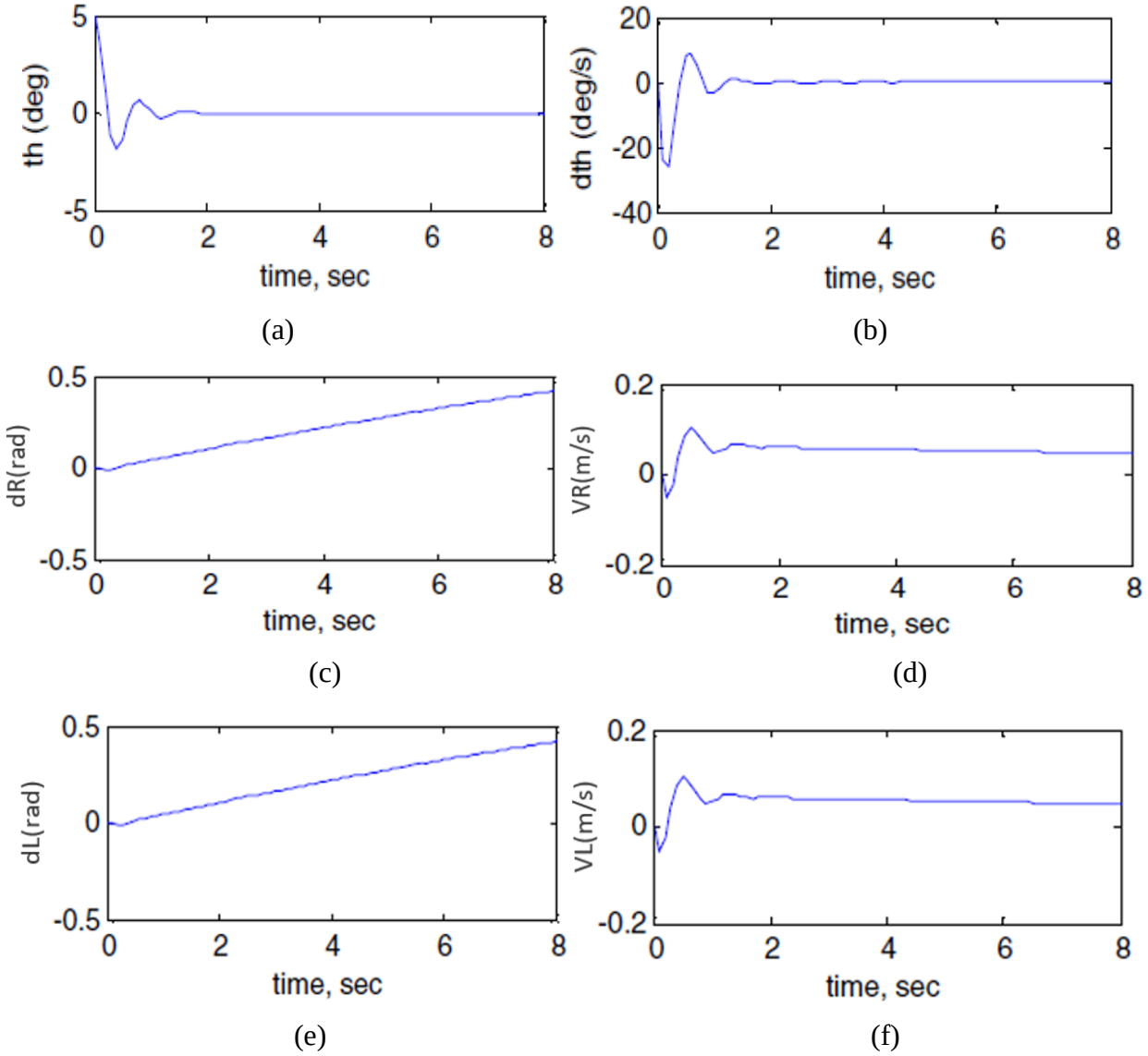

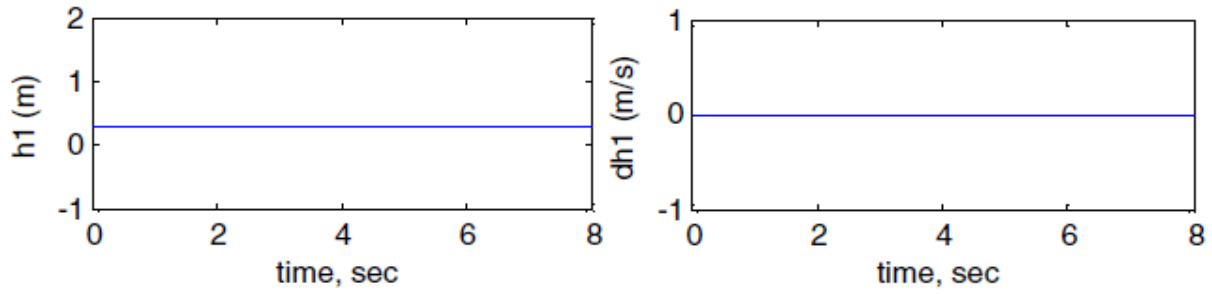

(g) (h)

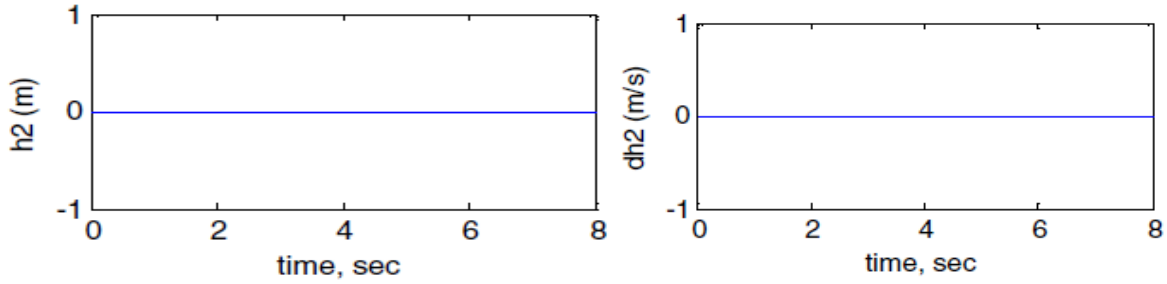

(i) (j)

Figure 4.3 (a)-(j): System output (h1 = h2 = 0) of unbounded wheels displacement

The controller is modified to minimize the motion of the TWMPPRM by restricting the linear displacement of the wheels. The modified controller helps the wheels to rotate the predefined fraction. As shown in Figure 4.4, the control method has the capability to achieve the TWMPPRM balance position (upright vertical position) within 2 seconds. On the other hand, the wheels ' steady state position is reached in approximately 4 seconds. Compared with the previous case, bounding the rotation of the wheels of the system has an effective impact on the stability of the vehicle.

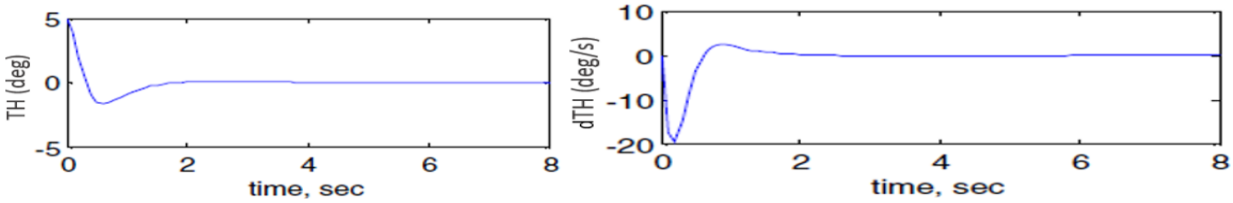

(a) (b)

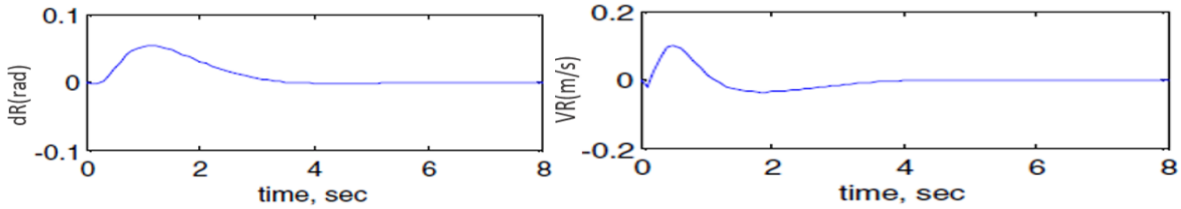

(c) (d)

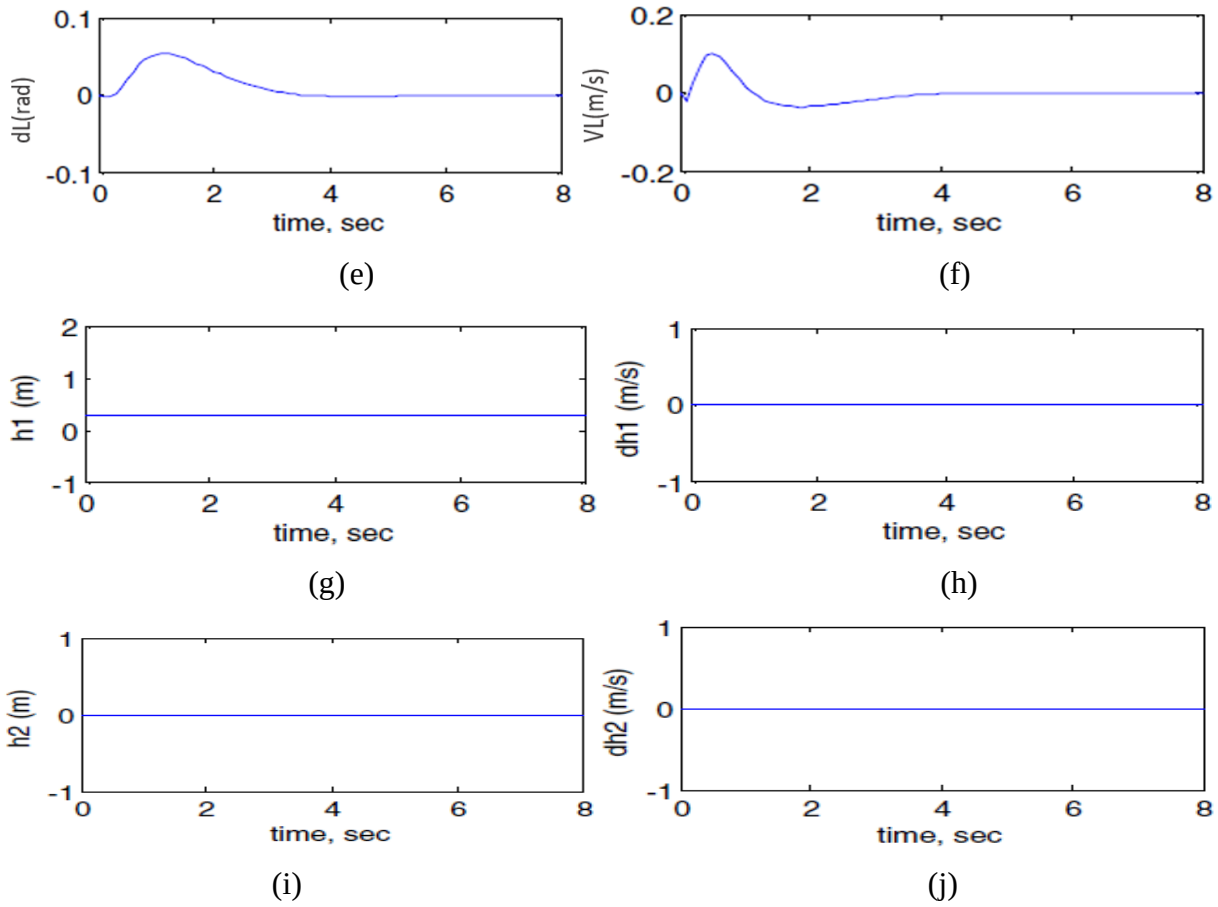

Figure 4.4 (a)-(j): Modified system output (h1 = h2 = 0) of bounded wheels displacement

B. Payload simultaneous horizontal and vertical motion (Vertical and horizontal linear actuators activated)

In this part, the effect of changing the robot COM by activating the linear actuator and extending simultaneously in two mutually perpendicular axes is investigated. As shown in Figure 4.5, and without considering the payload, the TWMPPRM has a longer transient period compared to the case previously examined. As a result of the COM position change in two different directions, the system took longer to achieve stability by increasing the overshoot. The system takes around 4s to reach stability, which is close to the time taken by both actuators to extend. When comparing these results with previous simulation results, it was noted that the system experienced a significant amount of vibration throughout the duration of the COM change in two directions. It will result in dramatic changes in the required control effort. The torques provided by both motor wheels is anticipated to be influenced by the aforementioned long transient period of instability, until the system reaches stability.

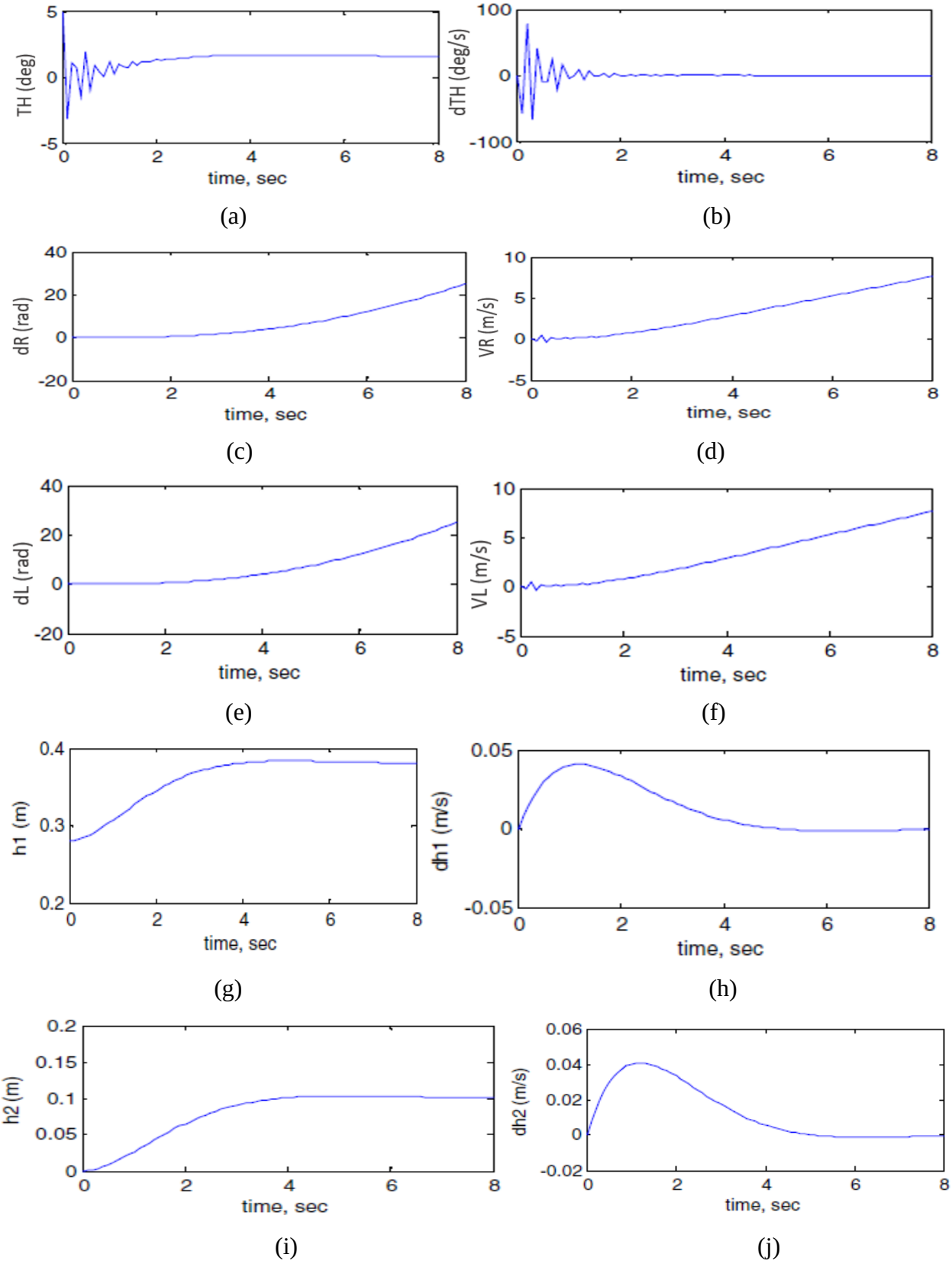

Figure 4.5 (a)-(j): System output (Vertical and horizontal linear actuators activated)

4.2.2 PID control with switching mechanisms

Since the proposed self-balanced TWMPPRM is mainly designed for picking and/or placing applications, it is desirable to stabilize the system first. The reason is to avoid any disturbance at the beginning of the operation as a result of the lifting of the object. The lifting of an object causes the COM to move during the stabilization mode, which in turn affects the stability state and disrupts the control effort.

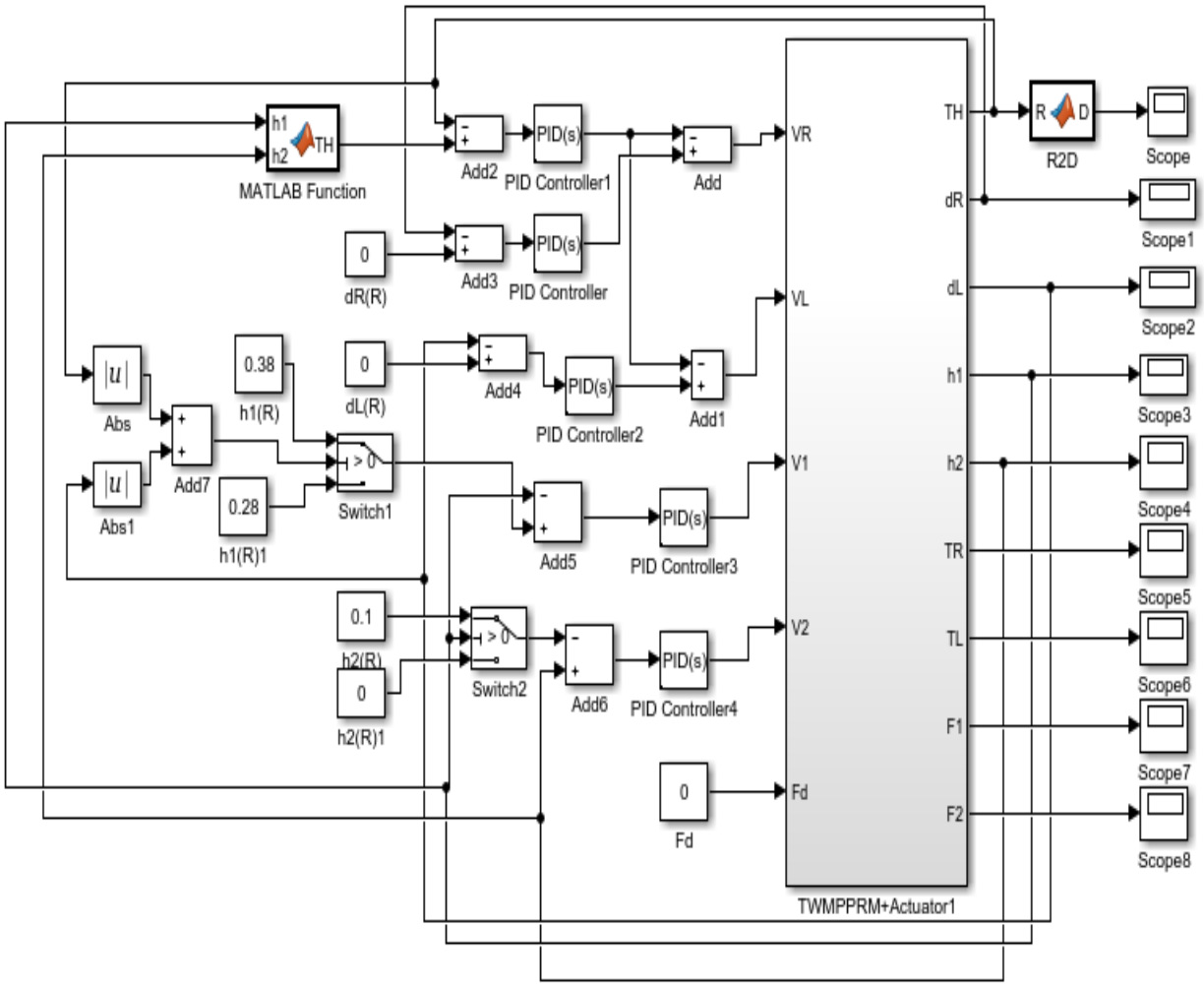

Figure 4.6 Simulink model of PID controller with switching mechanism

In order to avoid this case, the control scheme is modified as shown in figure 4.6. Two switching mechanisms are added to the system to ensure stability of the system before starting the handling of the object. The two mechanisms are developed in such a way that linear actuators will not be activated until the IB of the vehicle reaches a stable upright position. Three case studies are

known where only one linear actuator is allowed to operate at a time in the first two cases and, in the third case, the two actuators working simultaneously at the same time.

A. Payload Vertical Movement Only

In this case, the linear actuator along the IB is allowed to operate by moving up and down along the IB and z axis. This is actually implemented by extending and contracting the linear actuator rod, which leads to moving up and down the entire COM as per the control signal developed by the actuator. Figure 4.7 shows the system's output simulation starting with the initial conditions at $\theta = 5^{\circ}$, $h_1 = 0.28m$ and $h_2 = 0m$. The actuator starts to be extended by approximately 0.4 m after 5second from the start of the simulation. The control mechanism was robust enough to ensure that there was no interruption in the stabilization condition of the IB. The linear actuator accelerates to its maximum speed at around 7second and then decelerates to completely settle down when it reaches its target height.

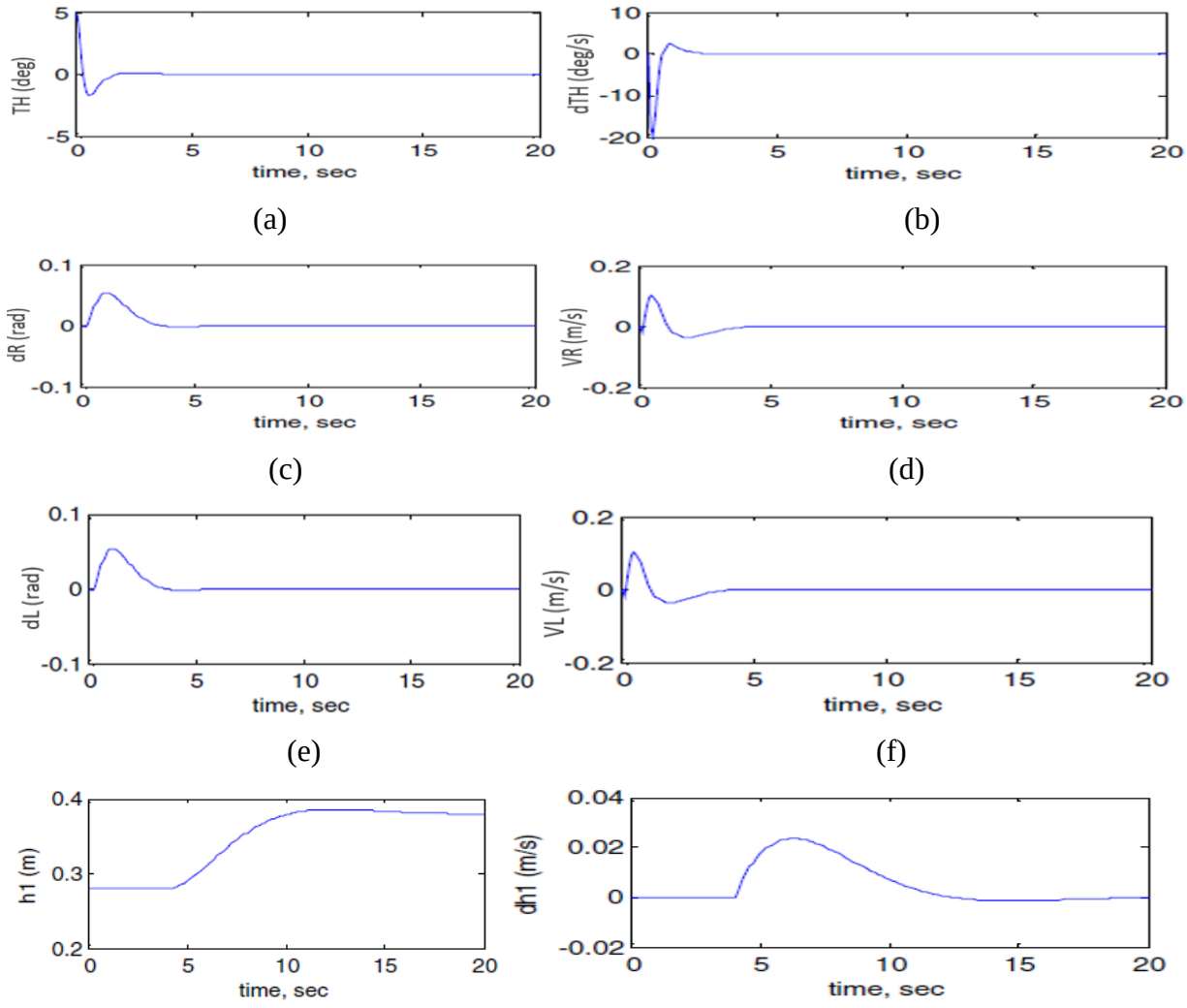

(g) (h)

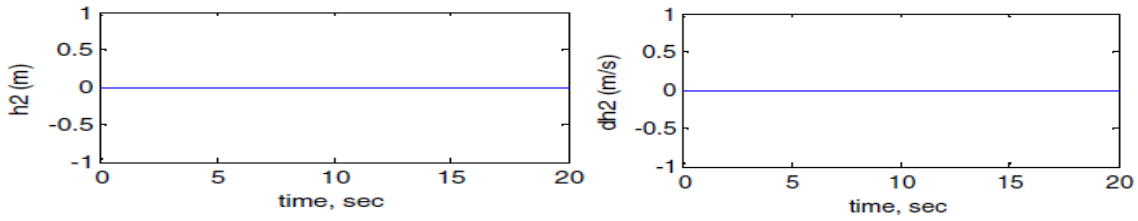

(i) (j)

Figure 4.7 (a)-(j): System output of payload vertical motion only

B. Payload horizontal movement only

During this case, the system is simulated to observe the impact of changing h_2 in a direction perpendicular to the axis of the IB and in the *x* direction. This condition is close to the IB's forward or back inclination, which simulates scenarios of wheeled robot going up or down an inclined surface. The initial conditions are set $\theta = 5^{\circ}$, $h_1 = 0.28m$ and $h_2 = 0m$. At this point, the actuator along the IB is kept locked, and the allowed motion will be the one from the other linear actuator that starts to operate after reaching a state of balance as shown in Figure 4.8. As observed from the figure, changing h_2 by only 10 cm at 5second will act as a sudden impact disturbance which hits the IB causing it to change its direction dramatically to the opposite side of Z axis as obvious from the tilt angle graph. However, the control algorithm was unable to push the IB to the vertical position and instead kept it inclined towards to the opposite side with a constant angle of tilt around. 7°. Changing h_2 in the aforementioned manner also influences the vehicle's linear motion in the X-direction as clear from both wheels ' fractional displacements.

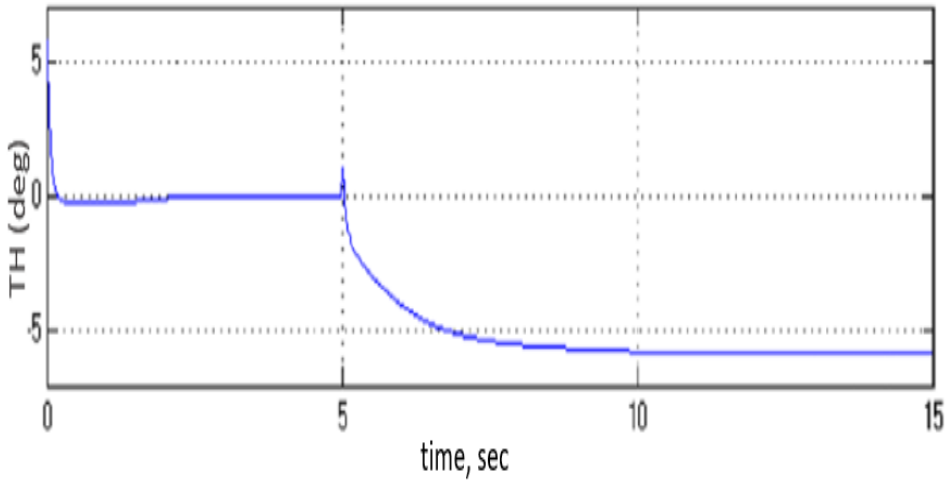

(a)

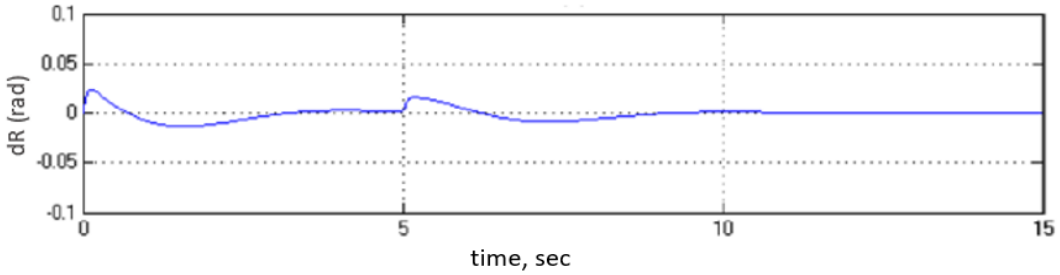

(b)

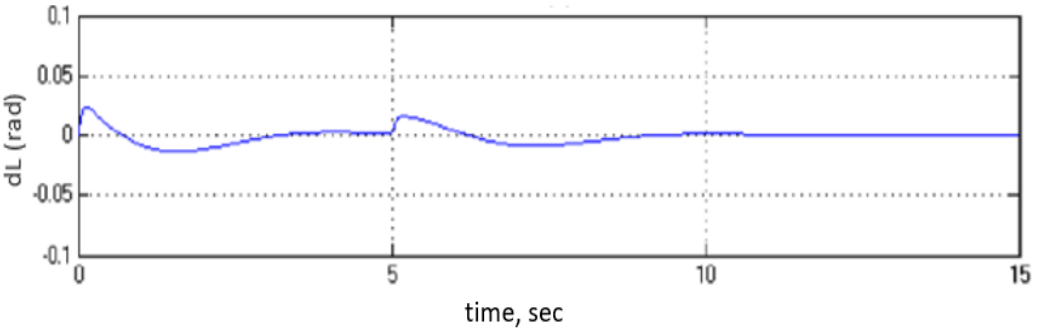

(c)

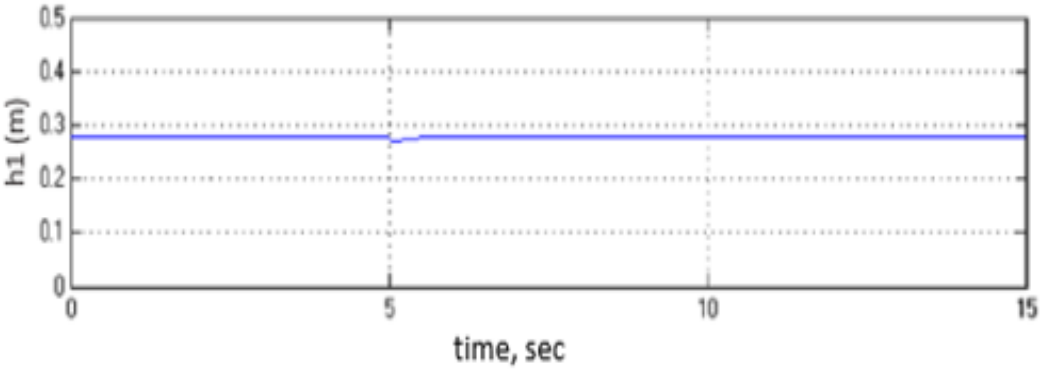

(d)

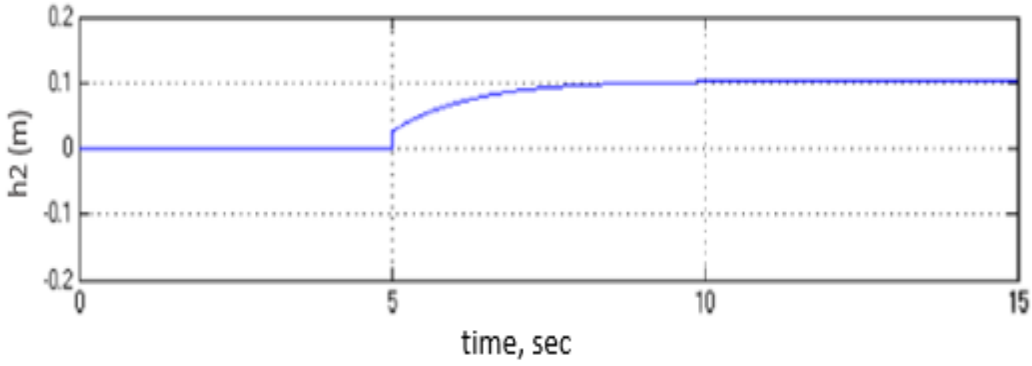

(e)

Figure 4.8 (a)-(e): System output of payload horizontal motion only

C. Payload simultaneous horizontal and vertical motion

The proposed control algorithm′s robustness is tested and Figure 4.9 demonstrates the system output considering the case where h_1 and h_2 change sequentially. For approximately 5.5second, h_1 is maintained fixed at 0.28 m prior starting the alteration process to the aimed elevation. The IB′s stabilization condition was not interrupted and at about 9.5second, h_2 starts to change and results in unanticipated changes in the IB′s stabilization along with a minor disturbance in h_1. Associated with the changes in h_2, the IB inclines in the opposite direction to overcome the COM′s position change due to the extension of h_2.

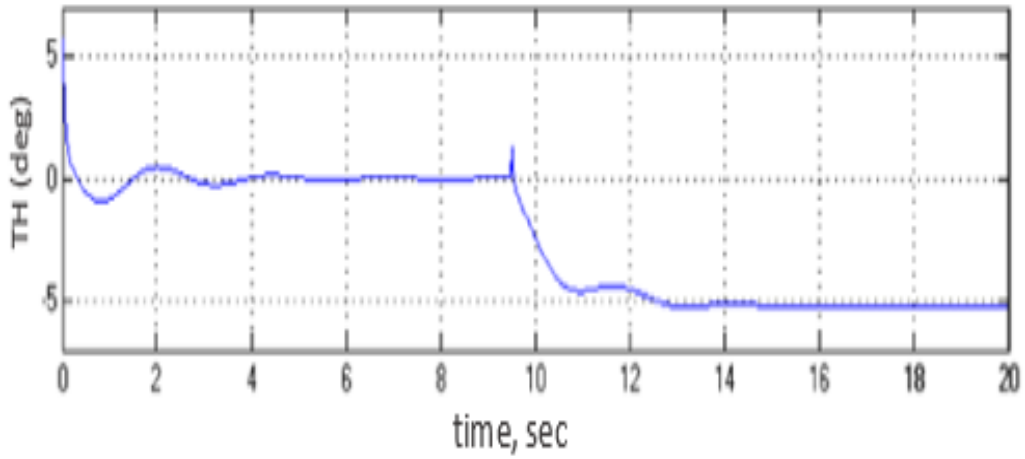

(a)

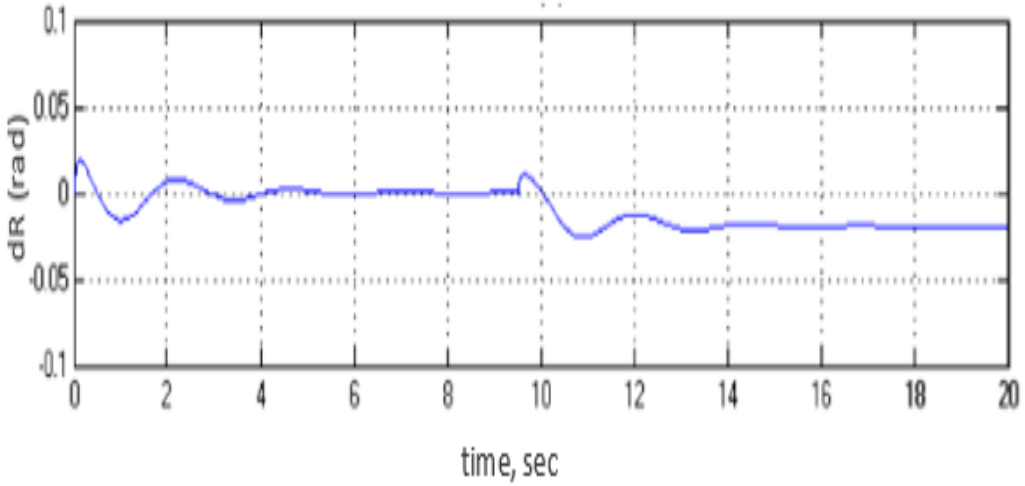

(b)

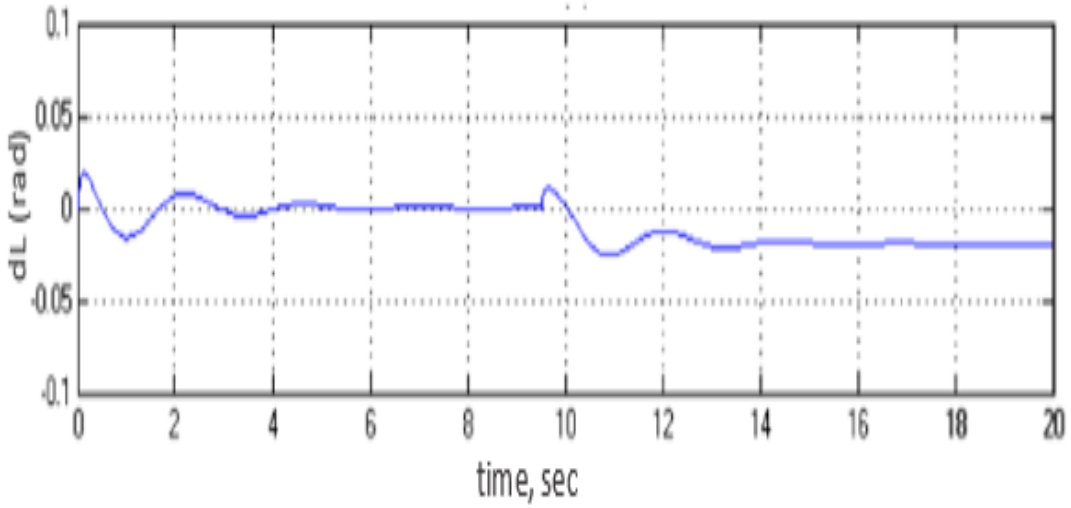

(c)

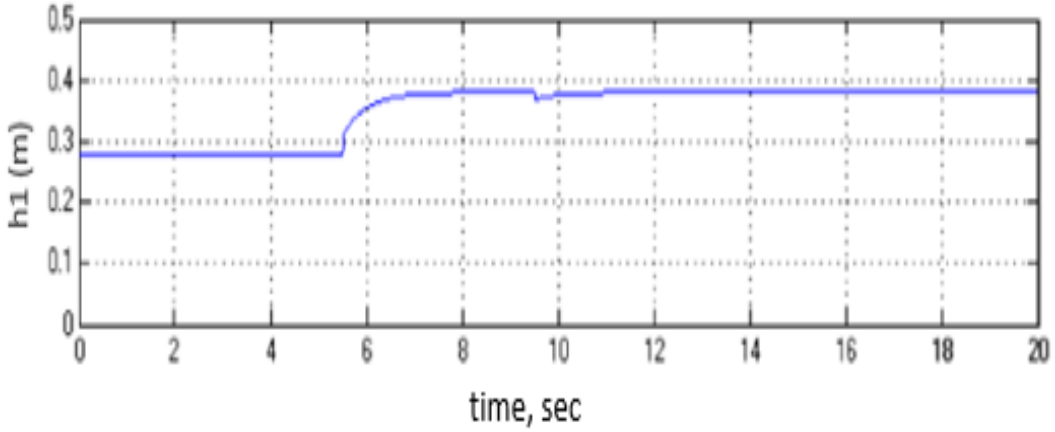

(d)

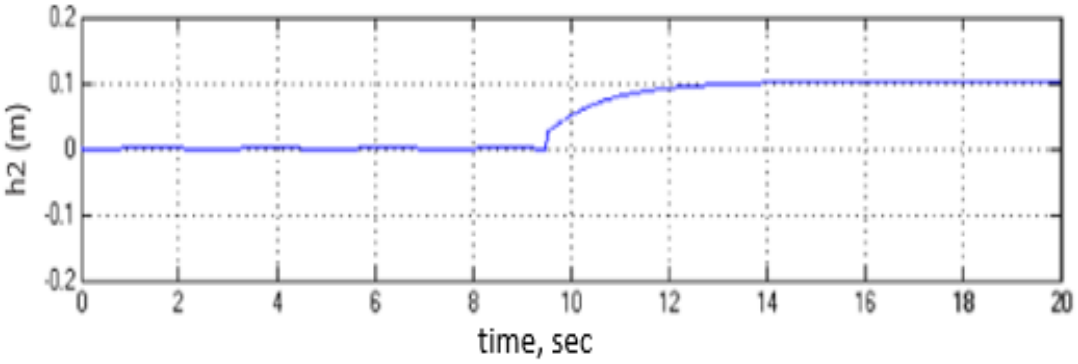

(e)

Figure 4.9 (a)-(e): System output (Vertical and horizontal linear actuators activated)

4.3 Fuzzy-PID control without and with switching mechanisms

4.3.1 Fuzzy-PID control without switching mechanisms

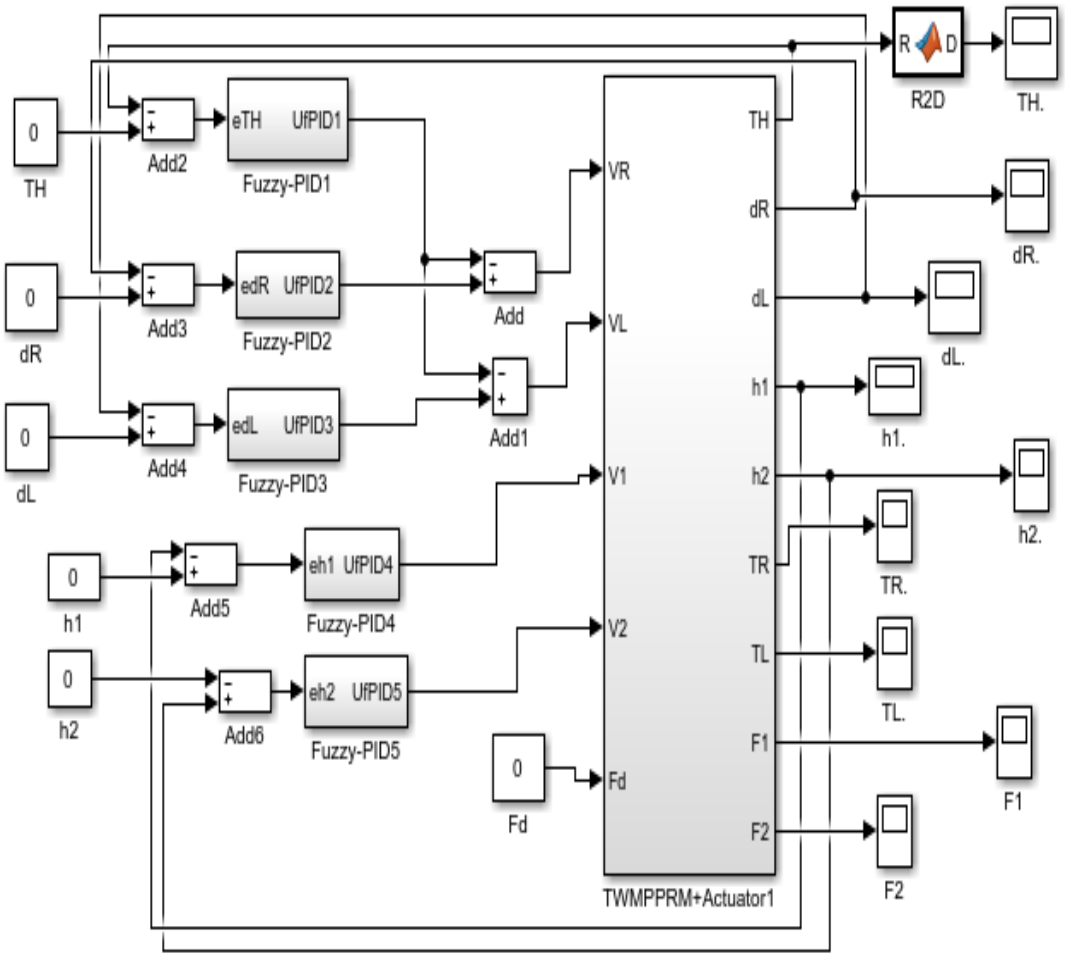

Figure 4.10 Simulink model of fuzzy-PID controller without switching mechanism

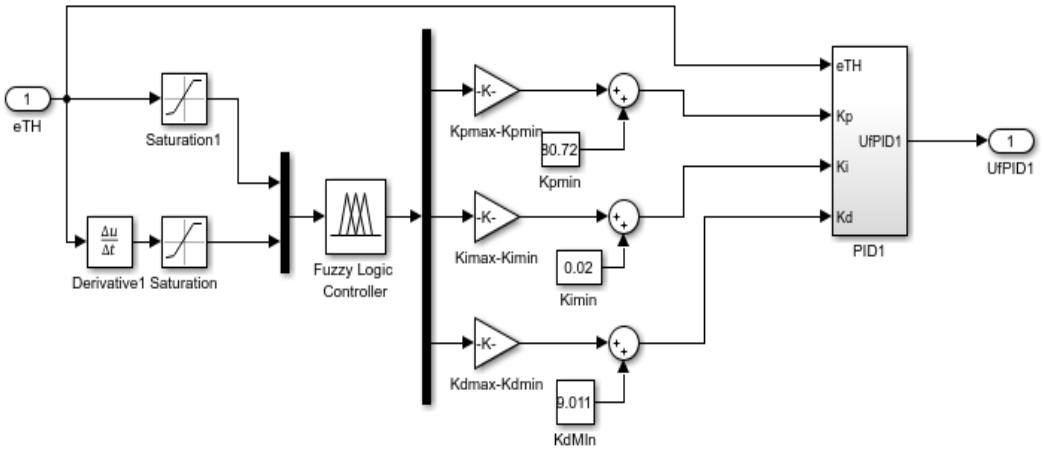

Figure 4.11 Simulink Block diagram of fuzzy-PID1

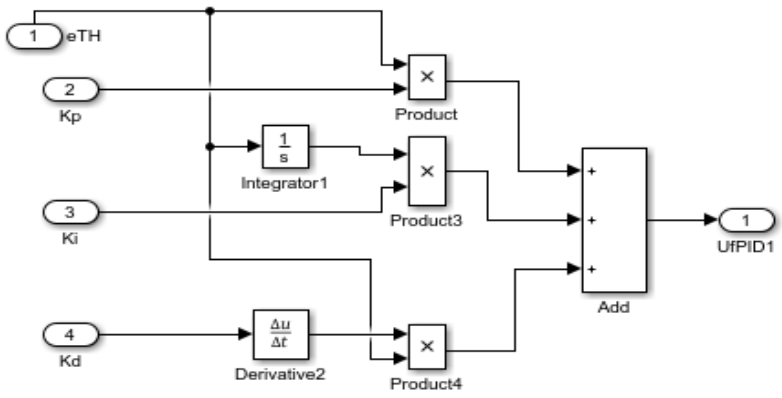

Figure 4.12 Simulink Block diagram of PID1

A. Payload free motion (Vertical and horizontal linear actuators not activated)

In view of different motion scenarios, the behavior of the system is observed for the tilting angle of the robotic vehicle, the angular displacement of the two wheels and the displacement of the linear actuators, Figure 4.13 shows the simulation results of the TWMPPRM performance and input control signals. The system is considered to commence at $\theta = -5^{\circ}$ and ignoring the linear actuators' effect h_1 and h_2 by setting them to zero throughout the TWMPPRM stabilization process. As can be shown, the control approach stabilizes the robot within less than approximately 1.5seconds and the steady state position of the two wheels was reached within almost 5second.

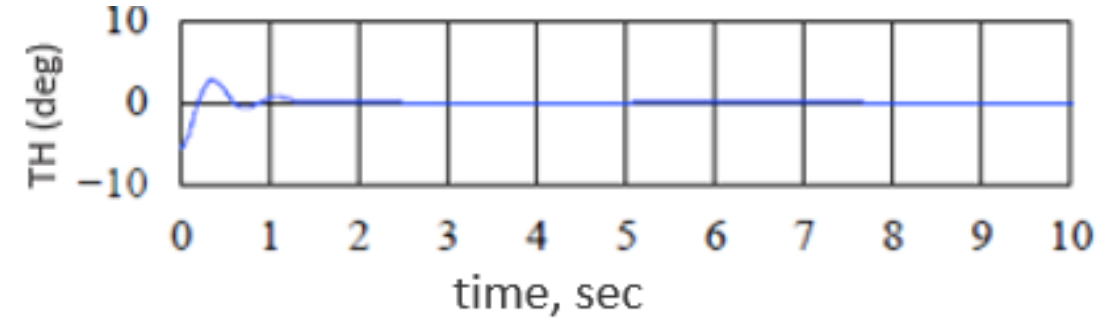

(a)

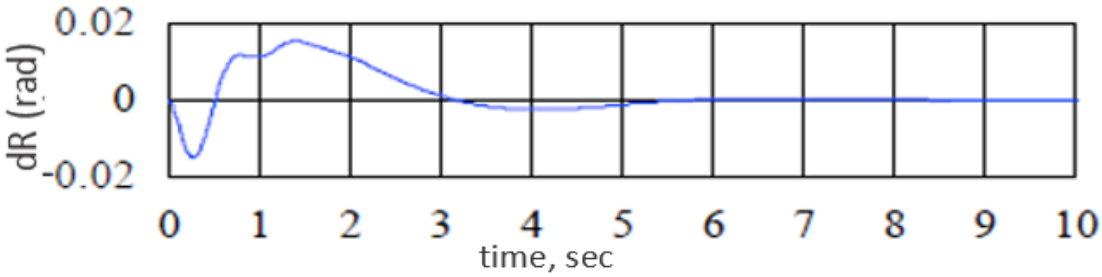

(b)

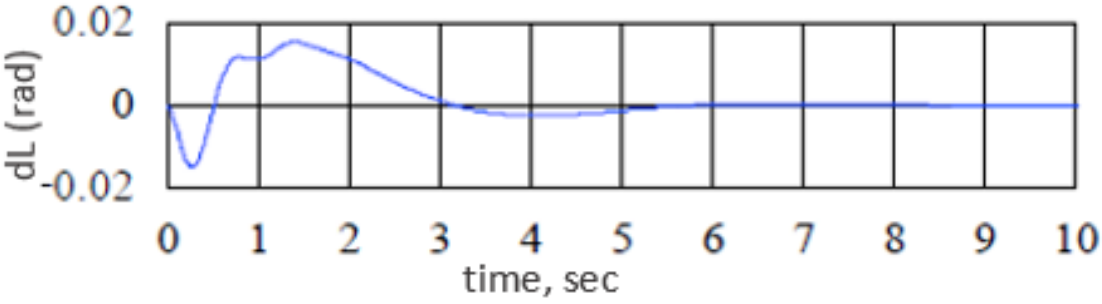
0.02
0
-0.02
dL (rad)
0 1 2 3 4 5 6 7 8 9 10
time, sec

(c)

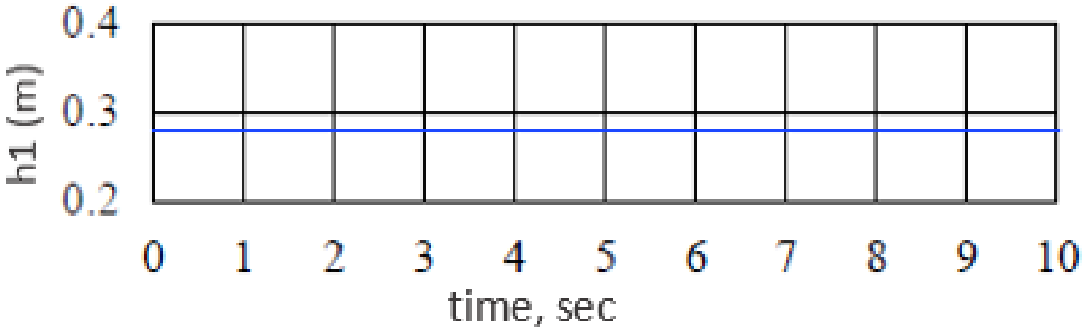
0.4
0.3
0.2
h1 (m)
0 1 2 3 4 5 6 7 8 9 10
time, sec

(d)

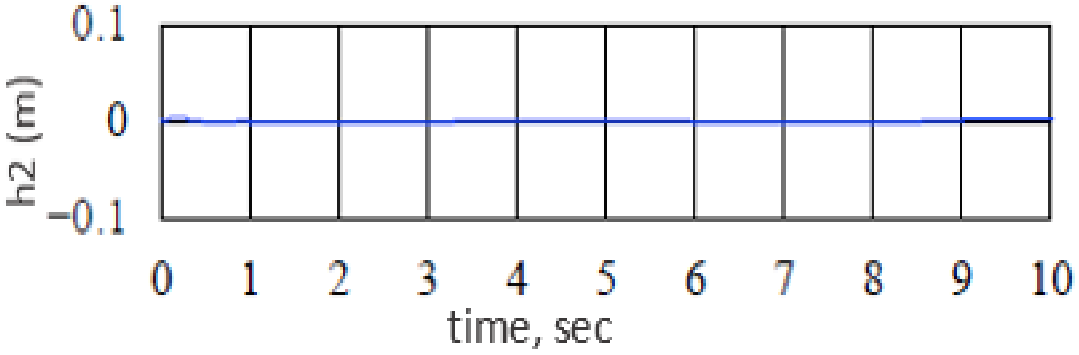
0.1
0
−0.1
h2 (m)
0 1 2 3 4 5 6 7 8 9 10
time, sec

(e)

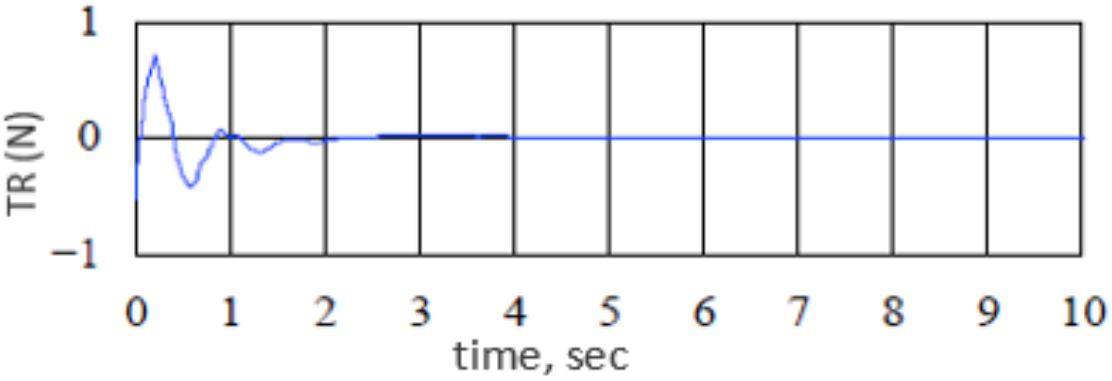
1
0
−1
TR (N)
0 1 2 3 4 5 6 7 8 9 10
time, sec

(f)

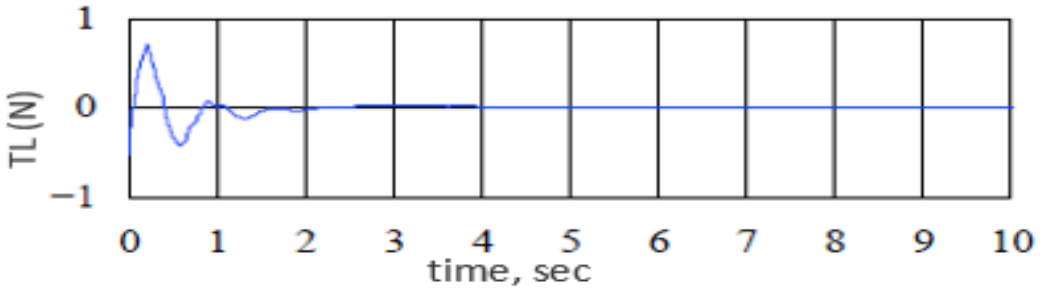

(g)

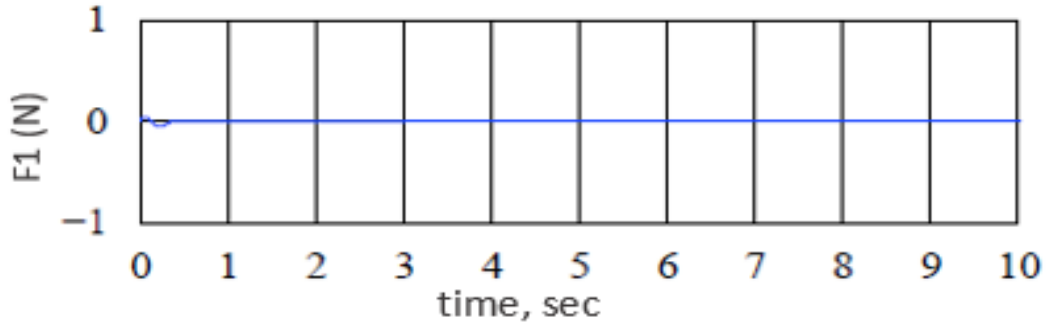

(h)

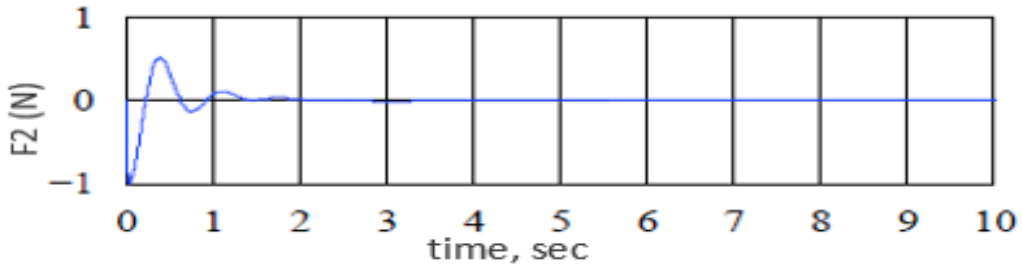

(i)

Figure 4.13 Fuzzy-PID controlled (a)-(e) system performance and (f)-(i) control efforts (Vertical and horizontal linear actuators not activated)

B. Payload horizontal movement only

The robot is permitted to move the carried payload in a direction parallel to the chassis ' axis (horizontal direction) to complete a handling task of picking and placing. The output response of the system, considering activation of the horizontal linear actuator only is shown in Figure 4.14. The attached load is maintained fixed at an elevation of 0.28 m. On the other hand, before resetting at a fixed position, the attached load is allowed to move horizontally at a distance of 0.07 m. With the following initial conditions: $\theta = -5^{\circ}$, $h_1 = 0.28m$ and $h_2 = 0m$, the controller was not capable of retrieving the robotic machine's IB back to the equilibrium upright position as can

be seen in Figure 4.13 (a-e). Rather than maintaining stability, the control mechanism kept it inclined at a fixed inclination angle (approximately 7° on the opposite side).

C. Payload vertical movement only

The robot's stability was tested against the effect of the vertical motion of the attached payload.

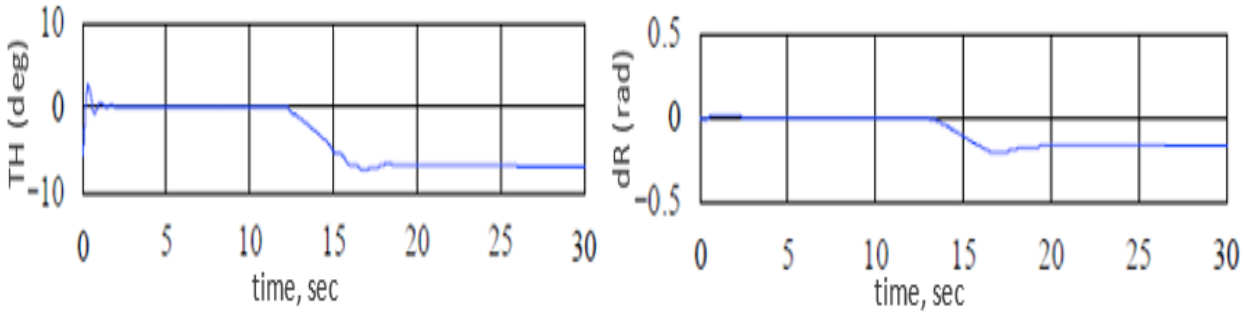

(a)

(b)

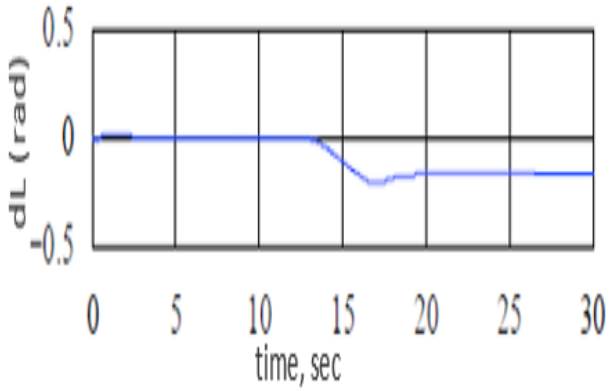

(c)

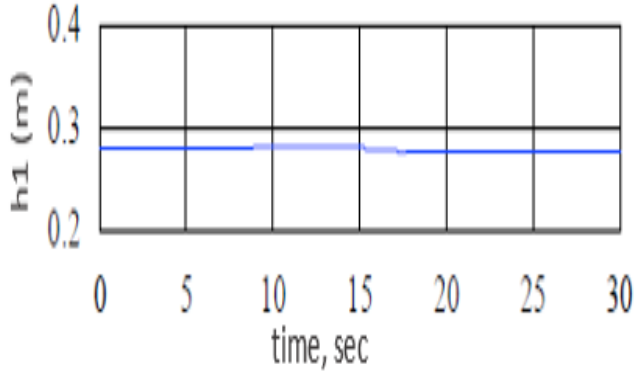

(d)

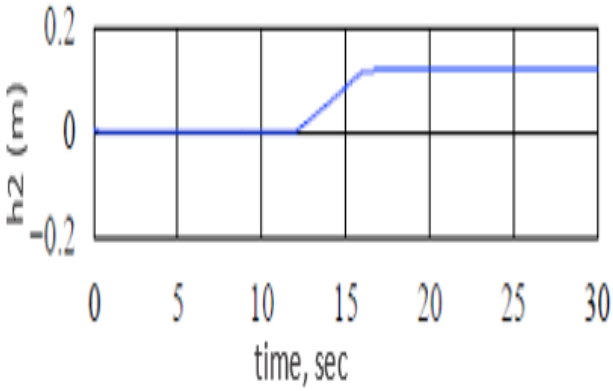

(e)

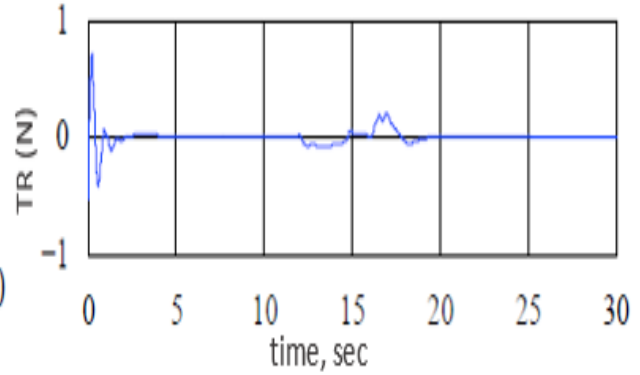

(f)

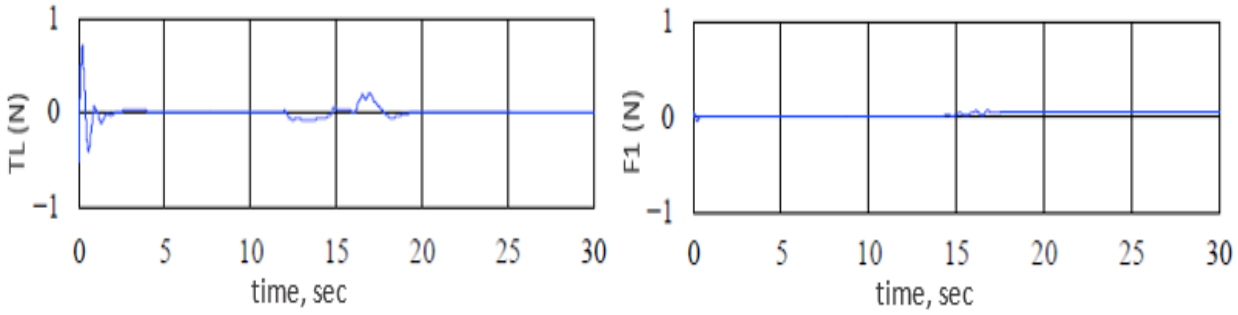

(g) (h)

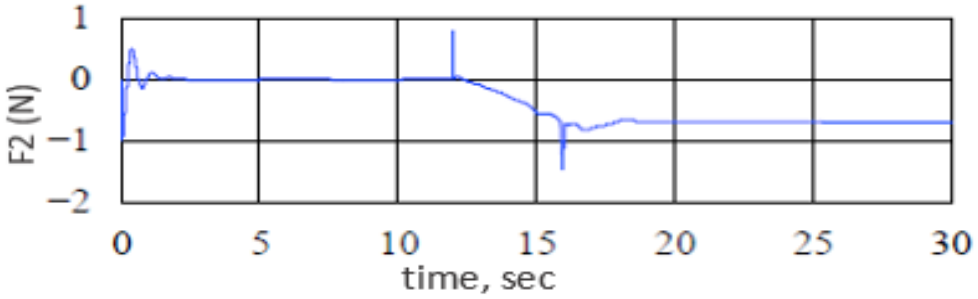

(i)

Figure 4.14 Fuzzy-PID controlled system performance (a)-(e) and control efforts (f)-(i) for payload horizontal movement only

The carried payload is kept fixed for a period of around 12 seconds. The system is then allowed to move the carried payload in a direction along the IB (vertical direction) for a distance of 0.1m before re-settling at an elevation of approximately 0.38 m away from the chassis of the robot. Neglecting the horizontal linear actuator′s effect h_2 and considering the following initial conditions: $\theta = -5^{\circ}$ and $h_1 = 0.28m$, Figure 4.15 shows simulation results for outputs and inputs of the system. From the results it appears clearly, given that no interruption affected the stabilization state of the IB, which the control mechanism developed was robust enough to maintain stability of the robot.

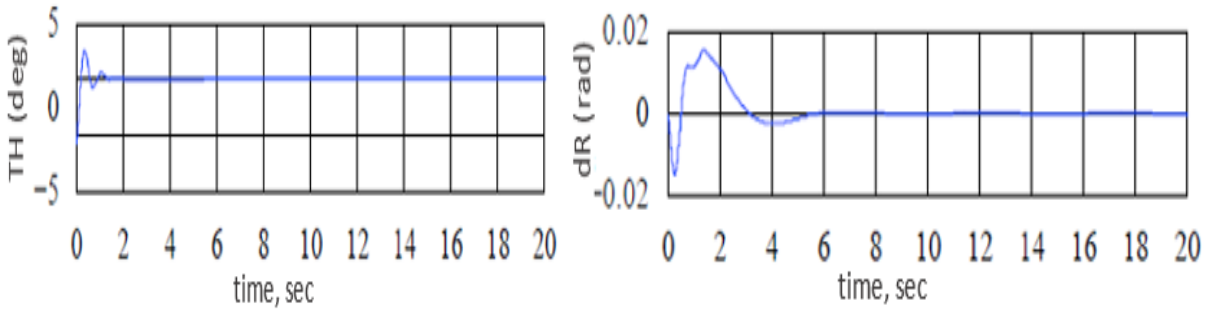

(a) (b)

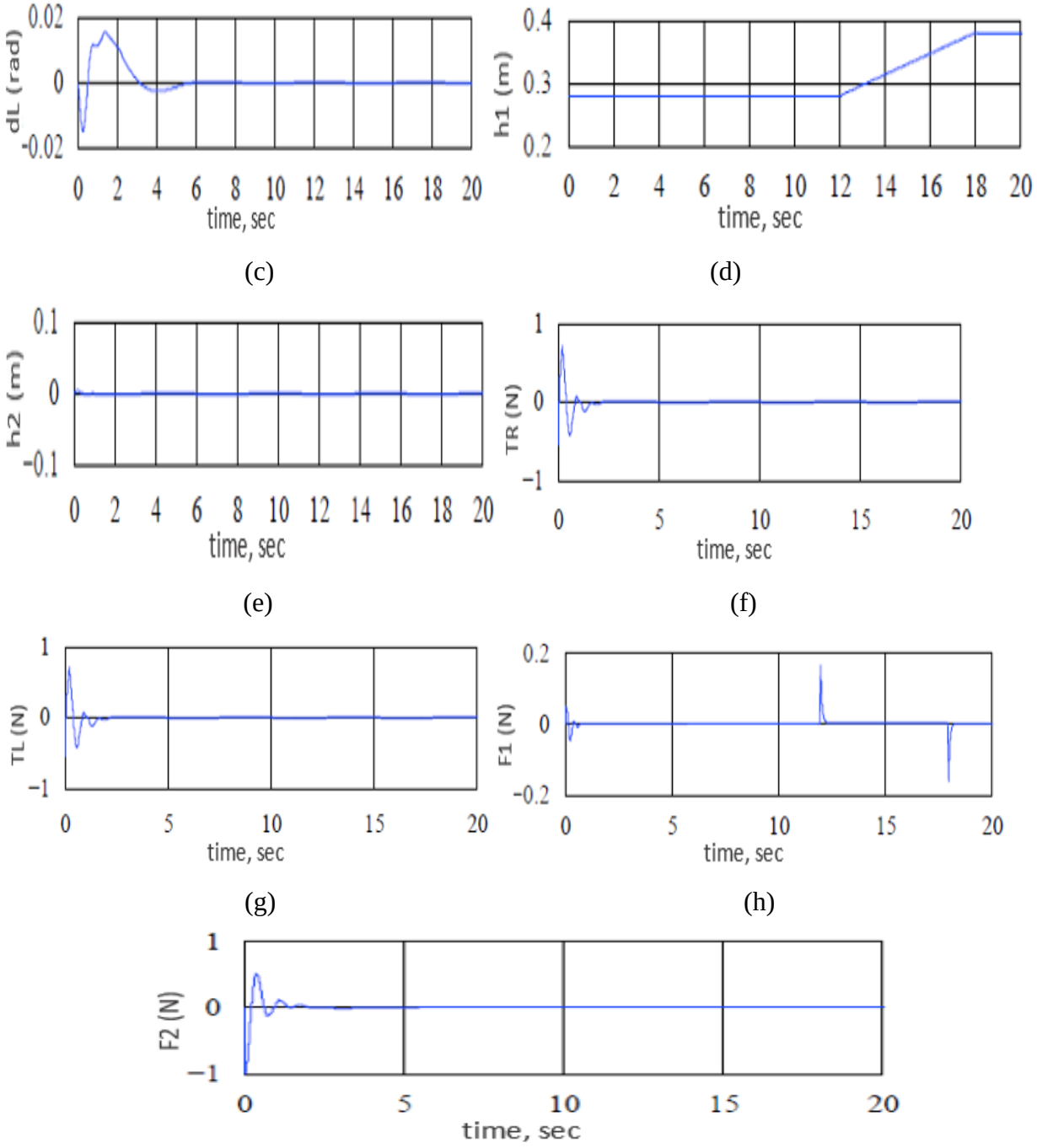

Figure 4.15 Fuzzy-PID controlled system performance (a)-(e) and control efforts (f)-(i) for payload vertical movement only

D. Payload simultaneous horizontal and vertical motion (Vertical and horizontal linear actuators activated)

Figure 4.16 shows the system output response, considering simultaneous activation of the two linear actuators. Setting the simulation′s initial conditions to $\theta = -5^{\circ}$, $h_2 = 0.28m$ and $h_2 = 0m$, the system remains stable without any interruptions during the entire vertical actuator activation process. However, sudden changes in the stability of the IB were observed when the horizontal actuator began to extend its end-effector with a small disturbance in h_1. For the sake of overcoming the COM's position alteration because of the extension of h_2, the IB tilts to the opposite direction.

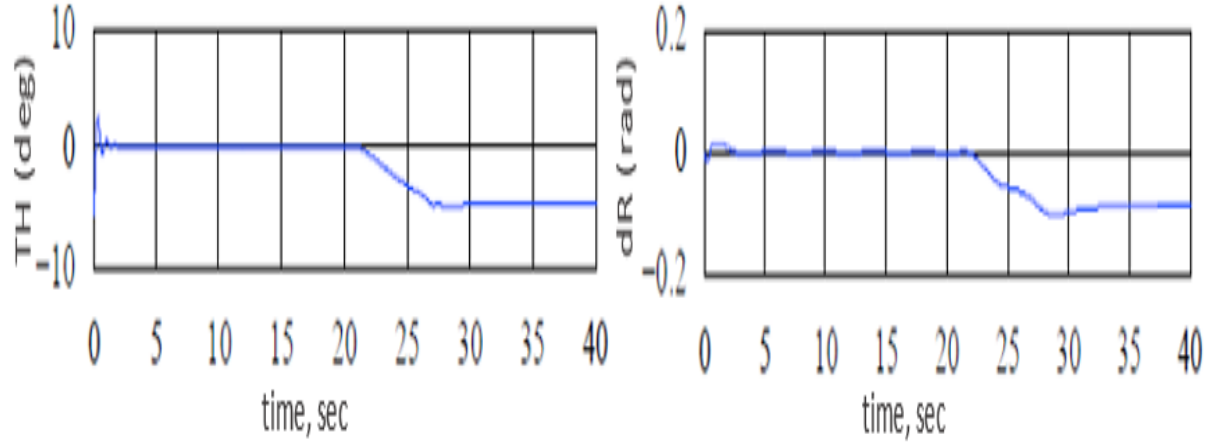

(a)

(b)

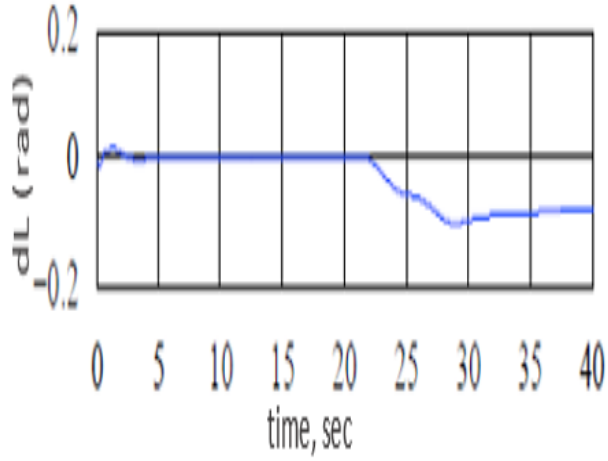

(c)

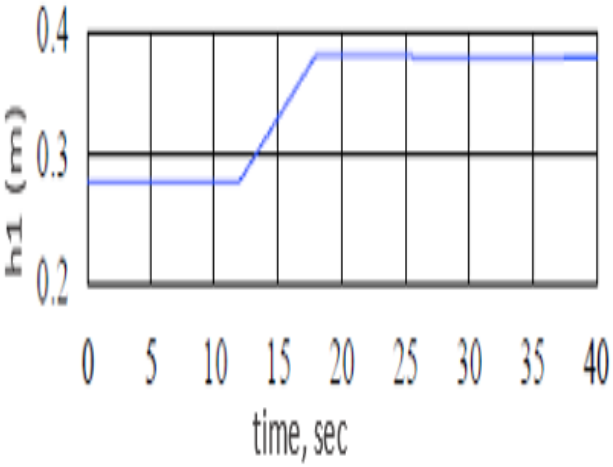

(d)

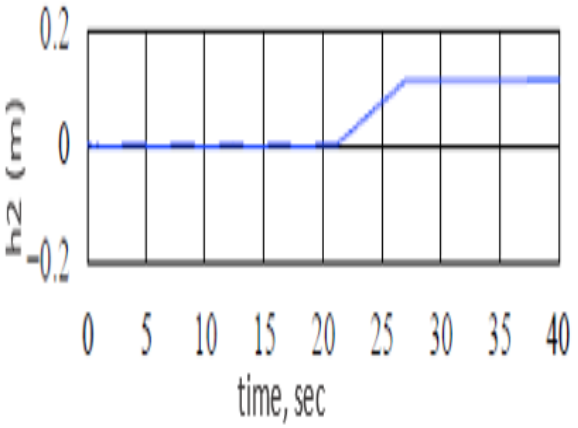

(e)

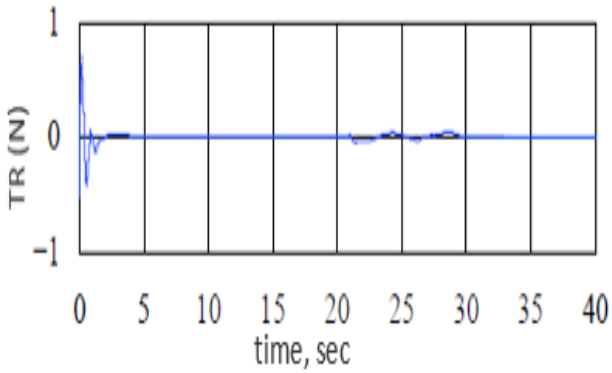

(f)

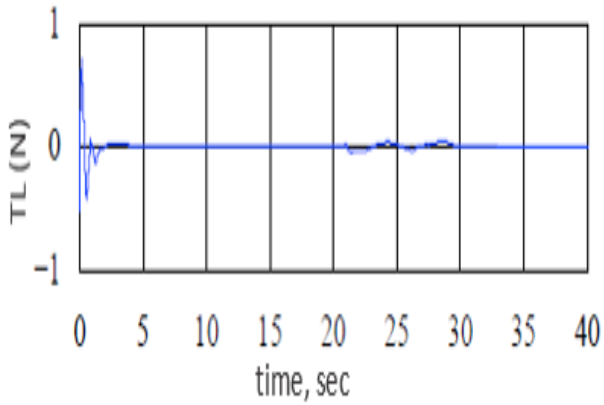

(g)

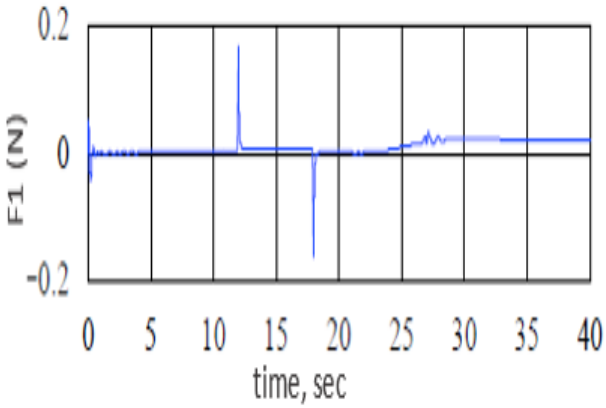

(h)

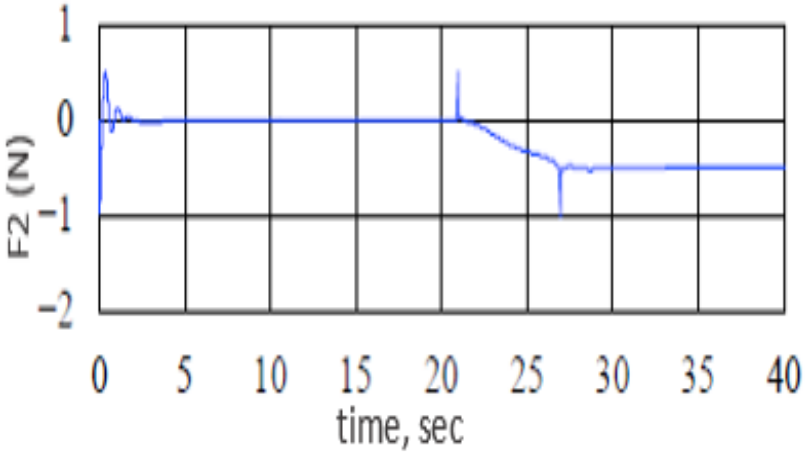

(i)

Figure 4.16 Fuzzy-PID controlled (a)-(b) system performance and (f)-(g) control efforts (Vertical and horizontal linear actuators activated)

4.3.2 Fuzzy-PID with switching mechanisms

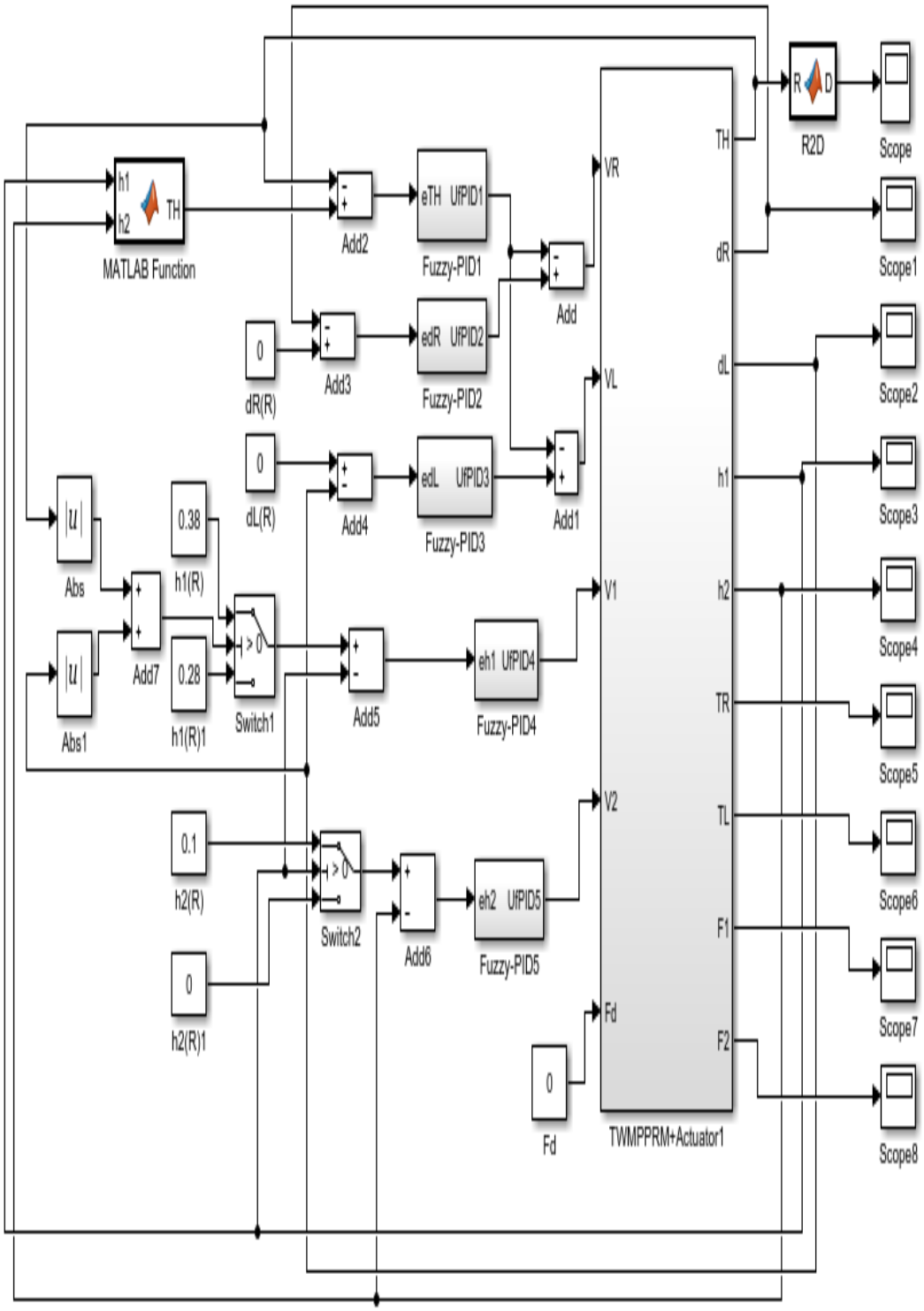

Figure 4.17 Simulink model of fuzzy-PID controller with switching mechanism

The system's stability was evaluated against both the TWMPPRM COM's vertical and horizontal linear motions. Figure 4.18 shows the output simulation of the system, which initially starts at $\theta = -5^{\circ}$, $h_1 = 0.28m$ and $h_2 = 0m$. After balancing the system, the TWMPPRM′s model is simulated to examine the effect of moving h_1 and h_2 in sequence. If the system is balanced, the vertical actuator then moves to its final displacement, the horizontal actuator starts moving until it reaches its final displacement. In the first stage, the stability state of the system is not affected by the activation of the vertical linear actuator. As for the second stage, starting at 10 second, operating the horizontal actuator yields an observable steady tilt in the IB found to be approximately 5°.

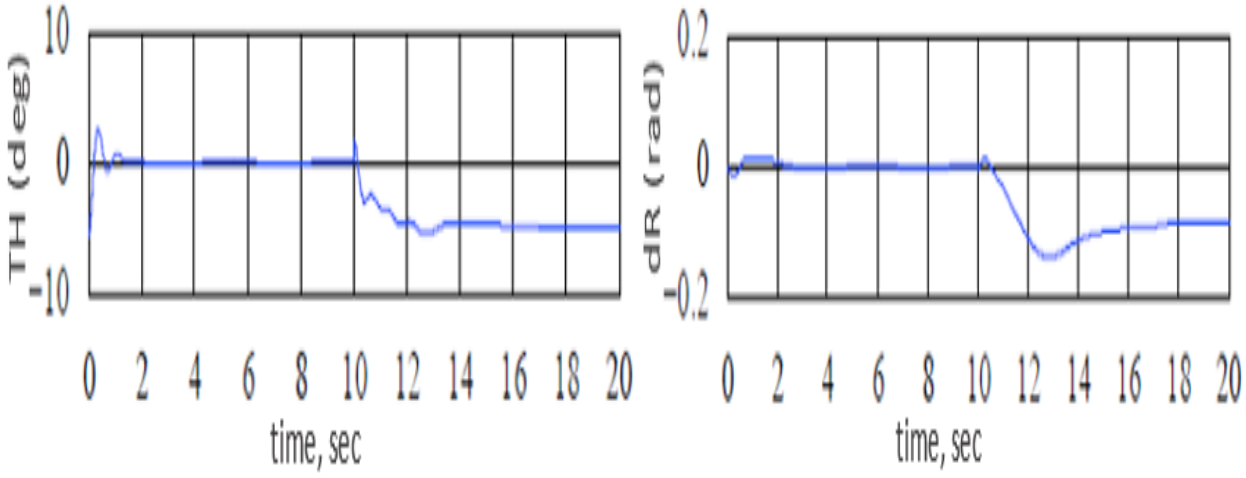

(a)

(b)

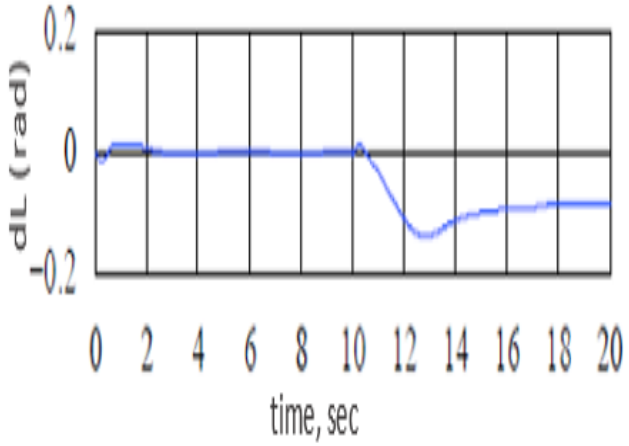

(c)

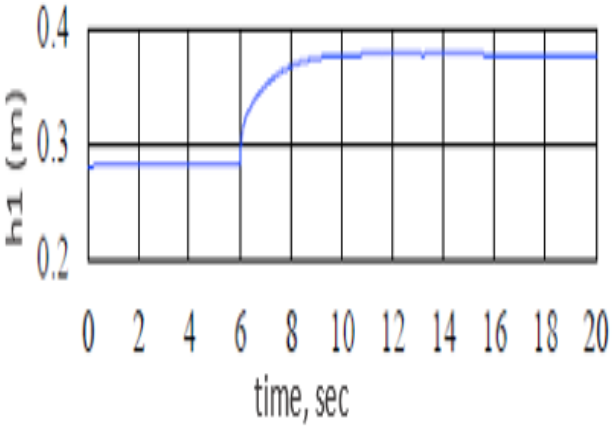

(d)

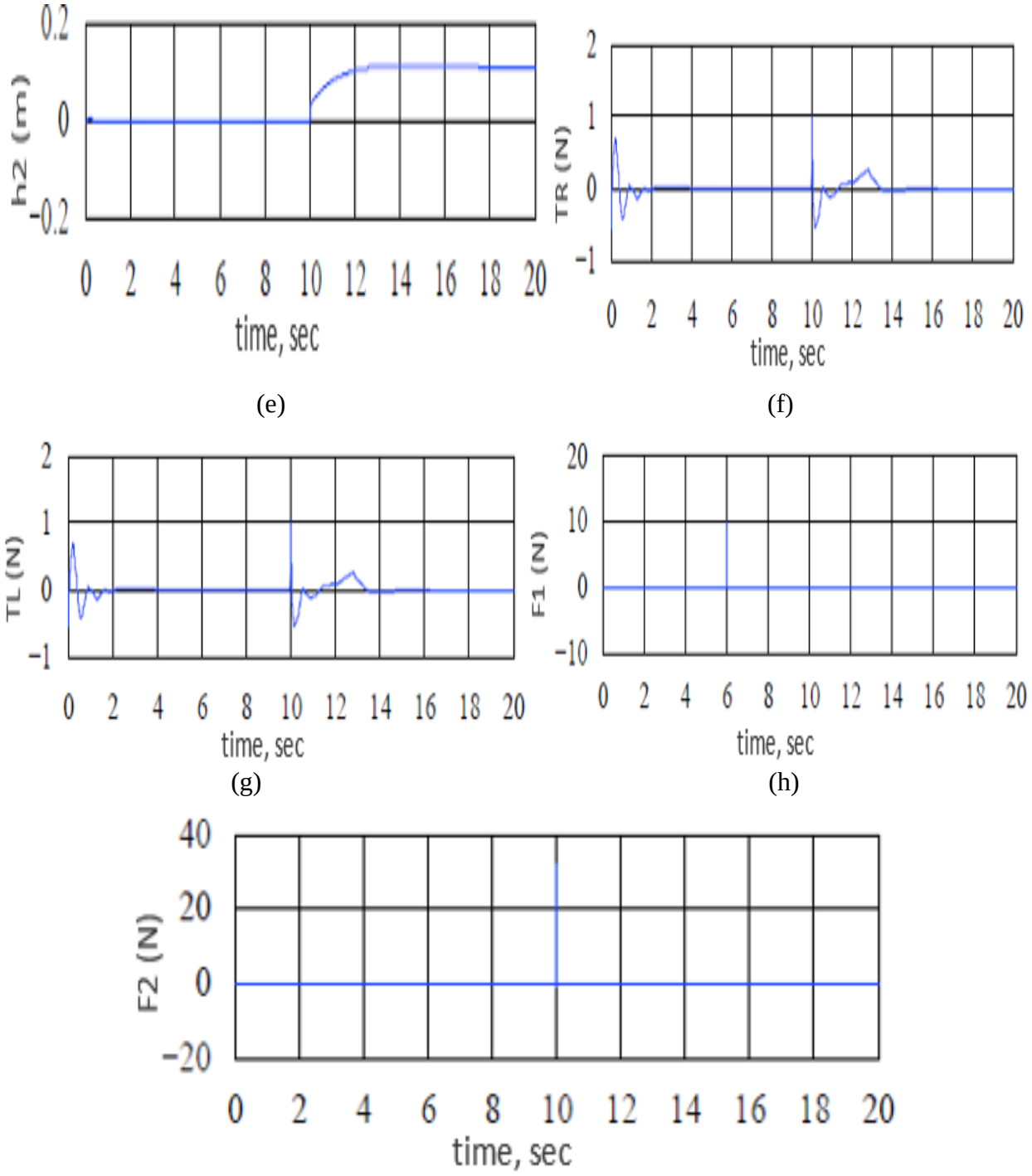

Figure 4.18 Fuzzy-PID controlled (a)-(e) system performance and (f)-(i) control efforts considering switching mechanism with considering switching mechanism (Vertical and horizontal linear actuator activated)

4.4 System response comparison between Fuzzy-PID and PID Controller

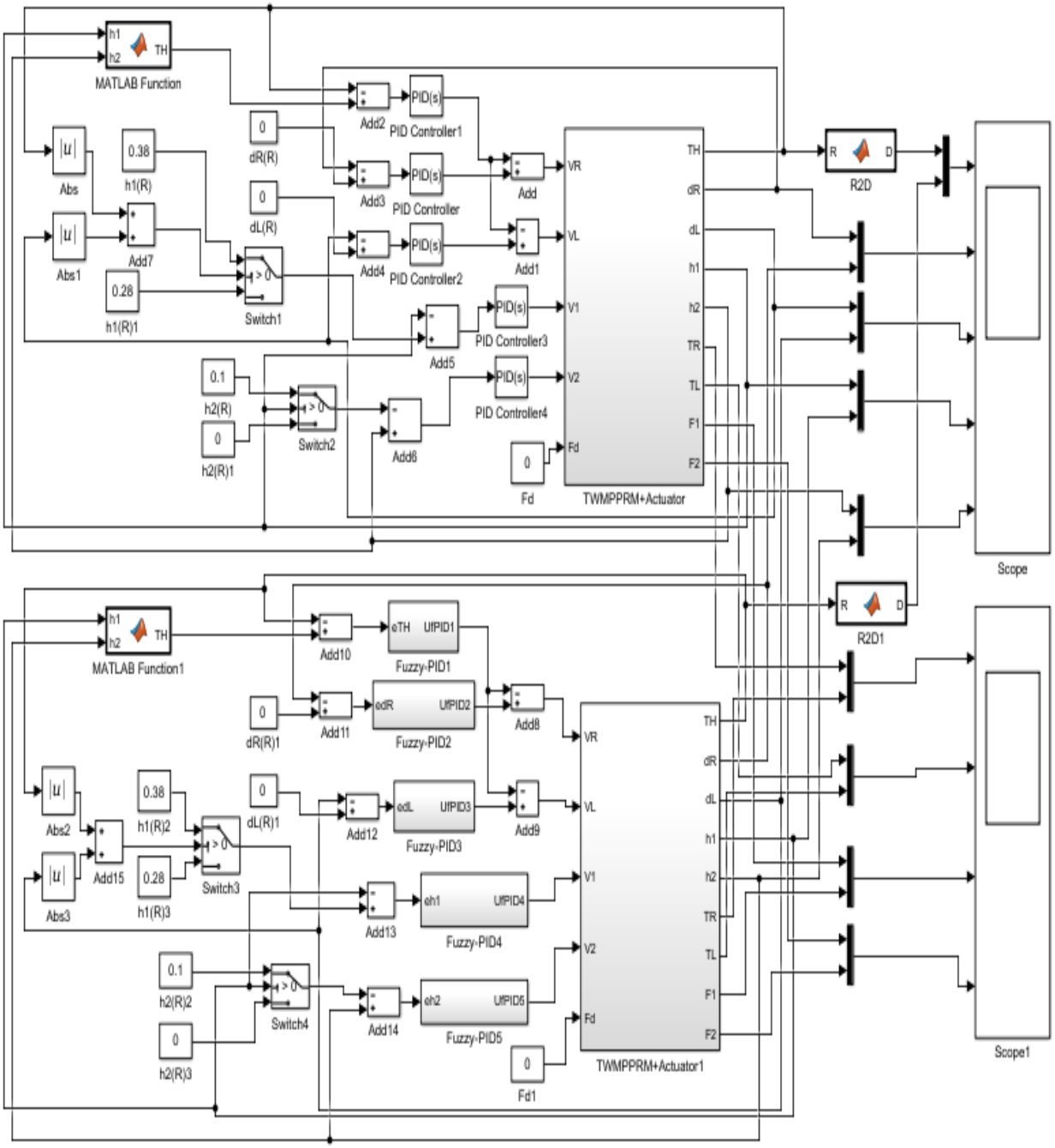

Figure 4.19 Over all Simulink model of PID and FPID controller

For the following situations, payload free movement, payload vertical movement only, payload horizontal movement only, simultaneous horizontal and vertical motion and 1-m straight-line motion of the vehicle; Figures, 4.20, 4.21, 4.22, and 4.23 show the output results of the simulated self-balancing TWMPPRM model and the applied control effort. It is clear from previous figures

that, the Fuzzy-PID controller provides better performance for the system and minimizes the applied force demanded for the TWMPPRM stabilization process. Observing the payload free movement ($h_1 = h_2 = 0$) scenario, as an example of how the Fuzzy-PID controller performance is better way than the PID, Table4.1 shows a comparison of system performance between the previously mentioned controllers in terms of settling time, peak time and raise time. Starting with system settling time, it is observable that the system takes around 2.2870 seconds to settle by implementing the PID control strategy, which is greater than the settling time (0.7800 seconds) of the Fuzzy-PID control strategy. Therefore, the control strategy for Fuzzy-PID optimizes the settling time. As in peak and rise time values, a slight reduction has been noticed when the Fuzzy-PID control method is implemented on the self-balanced TWMPPRM model and it can be concluded that the Fuzzy-PID based method produces both peak and rise time values better than the PID controller. From the scenarios where the horizontal linear actuator activates, payload horizontal movement only case (Figure 4.22) and simultaneous horizontal and vertical motion case (Figure 4.23), the issue of the continuous movement of the TWMPPRM resulting from the horizontal actuator activation has been compensated by the implementation of the FPID algorithm. In response to the PID control system, the horizontal actuator activation affects the stability of the system and allows the TWMPPRM to shift 10 cm away from its original position ($x_R = -0.1m, x_L = -0.1m$).

Where, $x_R = R\delta_R$ (4.1)

$x_L = R\delta_L$ (4.2)

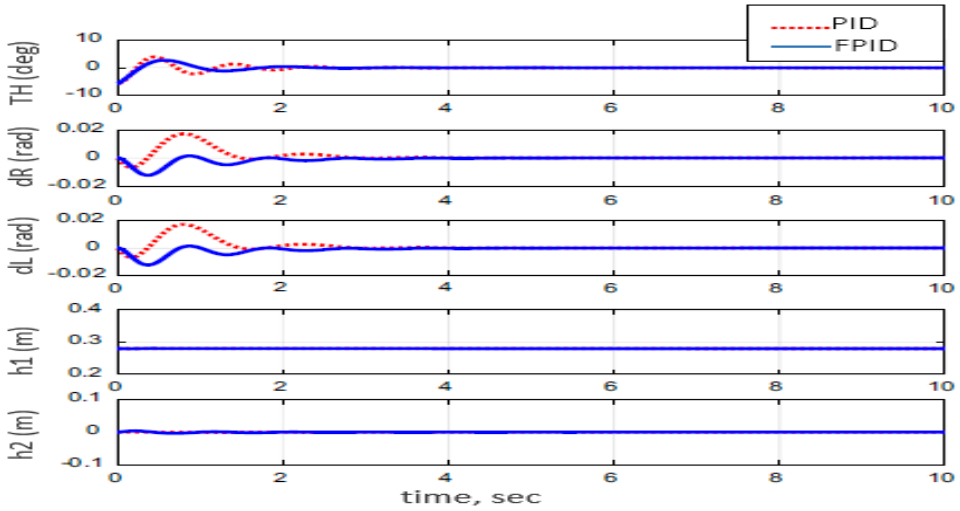

(a)

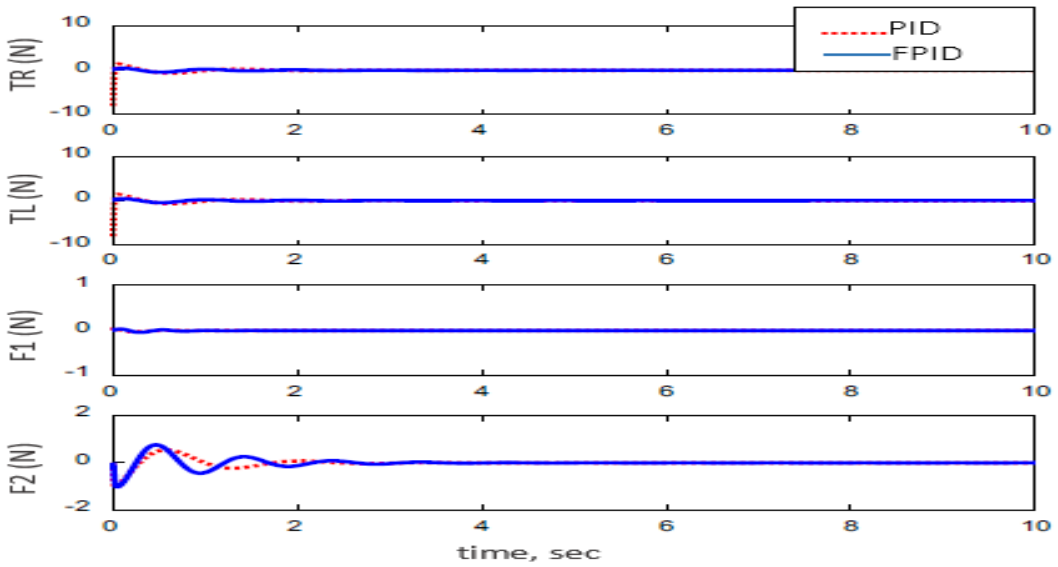

(b)

Figure 4.20 System outputs and inputs, payload free movement (h1 = h2 = 0). a) System outputs, b) System inputs

Table 4.1 Comparison between the system's performance using PID and Fuzzy-PID controller (payload free movement)

Control	Settling time (s)	Peak time (s)	Rise time (s)
PID	2.2870	0.5710	0.2790
Fuzzy-PID	0.7800	0.4400	0.2300

Where, the optimum controller values are based on the IAE criterion.

However, the Fuzzy-PID controller produces a satisfactory performance and robustness against the horizontal linear actuator's movement. In general, the FPID control approach provides much better system performance than the PID control system.

Investigating control system robustness

Considering the same disturbance force applied earlier to the system as shown in Figure 4.25, the robustness of the system was examined with the two control methods and the performance of the system is shown in Figure 4.26.

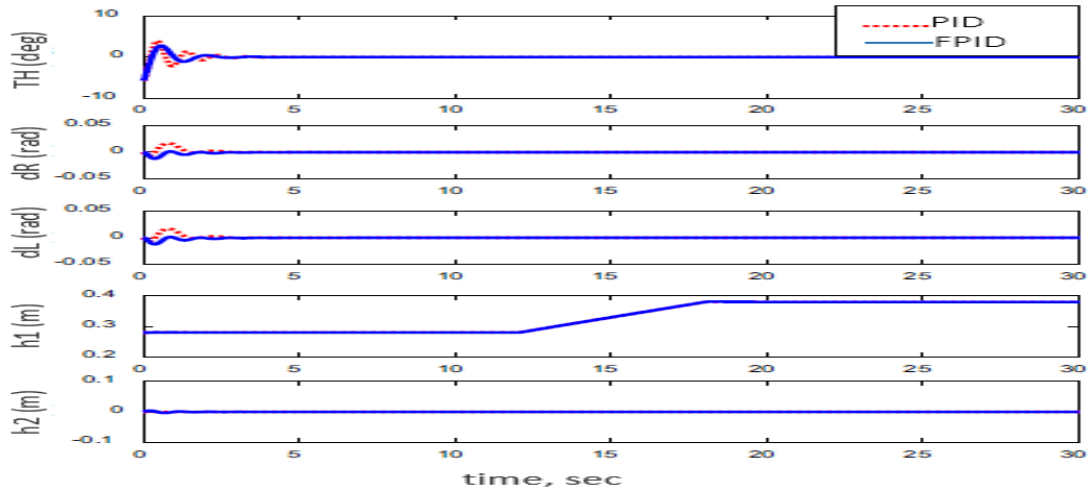

(a)

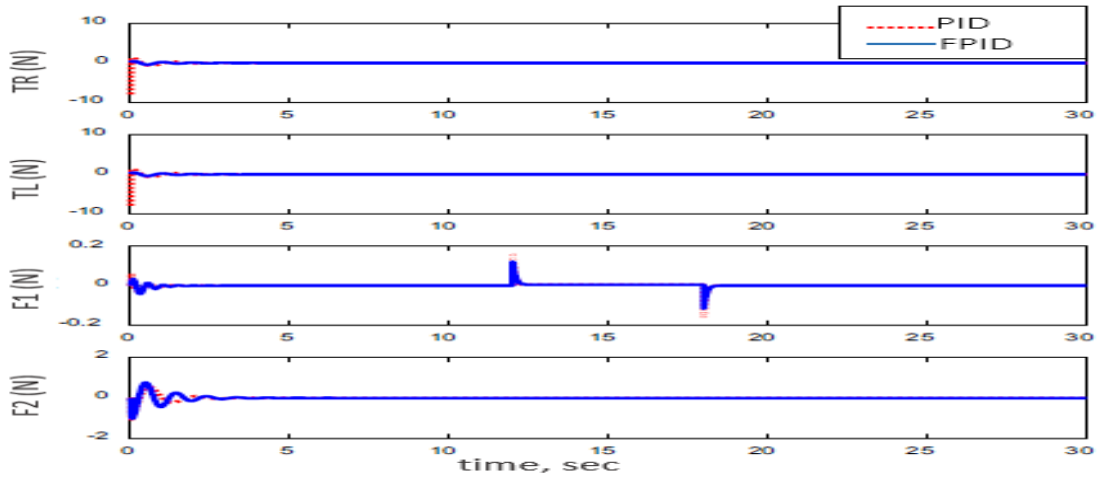

(b)

Figure 4.21 System outputs and inputs, payload vertical movement only. a) System outputs, b) system inputs

Table 4.2 Comparison between the system's performance using PID and Fuzzy-PID controller (payload vertical movement only)

Control	Settling time (s)	Peak time (s)	Rise time (s)
PID	2.2881	0.5921	0.2795
Fuzzy-PID	0.7809	0.4430	0.23070

Where, the optimum controller values are based on the IAE criterion.

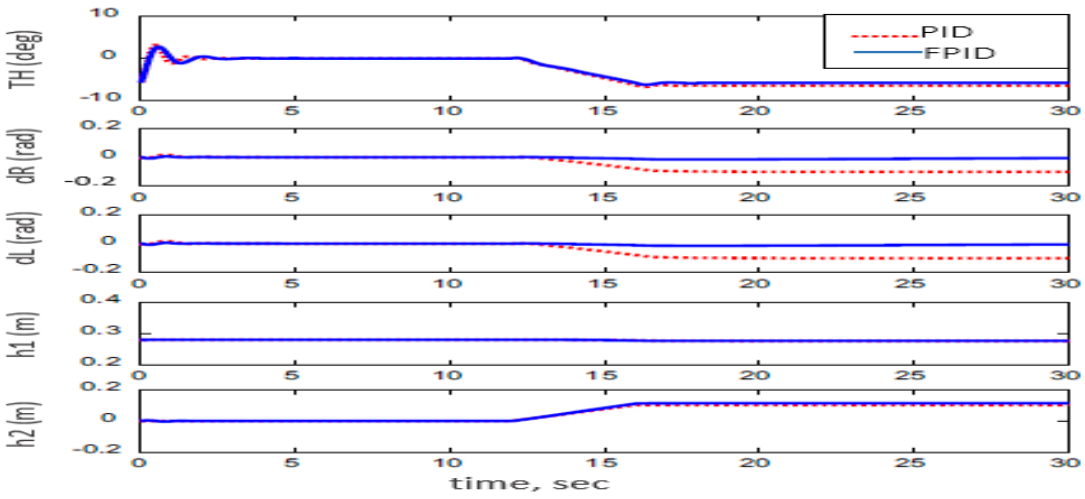

(a)

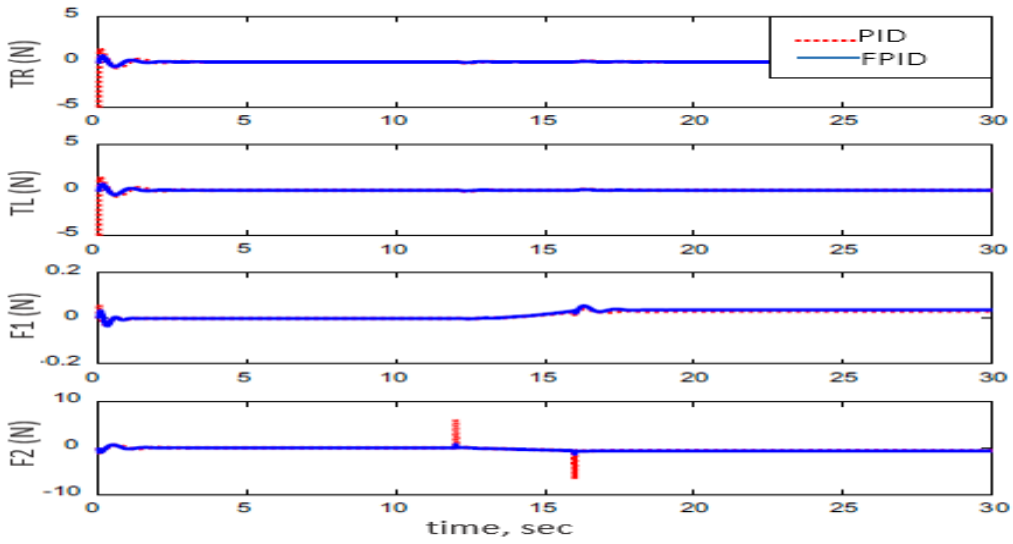

(b)

Figure 4.22 System outputs and inputs, payload horizontal movement only. a) System outputs, b) system inputs

Table 4.3 Comparison between the system's performance using PID and Fuzzy-PID controller (payload horizontal movement only)

Control	Settling time (s)	Peak time (s)	Rise time (s)
PID	2.2781	0.5899	0.2797
Fuzzy-PID	0.7811	0.4421	0.2317

Where, the optimum controller values are based on the IAE criterion.

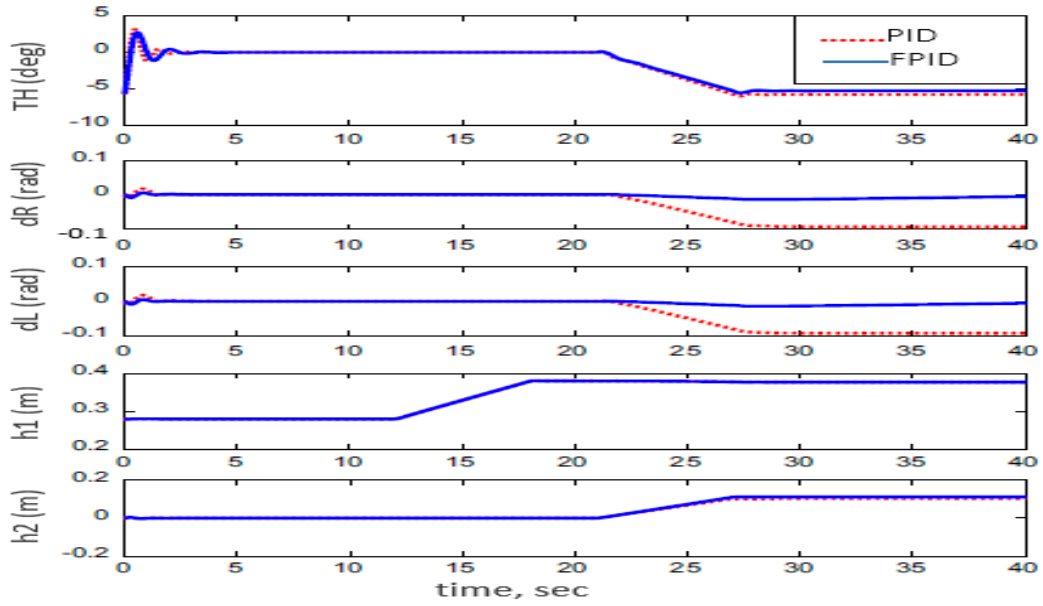

(a)

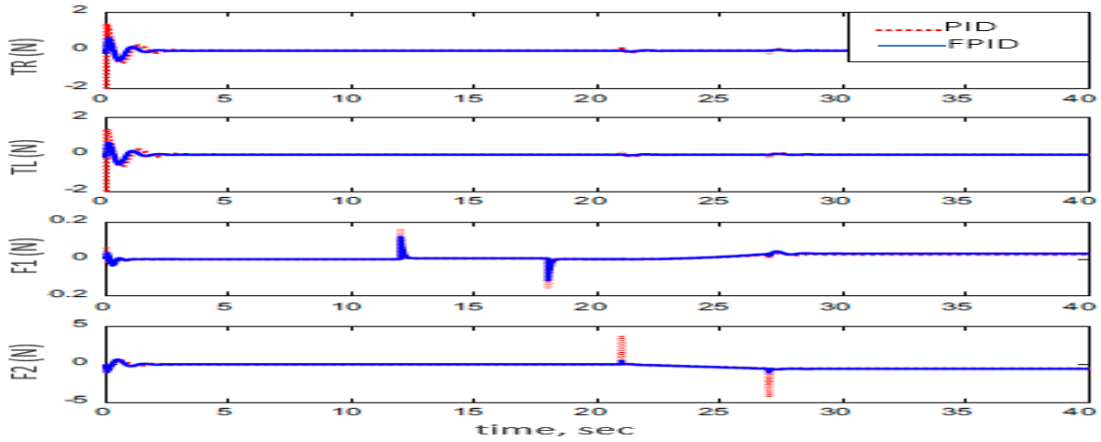

(b)

Figure 4.23 System outputs and inputs, simultaneous vertical and horizontal motion (h1 and h2 ≠ 0). a) System outputs, b) system inputs

Table 4.4 Comparison between the system's performance using PID and Fuzzy-PID controller (simultaneous vertical and horizontal motion)

Control	Settling time (s)	Peak time (s)	Rise time (s)
PID	2.2831	0.5889	0.2837
Fuzzy-PID	0.7923	0.4536	0.2357

Where, the optimum controller values are based on the IAE criterion.

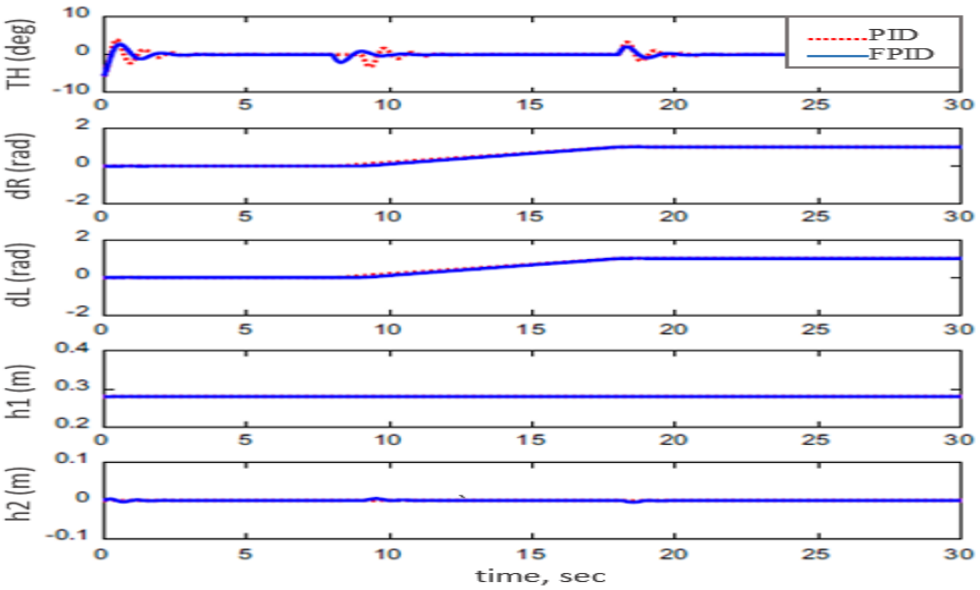

(a)

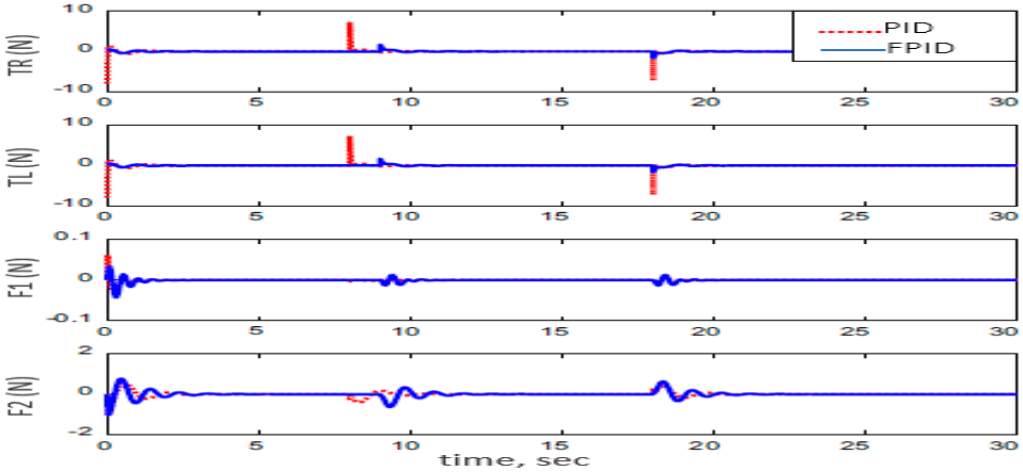

(b)

Figure 4.24 System outputs and inputs, a 1-m straight-line motion. a) System outputs, b) system inputs

Table 4.5 Comparison between the system's performance using PID and Fuzzy-PID controller (1-m straight-line motion)

Control	Settling time (s)	Peak time (s)	Rise time (s)
PID	2.2758	0.5892	0.2767
Fuzzy-PID	0.7843	0.4436	0.2382

Where, the optimum controller values are based on the IAE criterion.

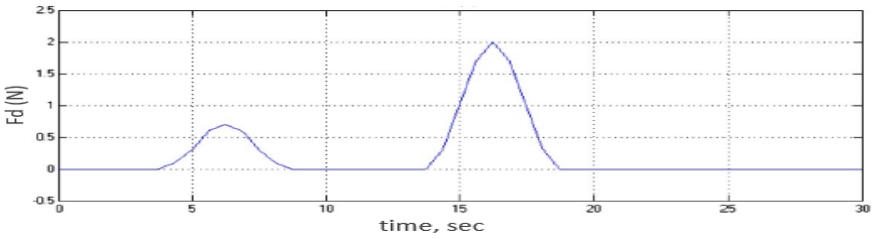

Figure 4.25 disturbance force

As can be observed, the system bounced back to its stability region around the vertical axis in all control methods and in a few seconds. However, the PID performance was not sufficient to withstand the effect of a disturbance on the angular displacement (δ_R, δ_L) of TWMPPRM wheels, and the horizontal linear actuator displacement (h_2). As a matter of fact, the Fuzzy-PID control method surpassed the PID control approach in terms of performance, robustness and instability minimization.

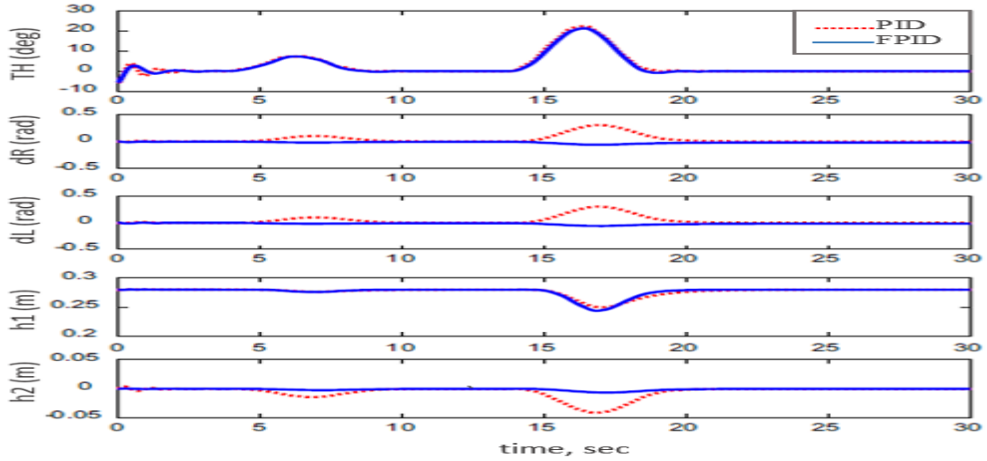

(a)

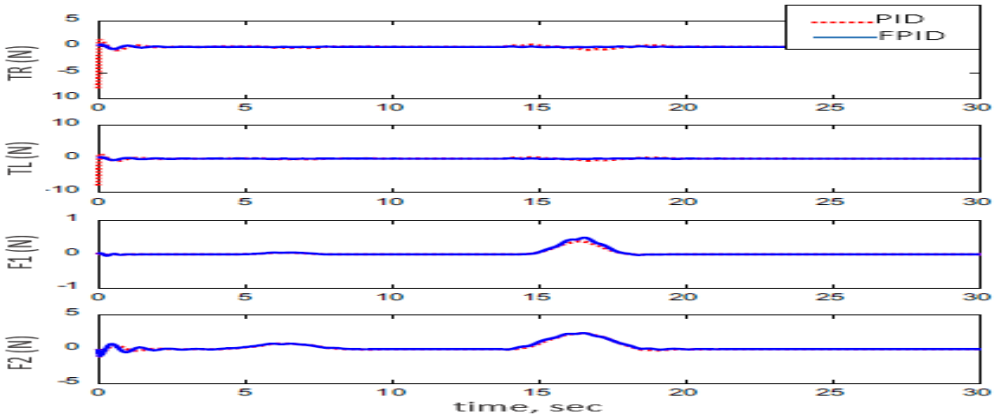

(b)

Figure 4.26 System outputs and inputs with a disturbance. a) System outputs, b) system inputs

Table 4.6 Comparison between the system's performance using PID and Fuzzy-PID controller (payload free movement of arms with disturbance forces)

Control	Settling time (s)	Peak time (s)	Rise time (s)
PID	2.2958	0.6134	0.2993
Fuzzy-PID	0.8343	0.4917	0.2798

Where, the optimum controller values are based on the IAE criterion.

CHAPTER FIVE

5. CONCLUSIONS AND RECOMMENDATIONS

5.1 Conclusions

Five DOFs self-balanced TWMPPRM has been presented in this thesis. The new self-balanced TWMPPRM system offers solutions for both industrial and service robotic applications involving work in limited spaces such as picking and placing objects. Mathematical model of the system was developed via the Lagrangian modeling approach. Considering the nonlinear model of the system, closed-loop PID and Fuzzy-PID controllers were designed to control the unstable 5 DOF self-balanced TWMPPRM. The stability of the nonlinear system was tested against different initial conditions, and the center of mass was moved during the system stabilization process. In addition, the control process was modified using a switching mechanism to avoid moving the center of mass during the stabilization of the system in order to achieve a steady state equilibrium position. It has been proved that the Fuzzy-PID method has improved the system response compared to the PID controller. It was shown by the outcomes of the simulation associated to each scenario.

5.2 Recommendation

The work done in this thesis was based on a FPID control structure, but it would be interesting to apply nonlinear controllers like PID self-tuning fuzzy neural controller for better performance of the system. In addition, more trajectory and different disturbance forces may be applied on the self-balanced TWMPPRM to investigate its performance and stability. The mechanical design can be modified by adding additional degrees of freedom and testing the robot using different types of end-effectors, and an extra degree of freedom may be used to maintain the end effector in a horizontal position while moving the horizontal actuator. This can be done either by adding another horizontal link moving in the reverse direction of the horizontal actuator or by adding a revolving joint to keep the horizontal actuator rotating parallel to the ground. Furthermore, implementing the designed controller practically using digital control system on DSP would be a very interesting extension of this work.

REFERENCES

[1] J. Angeles and J. Angeles, Fundamentals of robotic mechanical systems. Springer, 2002.

[2] R. Sehab and B. Barbedette, "Fuzzy PID Supervision for an Automotive Application: Design and Implementation," p. 101, 2012.

[3] M. A. Omar, T. Khedr, and B. A. Zalam, "Particle swarm optimization of fuzzy supervisory controller for nonlinear position control system," in 2013 8th International Conference on Computer Engineering & Systems (ICCES), pp. 138-145.

[4] Y. Yang, W.-G. Wang, D.-J. Yu, and G. Ding, "A fuzzy parameters adaptive PID controller design of digital positional servo system," in Proceedings. International Conference on Machine Learning and Cybernetics, 2002, vol. 1, pp. 310-314.

[5] M. Dotoli, B. Maione, and B. Turchiano, "Fuzzy-Supervised PID Control: Experimental Results," in EUNITE the 1st European Symposium on Intelligent Technologies, Hybrid Systems and their Implementation on Smart Adaptive Systems, 2001, pp. 31-35.

[6] J. Mayr, F. Spanlang, and H. J. M. Gattringer, "Mechatronic design of a self-balancing three-dimensional inertia wheel pendulum," vol. 30, pp. 1-10, 2015.

[7] J. Lee, H. Shin, S. Lee, and S. Jung, "Balancing control of a single-wheel inverted pendulum system using air blowers: evolution of mechatronics capstone design," vol. 23, no. 8, pp. 926-932, 2013.

[8] K. M. GOHER and M. Tokhi, "Balance control of a TWRM with a dynamic payload," in Advances In Mobile Robotics: World Scientific, 2008, pp. 39-46.

[9] M. Bettayeb, C. Boussalem, R. Mansouri, and U. Al-Saggaf, "Stabilization of an inverted pendulum-cart system by fractional PI-state feedback," vol. 53, no. 2, pp. 508-516, 2014.

[10] I. Boussaada, I.-C. Morărescu, and S.-I. Niculescu, "Inverted pendulum stabilization: Characterization of codimension-three triple zero bifurcation via multiple delayed proportional gains," vol. 82, pp. 1-9, 2015.

[11] R. Brisilla and V. Sankaranarayanan, "Nonlinear control of mobile inverted pendulum," vol. 70, pp. 145-155, 2015.

[12] R. Cui, J. Guo, and Z. Mao, "Adaptive backstepping control of wheeled inverted pendulums models," vol. 79, no. 1, pp. 501-511, 2015.

[13] E. V. Kumar and J. Jerome, "Robust LQR controller design for stabilizing and trajectory tracking of inverted pendulum," vol. 64, pp. 169-178, 2013.

[14] L. B. Prasad, B. Tyagi, and H. O. Gupta, "Optimal control of nonlinear inverted pendulum system using PID controller and LQR: performance analysis without and with disturbance input," vol. 11, no. 6, pp. 661-670, 2014.

[15] M. Olivares and P. Albertos, "Linear control of the flywheel inverted pendulum," vol. 53, no. 5, pp. 1396-1403, 2014.

[16] G. V. Raffo, M. G. Ortega, V. Madero, and F. R. Rubio, "Two-wheeled self-balanced pendulum workspace improvement via underactuated robust nonlinear control," vol. 44, pp. 231-242, 2015.

[17] M. Yue, S. Wang, and J.-Z. Sun, "Simultaneous balancing and trajectory tracking control for two-wheeled inverted pendulum vehicles: a composite control approach," vol. 191, pp. 44-54, 2016.

[18] L. A. Zadeh, "Fuzzy sets," vol. 8, no. 3, pp. 338-353, 1965.

[19] A. Visioli, "Tuning of PID controllers with fuzzy logic," vol. 148, no. 1, pp. 1-8, 2001.

[20] S. Sivanandam, S. Sumathi, and S. Deepa, Introduction to fuzzy logic using MATLAB. Springer, 2007.

[21] E. H. Mamdani, "Application of fuzzy logic to approximate reasoning using linguistic synthesis," no. 12, pp. 1182-1191, 1977.

[22] M. Legesse, "Speed ControlOf Vector Controlled PMSM Drive Using Fuzzy Logic-PI Controller," Addis Ababa University, 2011.

[23] Y. Maddahi, A. Maddahi, and N. Sepehri, "Calibration of omnidirectional wheeled mobile robots: method and experiments," vol. 31, no. 6, pp. 969-980, 2013.

[24] G. Ishigami, K. Iagnemma, J. Overholt, and G. Hudas, "Design, development, and mobility evaluation of an omnidirectional mobile robot for rough terrain," vol. 32, no. 6, pp. 880-896, 2015.

[25] M. F. Silva, J. T. Machado, and A. M. Lopes, "Modelling and simulation of artificial locomotion systems," vol. 23, no. 5, pp. 595-606, 2005.

[26] J. J. Craig, Introduction to robotics: mechanics and control, 3/E. Pearson Education India, 2009.

[27] A. Z. Alassar, I. M. Abuhadrous, and H. A. Elaydi, "Comparison between FLC and PID Controller for 5DOF robot arm," in 2010 2nd International Conference on Advanced Computer Control, vol. 5, pp. 277-281.

[28] L. Wang, M. Tian, and Y. Gao, "Fuzzy self-adapting PID control of PMSM servo system," in 2007 IEEE International Electric Machines & Drives Conference, vol. 1, pp. 860-863.

[29] K. H. Ang, G. Chong, and Y. Li, "PID control system analysis, design, and technology," vol. 13, no. 4, pp. 559-576, 2005.

[30] C. C. Hang, K. J. Åström, and W. K. Ho, "Refinements of the Ziegler–Nichols tuning formula," in IEEE Proceedings D (Control Theory and Applications), 1991, vol. 138, no. 2, pp. 111-118.

[31] P. N. Paraskevopoulos, Modern control engineering. CRC Press, 2017.

[32] A. Rohan, M. Rabah, K.-H. Nam, and S. H. Kim, "Design of fuzzy logic based controller for gyroscopic inverted pendulum system," vol. 18, no. 1, pp. 58-64, 2018.

[33] M. Rabah, A. Rohan, and S.-H. Kim, "Comparison of position control of a gyroscopic inverted pendulum using PID, fuzzy logic and fuzzy PID controllers," vol. 18, no. 2, pp. 103-110, 2018.

[34] Y.-J. Ryoo, "An autonomous control of fuzzy-PD controller for quadcopter," vol. 17, no. 2, pp. 107-113, 2017.

[35] D. Parhi and M. Singh, "Intelligent fuzzy interface technique for the control of an autonomous mobile robot," vol. 222, no. 11, pp. 2281-2292, 2008.

[36] A. Z. Alassar, I. M. Abuhadrous, and H. A. Elaydi, "Modeling and control of 5 DOF robot arm using supervisory control," in 2010 The 2nd International Conference on Computer and Automation Engineering (ICCAE), vol. 3, pp. 351-355.

[37] R. S. Ali, A. A. Aldair, and A, K. Almousawi, " Implementation and Design of Fuzzy Supervisory Controller for Mobile Robot Manipulator," vol.16,no.1,pp.243-259,2016.

[38] F. C. Liu, L. H. Liang, and J. J. Gao, " Fuzzy PID Control of Space Manipulator for Both Ground Alignment and Space Applications," vol.11,no.4,pp.353-360,2014.

[39] Z. Y. Zhao, M. Tomizuka and S. Isaka, " Fuzzy Gain Scheduling PID Controller," Vol. 23, No. 5, pp.1392–1398,2003.

APPENDIXES

A. COEFFICIENTS OF THE STATE SPACE MODEL

$$A_{63} = \left[\frac{4gR^2\left(J_w + m_w R^2\right)\left(m_2\left(m_1 l^2 + J_1 + J_2\right) + \left(m_1^2 l^2\right)\right)}{den_1} \right]$$

$$A_{65} = \left[\frac{4m_1 m_2 glR^2\left(J_w + m_w R^2\right)}{den_1} \right]$$

$$A_{66} = \left[\frac{8\left(m_1 l^2 + J_1 + J_2\right)\left(\left(J_w + m_w R^2\right)\left(\mu_w + \mu_c R^2\right)\right) + m_1 R^2\left(J_1 + J_2\right)\left(\mu_w + \mu_c R^2\right)}{den_1} \right]$$

$$A_{67} = \left[\frac{m_1 R^2\left(J_1 + J_2\right)\left(\mu_w + \mu_c R^2\right)}{den_1} \right]$$

$$A_{610} = \left[\frac{4\mu_2 R^2\left(m_1 l^2 + J_1 + J_2\right)\left(J_w + m_w R^2\right)}{den_1} \right]$$

$$A_{82} = \left[\frac{m_1 gl\left(4J_w + R^2\left(4m_w + m_1 + m_2\right)\right)}{den_2} \right]$$

$$A_{85} = \left[\frac{m_2 g\left(4J_w + 4m_w R^2 + m_1 R^2\right)}{den_2} \right]$$

$$A_{86} = \left[\frac{m_1 l\mu_c R^2 + m_1 l\mu_w}{den_2} \right],$$

$$A_{87} = \left[\frac{m_1 l\mu_c R^2 + m_1 l\mu_w}{den_2} \right],$$

$$A_{810} = \left[\frac{m_1 l\mu_2 R^2}{den_2} \right],$$

$$A_{94} = -\left[\frac{\mu_1}{m_2} \right],$$

$$A_{103} = \left[\frac{m_2 g\left(J_1 + J_2 + m_1 l^2\right)\left(4J_w + 4m_w R^2 + m_1 R^2 + m_2 R^2\right)}{den_3} \right]$$

$$A_{105} = \left[\frac{m_1 g l m_2^2 R^2}{den_3} \right],$$

$$A_{73} = A_{63} \quad A_{75} = A_{65}$$
$$A_{710} = A_{610}, A_{76} = A_{67},$$

$$A_{106} = \left[\frac{m_2 \left(J_1 + J_2 + m_1 l^2 \right) \left(\mu_w + \mu_c R^2 \right)}{den_3} \right]$$

$$A_{107} = \left[\frac{m_2 \left(J_1 + J_2 + m_1 l^2 \right) \left(\mu_w + \mu_c R^2 \right)}{den_3} \right]$$

$$A_{1010} = \left[\frac{\mu_2 \left(J_1 + J_2 + m_1 l^2 \right) \left(4 J_w + 4 m_w R^2 + m_2 R^2 \right) + \left(J_1 + J_2 \right) \left(m_1 R^2 \right)}{den_3} \right]$$

$$B_{64} = -\left[\frac{4 R^2 \left(J_1 + J_2 + m_1 l^2 \right) \left(J_w + m_w R^2 \right)}{den_1} \right], B_{93} = \left[\frac{1}{m_2} \right],$$

$$B_{81} = B_{82} = B_{84} = -\left[\frac{m_1 l R^2}{den_2} \right]$$

$$B_{101} = -\left[\frac{m_2 R^2 \left(m_1 l^2 + J_1 + J_2 \right)}{den_3} \right],$$

$$B_{72} = B_{62}, B_{71} = B_{62}$$
$$B_{74} = B_{64}$$

$$B_{102} = -\left[\frac{\left(J_1 + J_2 + m_1 l^2 \right) \left(4 J_w + 4 m_w R^2 + m_2 R^2 \right) + \left(J_1 + J_2 \right) \left(m_1 R^2 \right)}{den_3} \right]$$

Where,

$$den_1 = -4 \left[4 \left(J_1 + J_2 + m_1 l^2 \right) \left(J_w^2 + m_w^2 R^4 + 2 J_w m_w R^2 \right) + \left(J_1 + J_2 \right) \left(m_1 m_w R^4 + m_1 J_w R^2 \right) \right]$$

$$den_2 = \left[4 \left(J_1 + J_2 + m_1 l^2 \right) \left(J_w + m_w R^2 + 2 J_w m_w R^2 \right) \right] + \left[\left(J_1 + J_2 \right) m_1 R^2 \right]$$

$$den_3 = m_2 \left[4 \left(J_1 + J_2 + m_1 l^2 \right) \left(J_w + m_w R^2 \right) \right] + \left[\left(J_1 + J_2 \right) m_1 R^2 \right]$$

B. TWMPPRM SIMULATION PARAMETERS

Table B.1 TWMPPRM simulation parameters

Terminology	Description	Value	Unit
m_1	Mass of the chassis	3.1	Kg
m_2	Mass of the linear actuators	0.6	Kg
m_w	Mass of wheel	0.14	Kg
R	Wheel radius	0.05	M
L1	Length of arm/link one	0.5	M
L2	Length of arm/link two	0.5	M
J_1	Chassis moment of inertia	0.068	$kg.m^2$
J_2	Moving mass moment of inertia	0.0093	$kg.m^2$
J_w	Wheel moment of inertia	0.000175	$kg.m^2$
l	Distance of chassis′ center of mass for wheel axle	0.14	M
μ_1	Coefficient of friction of vertical linear actuator	0.3	Ns/m
μ_2	Coefficient of friction of horizontal linear Actuator	0.3	Ns/m
μ_w	Coefficient of friction between wheel and ground	0	Ns/m
μ_c	Coefficient of friction between chassis and wheel	0.1	Ns/m
g	Gravitational acceleration	9.81	m/s^2

C. MATHEMATICAL CALCULATION OF CONTROL PERFORMANCE INDEX

$$ISE = \int e^2(t)dt$$

$$IAE = \int |e(t)|dt$$

$$ITSE = \int te^2(t)dt$$

$$ITAE = \int t|e(t)|dt$$

D. FLC 25 RULES

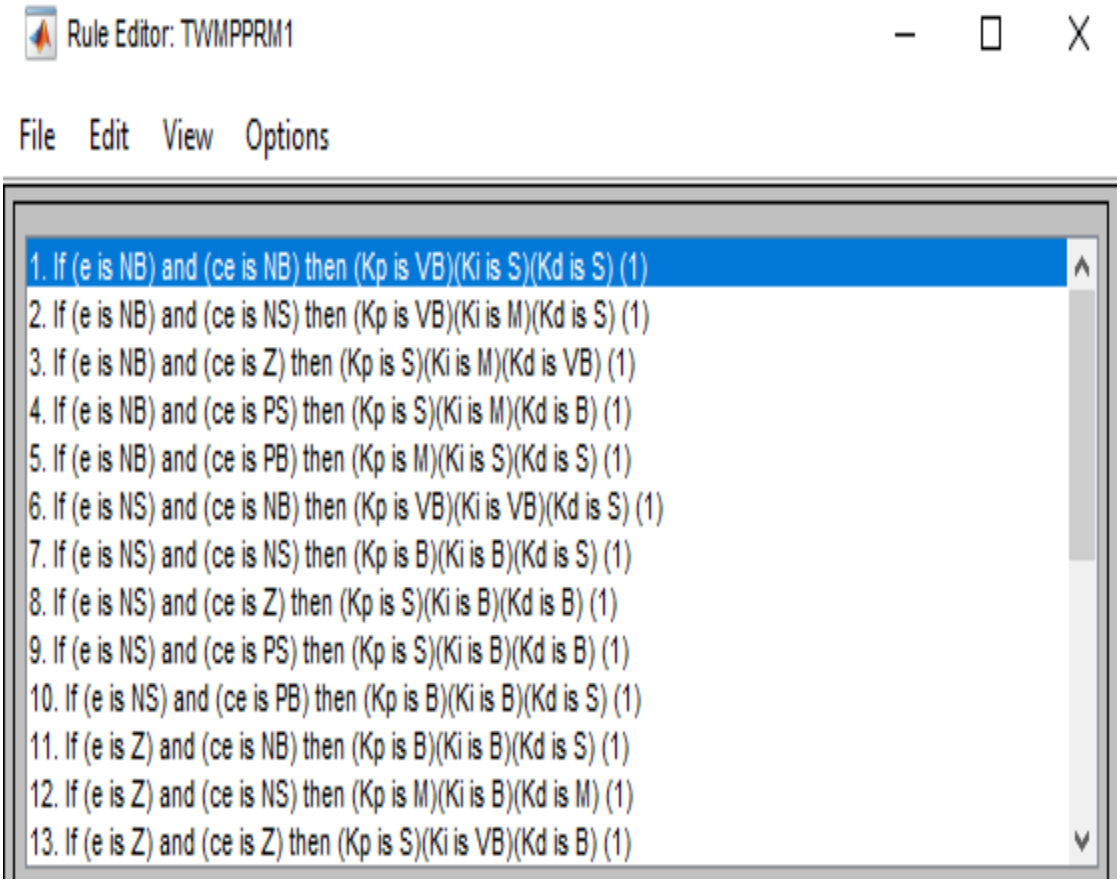

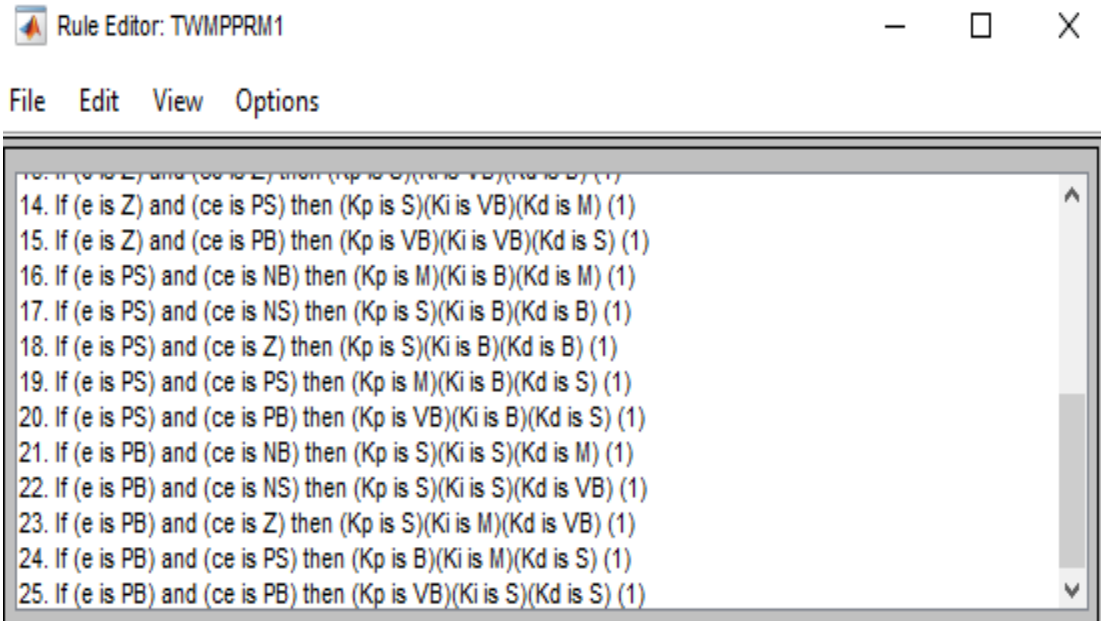

E. RULE VIEWS OF THE FIS